1983

Analysis of the electromagnetic interference field by the radiation method for transposed and untransposed transmission lines

Salah Leulmi
Iowa State University

Leulmi, Salah

ANALYSIS OF THE ELECTROMAGNETIC INTERFERENCE FIELD BY THE RADIATION METHOD FOR TRANSPOSED AND UNTRANSPOSED TRANSMISSION LINES

Iowa State University PH.D. 1983

Analysis of the electromagnetic interference field by the radiation method for transposed and untransposed transmission lines

by

Salah Leulmi

A Dissertation Submitted to the
Graduate Faculty in Partial Fulfillment of the
Requirements for the Degree of
DOCTOR OF PHILOSOPHY

Department: Electrical Engineering
Major: Electric Power Systems

Approved:

Signature was redacted for privacy.

In Charge of Major Work

Signature was redacted for privacy.

For the Major Department

Signature was redacted for privacy.

For the Graduate College

Iowa State University
Ames, Iowa

1983

TABLE OF CONTENTS

I. INTRODUCTION

A. Historical Background

Corona has been the subject of detailed theoretical study for many years [1, 2, 3]. The power loss due to corona was initially developed by Peek in the 1920s [4, 5]. However, not much was done in the radio noise area until the late '30s and early '40s.

The term "radio noise" has been defined as "any unwanted disturbance within the radio frequency band, such as undesired electric waves in any transmission channel or device" [6]. Electric power transmission lines generate radio noise during their normal operation as a by-product of corona generation and gap discharges.

To provide reasonably efficient transmission of energy over distances ranging from a few miles to hundreds of miles, the maximum transmission voltage levels have increased from approximately 35 kV in 1900 to a nominal 765 kV in 1980. With this advent in transmission line voltage levels, EMI assumed a great influence, both in design and choice of the right of way (ROW) of transmission lines. The prospect in the near future of the UHV (ultra high voltage) transmission lines further emphasizes the importance of this EMI parameter. In fact, transmission line designs are EMI-limited and not capacity-limited at these higher voltage levels.

Radio noise from transmission lines has been a concern of the electric utility industry for many years. Thus, one of the objectives of transmission line designers is to find methods to effectively reduce the EMI. Research in this area over the last 40 years has enabled the

different physical mechanisms that cause and produce the EMI to be analyzed and better understood. Furthermore, analysis and quantitative predetermination of the EMI as a function of the main parameters of transmission lines were developed in the past few years. This work was initially undertaken by G. E. Adams [7-11].

However, the phenomenon connected with the corona effect also is sensitive to a large number of variables that are difficult to measure. The determination of these variables is of a statistical nature [12-14] and may be treated as statistical models [6, 12, 15-17].

B. Problem Formulation

Radio noise interference and corona power losses have been extensively investigated in the field and laboratories [6, 9, 10, 16, 17, 18-23]. Some theoretical analysis has been used to calculate the radio noise and corona power loss on high voltage transmission lines [7, 8, 19-22]. Many approaches to analyze radio frequency interference were tried. The influence of the various line parameters as well as the influence of the different weather conditions on radio frequency interference and corona power loss also have been analyzed [6, 12-15].

A number of authors have studied the EMI problems on multiconductor systems in terms of symmetrical component, 0-α-β component [8, 9, 20, 21], or modal (eigenvalue) propagation on unbalanced high voltage transmission lines [6, 24, 25]. However, no data have been found to compare the EMI level between transposed and untransposed lines taking into account the frequency dependence of the electrical line parameters.

Furthermore, in all the EMI analysis literature, the interference field evaluations are based on the quasi-static method. It is well-known that the quasi-static method is an approximation method and is not valid for frequencies higher than the AM radio stations, 535 kHz-1605 kHz. Therefore, a method for EMI analysis that would be valid beyond these frequencies is needed. Such a method will extend and validate the study of the EMI spectrum to the FM and television frequencies.

C. Research Objective

The objective of this investigation is to analyze and determine the impact of the transposed and untransposed transmission lines on the EMI level due to line corona. This study will enable the transmission line designers to decide whether or not complete or partial transposition is needed based on radio and television frequency interference.

Furthermore, a radiation method is introduced to extend and validate the study of the EMI to FM and television frequencies. Finally, a general FORTRAN computer algorithm will be developed for simulation of the EMI analysis.

D. Research Outline

The purpose of this work is to summarize the present art of knowledge and to enable one to calculate the effects of transposition and nontransposition of the transmission line on the EMI.

While the first chapter deals with an introduction and formulation of this problem, the second chapter is devoted to a description of the basic mechanisms which are at the origin of the EMI.

Chapters III, IV and V constitute the practical guide in analyzing and determining corona currents and voltages with the similarity transformation or direct modal analysis. They deal, also, in some detail with the frequency dependent parameters of the transmission lines, the definition and determination of the excitation function, and the modeling of the completely transposed line. Corona currents and voltages are calculated under two assumptions, namely, single corona source per phase and uniformly distributed corona over all the phases.

Chapter VI focuses on methods to calculate the EMI, based on the knowledge of the corona currents and voltages. The quasi-static approximation and the radiation method for the untransposed transmission line as well as for the completely transposed transmission line were used.

The last chapter includes results and model comparison based on a developed digital algorithm for three different configurations. The three configurations are the horizontal, the vertical and the triangular (delta) configurations.

II. GENERAL PROPERTIES OF CORONA

A. Introduction

The term 'discharge' is usually used to describe the flow of current through a gaseous medium. The requirements for such a passage of current are that some of the gas particles should be ionized, by whatever means are available. There should exist an electric field to drive the produced charged particles to form a current. The behavior of a gas discharge is in general influenced by the properties of the electrical circuit of which it forms a part. These discharges may be steady state process or transients of very short duration [26].

Gas discharges in the steady state may conveniently be classified in three types according to the magnitude of the current which they carry. They are:

(1) The Townsend or dark avalanche, $I \leq 10^{-6}$ A.

(2) The glow discharge, $10^{-6} < I \leq 10^{-1}$ A.

(3) The arc discharge, $I > 10^{-1}$ A.

However, transient discharges can occur over a wide range of current and pressure. Their initiation is usually accomplished through breakdown; the discharge will last for a time which depends on the source of energy or on the onset of instability. If the duration of a transient discharge is long enough, it has many attributes of the steady state. Transient discharges are not easy to classify. In many cases, the breakdown itself is the principal feature of interest.

A.C. discharges at low frequencies may be classified much as the

D.C. cases; but increasing frequency changes the behavior radically and distributions become less clear [26].

Corona is either a pulsating discharge or a pulseless glow. While the former is the source of the electromagnetic interference, the latter is noiseless. Both forms of discharges are accompanied by power losses.

As pulsating corona discharges are the major sources of the EMI on high voltage transmission lines, many experimental investigations have been made to study corona current pulse and EMI characteristics of various conductor arrangements [13]. Further, the transition from pulsating to steady state glow corona has been experimentally studied [27]. An excellent up-to-date review of the subject may be found in Loeb's book [28].

The phenomenon is of particular importance in high voltage (transmission systems) where nonuniform fields are unavoidable especially on a conductor surface, an irregularity such as a contamination which can become the point source of a discharge.

Corona phenomenon is responsible for a considerable power loss from H.V. transmission lines. It often leads to deterioration of insulating materials by the combined action of the discharge ions bombarding the surface and the action of chemical compounds that are formed by the discharge [29, 30]. Corona can also be the source of harmonics, conductor vibrations [29], audible noise, ozones and other products. Besides, a broad spectrum of electromagnetic radiation develops and often creates severe interference with broadcast and communication channels.

B. Townsend Avalanche

There is always a certain number of ion-electron pairs in the air created from sources such as cosmic radiation and natural radioactivity. In the presence of a strong electric field, these free electrons and positive ions will be accelerated in opposite directions. If this field is intense enough, the energy which they acquire becomes sufficient to cause the ionization of neutral molecules by collision. One electron can multiply and cause an avalanche. Other processes, including photoionization and attachment, become very important. The positive ions and photons bombard the cathode (conductor surface) and release new electrons. This liberation of electrons from the cathode represents a secondary emission process, while the normal ionization by collision in the gas represents a primary process.

Taking into account the above-mentioned processes and the effect of attachment, the total current can be shown to be given by [26, 31]:

$$I = \frac{I_0 \, \alpha e^{(\alpha-\beta)d} - \beta}{(\alpha-\beta) - \alpha\gamma(e^{-(\alpha-\beta)d} - 1)} \qquad (2.1)$$

where:

I_0 is the electron current at the cathode and is dependent only on the photoelectric effect of external radiation.

α is the Townsend's first ionization coefficient.

γ is the Townsend's second ionization coefficient.

β is the attachment coefficient or loss of electrons by attachment.

d is the distance between electrodes.

This equation shows that the Townsend current, I, becomes theoretically infinite if:

$$(\alpha - \beta) - \alpha\gamma(e^{-(\alpha-\beta)d} - 1) = 0 \qquad (2.2)$$

which reduces to the Townsend criterion for $\beta = 0$ to:

$$1 - \gamma(e^{-\alpha d} - 1) = 0 \quad .$$

In applying the Townsend discharge to nonuniform field, the product $(\alpha-\beta)d$ must be replaced by an integral form:

$$\int_0^d (\alpha - \beta)\, dx \quad . \qquad (2.3)$$

Therefore, the avalanche can only progress in regions where α exceeds β. That is, where the electric field is greater than a critical value E_{min}. Practically E_{min}, for the air, approaches 30 kV/cm at the standard temperature and pressure.

It is worthwhile to point out that Townsend discharge is characterized by its very small current; it is invisible because the density of excited atoms which emit visible light is correspondingly small. It is not a self-sustaining discharge in that it does not entirely provide its own ionization but requires external agencies to produce electrons either in the gas itself or from a negative electrode. These agencies may be ultraviolet light, x-rays, cosmic rays or an electric field. The gas itself is not truly broken down.

C. The Discharge Process

Before an avalanche can develop into a discharge with significant generating properties, it must reach a critical value. Above the critical field intensity for a given environmental condition, the Townsend discharge is increased. As the avalanche growth attains a very high amplification, the space charge developed by this latter, under certain conditions, transforms the avalanche into a plasma streamer [32]. The condition for which this phenomenon takes place is roughly when the avalanche space charge field equals the applied field and the photoelectrons directed to the avalanche stem help in generating the plasma discharge [33]. The conductivity in the avalanche stem then grows rapidly and breakdown occurs in the channel of the avalanche. The current will at this state increase sharply by several orders of magnitude. Once breakdown has occurred, the discharge becomes self-sustained and takes the form of a glow or an arc discharge, depending on the gas and circuit conditions. In either case, the gas becomes luminous.

On high voltage wires at high pressure, there is a distinct difference in the visual appearance of corona under the two polarities. Under positive voltage, corona appears in the form of a uniform bluish-white sheath over the entire surface of the wire [30]. However, on negative wires, the corona appears as reddish glowing spots distributed along the wire. The number of spots increases with the current.

Stroposcopic studies show that A.C. corona has the same appearance as D.C. corona.

Detailed studies of streamer formation and propagation criteria

have been extensively carried out by Essam Nasser [34] and many other authors.

D. Modes of Corona Discharges in Air

The transient and repetitive nature of the discharges, both positive and negative, are caused by space charge formation, blocking of the avalanche and space charge decay. This is usually called a relaxation process [30].

The modes of positive corona possible under D.C. and A.C. conditions are (1) onset pulses or preonset streamer, (2) positive pulseless glow or Hermstein glow, and (3) positive streamers or prebreakdown. Occasionally, burst pulses appear as frustrated discharges creeping on the conductor surface at the corona threshold voltage.

The negative corona modes are (1) Trichel pulses, (2) pulseless glow, and (3) prebreakdown streamers.

The positive and negative prebreakdown streamers occur at voltages considerably larger than the corona inception levels and therefore would not normally take place in fair weather on transmission lines of rational design.

The onset pulses and the Trichel pulses are thus the main types of corona producing and generating interference fields on transmission lines in their normal operating voltage levels.

In any event, breakdown will start with Trichel pulses on the negative half cycle, and burst pulses and pre-onset on the positive half.

1. Negative corona pulses: Trichel pulses

The first systematic study of negative corona was made by Trichel [35]. Trichel's explanation of the regular pulsed negative corona was as follows. After a number of generations of electrons, by the primary and secondary Townsend process or avalanche, a dense cloud of positive ions is formed near the cathode with the electrons moving away into the air where they form negative ions by attachment. This slowly-moving negative ion space charge region will grow more rapidly than the positive ions space charge. This phenomenon is based on the fact that the negative ions rapidly accumulate in the weak field region and cause a reduction in the field, while the positive ions which are near the cathode are withdrawn from the field by neutralization in the cathode. As the field near the cathode returns to normal, the ionization process commences again and the field is distorted. This creation and elimination of the ionized regions cause short bursts of current to flow. These pulses have been named after their discoverer as Trichel pulses. The Trichel pulse is intermittent and is choked off by the space charge developed [28, 36]. These discharges propagate radially into space [36]. The pulses themselves appear to be approximately the same shape. Their repetition rate increases with the applied field to a critical frequency, depending on the electrode geometry [36]. These sharp pulses will contain a broad spectrum of electromagnetic energy, but will be particularly strong at the frequency represented by the pulse separation. Due to the radial propagation of these pulses, the radiation method would probably be a more suitable method to analyze the electromagnetic

interference field.

With further increase of the applied field, the Trichel pulses change into the mode of corona pulseless glow [22].

Some experiments have reported that the negative pulses are steeper and shorter than the positive ones. They follow the form [37, 38, 39]:

$$i(t) = K_1 i_p t^{-(3/2)} e^{-(K_2/t + K_3 T)} \quad . \qquad (2.4)$$

The parameters K_1, K_2, and K_3 are functions of configuration and voltage level.

2. Positive corona pulses

The literature on the subject of positive point corona is very extensive and has been recently reviewed by Loeb [28].

Positive onset pulses and prebreakdown streamers operate by high, very localized space charges developed from large electron avalanche and photoelectric ionization in the gas. Near threshold, onset streamers are quenched by their own space charge or by the formation of a Hermestein sheath glow corona. The space charge choking makes them intermittent [28, 38].

Hermestein's findings showed that the negative ions play an important role in the sequence of preonset streamers, corona bursts, prebreakdown streamers and the filamentary spark.

The steps of formation of an onset pulse would be as illustrated in Fig. 2.1 [39]. The paths shown in Fig. 2.1 are close to what occurs

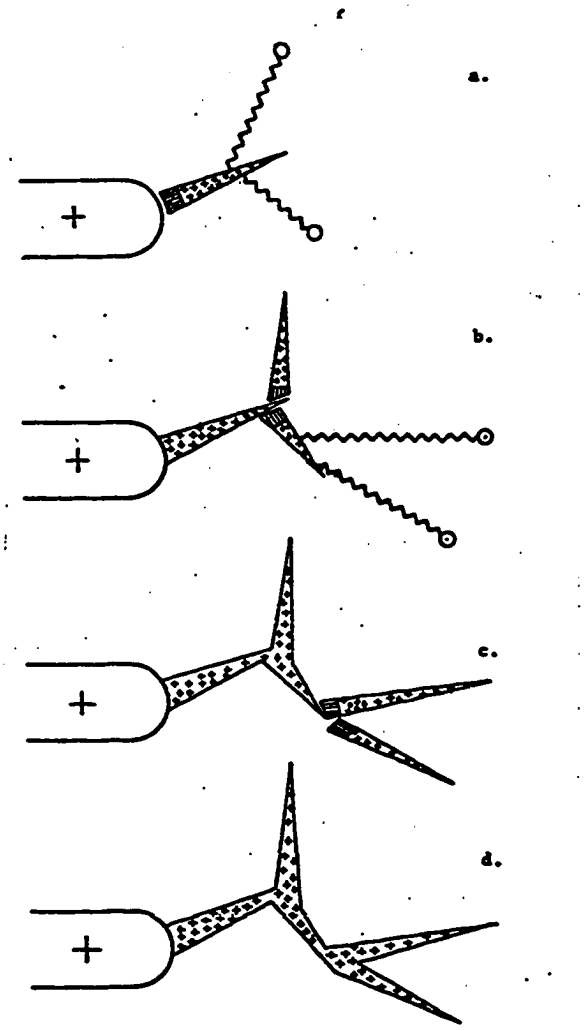

Fig. 2.1. Discharge mechanism schematic and idealized in four steps of few nanosecond intervals [39]

in practice but are of random orientation and are not at all easy to predict. There are successive generations of avalanches [34]. Any generation of avalanches produces photons which trigger the subsequent generation. The avalanches of the subsequent generation proceed to the anode partly, through the channels of the preceding generation [34]. This concept of successive generations of avalanches has been established by Raether [32] in both uniform and nonuniform fields and by Nasser in nonuniform fields [30]. This phenomenon is valid for corona streamers. However, with prebreakdown streamers, the first generation may produce plasma or lead by itself to complete breakdown of the air gap. These cases are beyond the scope of this work.

The shape of the positive pulse is a double exponential form:

$$i(t) = K_4 \, i_p (e^{-K_5 t} - e^{-K_6 t}) \quad . \tag{2.5}$$

The parameters K_4, K_5, and K_6 are functions of the line arrangement, voltage level and the atmospheric conditions. The repetition rate of these pulses is variable. It has been found that this repetition rate has a considerable sensitivity to atmospheric variations, especially humidity [38].

It should be pointed out that the onset streamers may be followed by a burst of pulses [29, 38].

E. Impulse Spectrum

These impulses may be represented by a Fourier frequency spectrum. The spectral density, $S(\omega)$, is related to the corona pulse current

i(t) by the expression:

$$S(\omega) = \int_0^\infty i(t)\ e^{-j\omega t}\ dt \qquad (2.6)$$

where $\omega = 2\pi F$ is the angular frequency.

For the negative corona pulses, the spectral density is given by:

$$S(\omega) = K_1\ i_p \int_0^\infty t^{-3/2}\ e^{-(K_2/t + K_3 T)}\ dt \quad . \qquad (2.7)$$

Using the integrals handbook [40], equation 2.7 becomes

$$S(\omega) = K_1\ i_p \left[\frac{2\ K_2}{K_3 + j\omega}\ \kappa_{(-1/2)}\left(2\sqrt{(K_3 + j\omega)\ K_2}\right)\right] \qquad (2.8)$$

for

$$R_e(K_3 + j\omega) > 0 \qquad (2.9)$$

$$R_e(K_2) > 0 \quad . \qquad (2.10)$$

The last two conditions are satisfied for this type of problem. The function $\kappa_{(-1/2)}(x)$ is given by [40] as:

$$\kappa_{(-1/2)}(x) = \sqrt{\frac{\pi}{2x}}\ e^{-x} \quad . \qquad (2.11)$$

However, the positive corona pulses have a simplified spectral density which is given by:

$$S(\omega) = K_4\ i_p \left(\frac{1}{K_5 + j\omega} - \frac{1}{K_6 + j\omega}\right) \quad . \qquad (2.12)$$

It is worthwhile to note both negative and positive corona pulses spectral density are decreasing function with the increase in frequency.

F. Critical Surface Gradient Calculation

Corona is charged ions and their presence will modify the electric field significantly.

High voltage transmission lines are designed so that the gradient is not large enough to produce corona at normal fair weather. However, the presence of irregularities will cause corona discharges which may contain all or some of the mentioned modes. Therefore, the dominant source of corona would then be irregularities.

From the electrostatic theory, the electric field at the surface of any conductor or set of conductors may be easily determined in the absence of corona. That is assuming a zero space charge. Due to the presence of highly variable ions in the corona processes, it is somewhat difficult to calculate the electric field in the presence of corona. However, the field equations are:

$$\overline{E} = -\overline{\nabla}\, V \tag{2.13}$$

$$\nabla \cdot \overline{D} = -q \tag{2.14}$$

$$\overline{D} = \varepsilon_0 \overline{E} \tag{2.15}$$

where:

$\overline{E}$ is electric field intensity in volts per centimeter.

V is the voltage in volts.

$\overline{D}$ is the electric flux density in coulombs per square meter.

q is the electric charge density of corona in coulombs per cubic meter.

ε_0 is the permitivity of vacuum, which is $8.854\ 10^{-12}$ farad per meter.

Since ε_0 is constant, the above equations (2.13 to 2.15) will lead to Poisson's equation:

$$\nabla^2 V = \frac{-q}{\varepsilon_0} \quad . \tag{2.16}$$

In the absence of corona, q = 0 and Poisson's equation reduces to Laplace's equation:

$$\nabla^2 V = 0 \quad . \tag{2.17}$$

The solution of equation 2.17 will only evaluate the onset of corona or the potential gradient at which corona will be initiated in the absence of the irregularities. It should be pointed out that it is very difficult to model the type, shape, etc. of the irregularities that could exist on the transmission lines. These influences are difficult to quantify and are usually taken into account by the introduction of an average coefficient for the surface state, m, usually deduced from experimental tests. A typical value of m, caused by stranding alone, is 0.9. However, rain may reduce the value of m to 0.6 or even lower. Atmospheric conditions likewise play an important role. Drops of water may be formed on the surface of the conductor. These drops are caused by rainy weather, fog, dew and snow. Their effect is to intensify the electric field and therefore generate more corona discharge. The onset voltage will then be reduced. To determine the onset gradient E_c of a cylindrical conductor, Peek's well-known formula has

been used:

$$E_c = 30\ m\ \delta\left(1 + \frac{0.426}{\sqrt{\delta d}}\right) \quad (kV/cm) \quad . \tag{2.18}$$

For A.C. voltages, E_c is the peak value of the field intensity, d is the diameter of the conductor in centimeters, δ is the relative density of air and is expressed by

$$\delta = \frac{3.92\ p}{273 + t} \tag{2.19}$$

where:

p is the atmospheric pressure.

t is the temperature in degrees Celsius.

The solution of equation 2.16 leads to the onset voltage.

$$V_1 = \frac{q}{2\pi\epsilon_0} \ln \frac{4h}{d} \tag{2.20}$$

for

$$h >> d \quad . \tag{2.21}$$

Fig. 2.2 illustrates the present configuration. However, the field strength at the surface of the conductor is given by

$$E = \frac{q}{\pi\epsilon d} \quad . \tag{2.22}$$

Substituting equation 2.22 into the voltage V_1 equation, equation 2.20 becomes

$$V_1 = E\,\frac{d}{2} \ln \frac{4h}{d} \quad . \tag{2.23}$$

When in equation 2.23 the electric field intensity E at the conductor reaches the critical onset gradient E_c for visual corona, the voltage V_1 will reach the critical value V_c.

$$V_c = 30\ m\ \delta\left(\frac{d}{2}\right)\left(1 + \frac{0.426}{\sqrt{\delta d}}\right)\ln\frac{4h}{d} \quad . \tag{2.24}$$

This equation can be generalized to include all three phases in a transmission system by the introduction of matrix notation.

If a solid conductor is replaced by a multiple conductor set, consisting of N subconductors each of diameter d arranged on the circumference of a circle, with an equivalent cross-section of the set or bundle of subconductors equal to that of the single conductor (that is the latter has a diameter $d\sqrt{N}$), then the visual critical corona voltage V_c would be increased mainly for two reasons:

(1) For the same voltage, the maximum surface electric field would be less.

(2) The surface field has to reach a greater value for corona to be visible for a small conductor than for a large one, so that the system voltage can be raised when bundle conductors are used.

A. E. Guile and W. Paterson [41] illustrated the order of magnitude of these factors by a simple example. They found that the maximum stress for Fig. 2.3 is

$$E_{a2} = \frac{Q}{2\pi\varepsilon}\left[\frac{1}{r} + \frac{1}{r+s} + \frac{1}{2(D-s-r)} + \frac{1}{2(D-r)} + \frac{1}{2(2D-s-r)} + \frac{1}{2(2D-r)}\right] \tag{2.25}$$

They also compared this maximum stress to the maximum stress of the

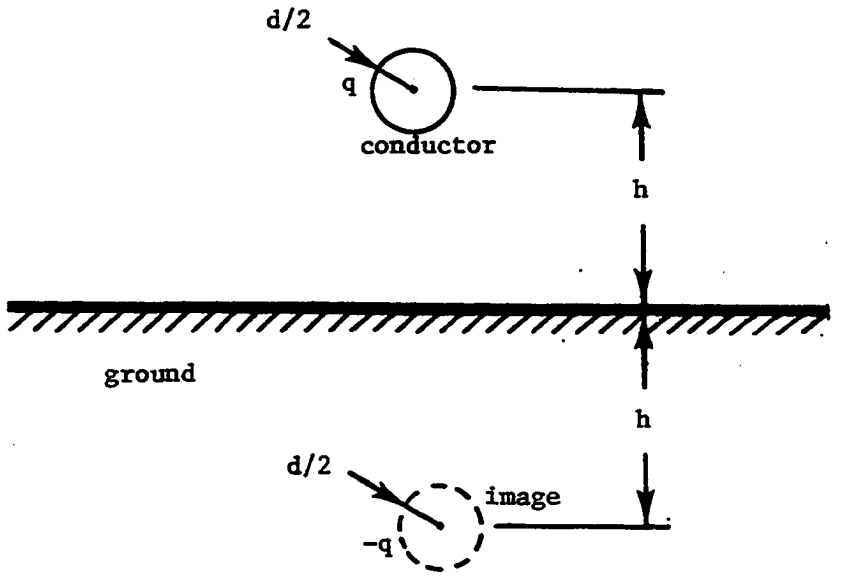

Fig. 2.2. Single conductor above ground

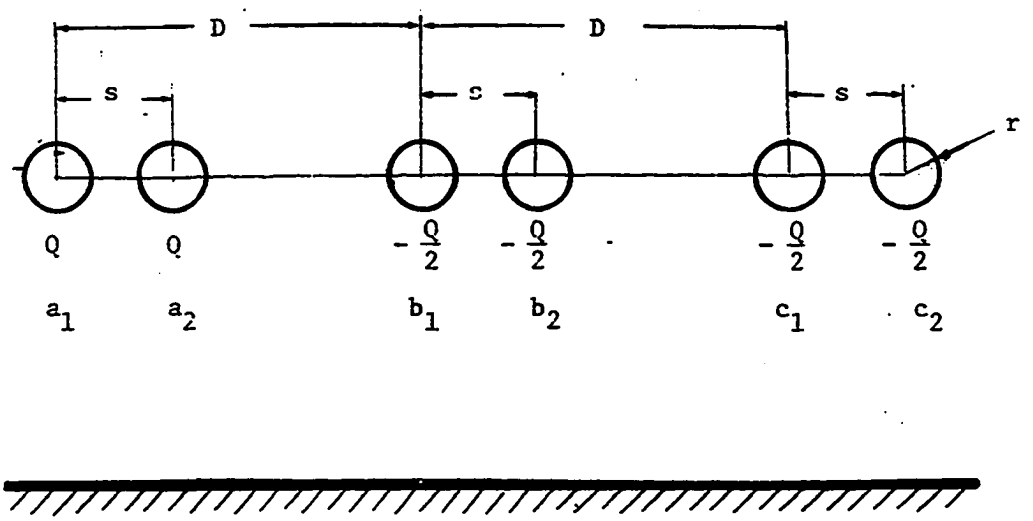

Fig. 2.3. Single-circuit line with two conductors/phase in one horizontal plane

alternative single-conductor per phase system of Fig. 2.4. The electric field intensity for the latter configuration is:

$$E_a = \frac{Q_a}{2\pi\varepsilon}\left[\frac{1}{r\sqrt{2}} + \frac{1}{2(D - r\sqrt{2})} + \frac{1}{2(2D - r\sqrt{2})}\right] \quad . \tag{2.26}$$

Equations 2.25 and 2.26 were derived under the following reasonable assumptions:

(1) The charge distribution depends upon balanced capacitances to earth. Thus, the charges are of equal amplitudes and in phase with respect to earth.

(2) Earth effect and ground wires are neglected.

(3) The conductors of one phase all have the same total charge on them at any instant, and these charges are distributed uniformly over the surface.

They plotted the maximum stress E_{a2} and E_a in units of $\frac{V_{ab}}{r}$ as a function of the ratio S/r. This is shown in Fig. 2.5 for D/r = 700 and shows that there is a range of values of S/r where a reduction in maximum stress is up to 11% for this specific example. It was also shown that the second factor mentioned in (2) raises the stress for visual critical corona E_c by a factor η given by

$$\eta \simeq \frac{1 + 0.426\, d^{-1/2}}{1 + 0.426\, (\sqrt{N}\, d)^{-1/2}} \tag{2.27}$$

where a single conductor is replaced by one with N conductors per phase. The increase in E_c for N = 2 and N = 4 is approximately 4 and 13%, respectively.

Therefore, it is possible to obtain an increase in the corona

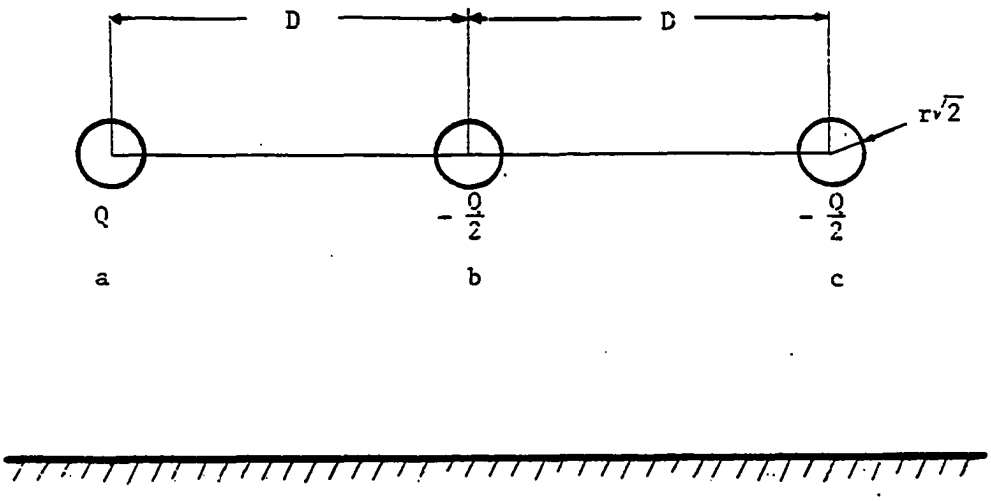

Fig. 2.4. Single-circuit line with one conductor/phase in one horizontal plane

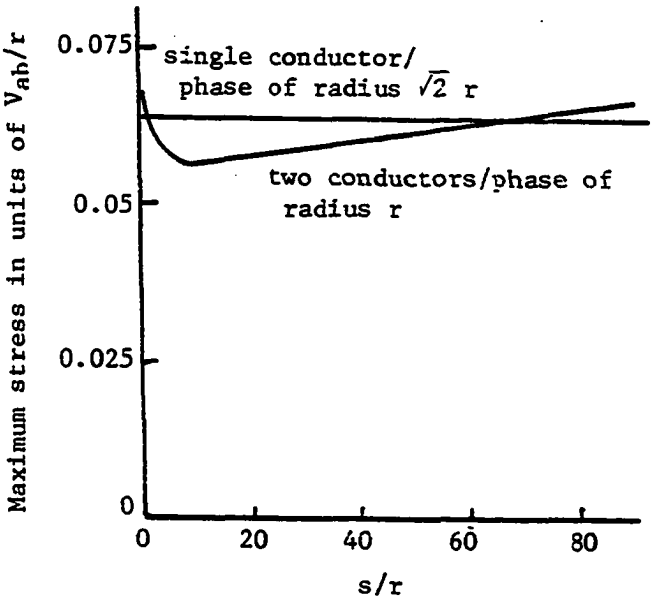

Fig. 2.5. Variation of maximum electric stress with ratio s/r for D/r = 700 [41]

voltage by replacing a single conductor system by a bundle conductor system with the same total cross-section. That is, to use a higher voltage level, or for a given system system voltage to reduce the radio interference and corona losses.

There is an additional advantage which is related to the increase of the natural load because of the decrease of the inductance and the increase of the capacitance by using bundle conductors, as will be explained in Chapter III.

III. ELECTRICAL LINE PARAMETERS CALCULATION

A. Introduction

Most high voltage transmission lines are operated above ground with the conductors suspended from large towers by insulator strings. The conductors are spaced far enough apart to prevent mechanical disturbance due to vibrations of the conductors and the generation of excessive corona discharges due to high intensity electric fields. These lines may be spaced horizontally or vertically either in a planar or staggered geometrical configuration. In some cases, two or more three phase circuits may be mounted on the same towers. Shielding wires are generally mounted above the power lines to provide a grounding path for lightning discharges or strokes independent of the power circuits themselves.

Any transmission line is characterized, electrically, by four distributed line parameters, namely, the resistance R, the inductance L, the conductance G and the capacitance C per unit length. The conductance G and the capacitance C are assumed constant, whereas the resistance R and the inductance L are functions of the frequency. These parameters are truly distributed parameters over tens or hundreds of kilometers. Usually the conductance G has a very small value and can be neglected.

B. Calculation of the Capacitances

The capacitances of any polyphase transmission line with or without ground wires can be calculated from the following equation:

$$[V_p] = [P_p][Q_p] \tag{3.1}$$

where:

$[V_p]$ is the phase voltage matrix in volts.

$[Q_p]$ is the charge matrix in coulombs per unit length.

$[P_p]$ is the potential coefficient matrix in $(\text{Farad})^{-1}$ unit length whose elements are given by:

$$P_{ii} = (\alpha/2) \ln (2H_{ii}/D_{ii}) \tag{3.2}$$

$$P_{ij} = (\alpha/2) \ln (H_{ij}/D_{ij}) \tag{3.3}$$

where:

α is equal to $36\ 10^9\ (\text{F/m})^{-1}$;

H_{ij} is the distance between conductor i and the image of conductor j;

D_{ij} is the distance between conductor i and conductor j; and

D_{ii} is the diameter of conductor i.

For clarification purposes, let "p" be the subscript for phase quantities and let "e" be the subscript for the earth or ground wires. Equation 3.1 would become:

$$\begin{bmatrix} V_p \\ V_e \end{bmatrix} = \begin{bmatrix} P_p & P_{pe} \\ P_{ep} & P_e \end{bmatrix} \begin{bmatrix} Q_p \\ Q_e \end{bmatrix} \tag{3.4}$$

Since $V_e = 0$, equation 3.4 can be Kron-reduced to equation 3.8 as follows:

$$[V_p] = [P_p][Q_p] + [P_{pe}][Q_e] \tag{3.5}$$

$$0 = [P_{ep}][Q_p] + [P_e][Q_e] \tag{3.6}$$

From equation 3.6, we can determine

$$[Q_e] = -[P_e]^{-1}[P_{ep}][Q_p] \quad . \tag{3.7}$$

Substituting equation 3.7 into 3.5, we get

$$[V_p] = [P_p - P_{pe}P_{ep}^{-1}][Q_p] \tag{3.8}$$

which is of the form of equation 3.1.

By finding the elements of $[\hat{P}_p] = [P_p - P_{pe}P_e^{-1}P_{ep}]$, then the capacitance matrix can be obtained from:

$$[C_p] = [\hat{P}_p]^{-1} \quad . \tag{3.9}$$

C. Skin Effect and Internal Impedance Calculation

Fields that change rapidly in time do not penetrate very far into good conductors. They are screened out by currents that flow at or near the surface [42]. In transmission line circuits, the current density may be nonuniform in the conductors. The tendency of alternating current to flow with greater density near the outside of conductors is called 'skin effect'. Because of the skin effect, the metal making up the conductors is not fully utilized in the current carrying processes. The change of the internal impedance from its value at D.C. is also attributed to 'skin effect' [43]. The magnitude of the components of the internal impedance is a function of frequency, size of the conductors and the conductivity. The results of skin effect are (1) reduction of the effective cross section of a conductor which increases the A.C. resistance per unit length, and (2) reduction of the internal flux

linkages within the conductor which reduces its internal impedance. These two components compose the internal impedance of a conductor.

The internal impedance can be evaluated quantitatively by the use of Maxwell's equation. A brief presentation will be given here. The usual 'skin effect' studied in the literature is developed for single frequency, steady state conditions subject to appropriate boundary conditions.

$$\nabla \times H = j\omega\epsilon E + J \tag{3.10}$$

$$\nabla \times E = -j\omega\mu H \quad . \tag{3.11}$$

Taking the curl of equation 3.11 and using equation 3.10, we get:

$$\nabla \times \nabla \times E = -j\omega\mu\ (j\omega\epsilon + \sigma)E \tag{3.12}$$

where:

$$J = \sigma E \quad . \tag{3.13}$$

The current of great interest to us at this stage is the current density J. With a constant conductivity σ, we can replace equation 3.12 by 3.14:

$$\nabla \times \nabla \times J = -j\omega\mu(j\omega\epsilon + \sigma)J \tag{3.14}$$

or equivalently

$$-\nabla^2 J + \nabla(\nabla_0 J) = -j\omega\mu(j\omega\epsilon + \sigma)J \quad . \tag{3.15}$$

A good conductor is characterized by (1) free charge term $\rho = 0$,

(2) conduction density current proportional to the electric field intensity, $J = \sigma E$ and (3) displacement current is usually zero. For constant σ and $\rho = 0$, we have

$$\nabla_0 J = \nabla_0 \sigma E = 0 \quad . \tag{3.16}$$

Therefore, equation 3.15 becomes:

$$\nabla^2 J = j\omega\sigma\mu J \quad . \tag{3.17}$$

The current displacement, $j\omega\varepsilon J$, was neglected in equation 3.17. This assumption is valid as long as ω is of the order of 10^{14} since σ is of the order of 10^{7} while ε is of the order of 10^{-11}.

The solution of equation 3.17 leads to a current density in terms of the first kind, zero order Bessel function of a complex argument.

$$J(r) = AJ_0(kr) \tag{3.18}$$

where:

$J_0(x)$ is the first kind, zero order Bessel function.

A is constant of integration.

$$k = \sqrt{-j\omega\mu\sigma} \quad . \tag{3.19}$$

By definition, the internal impedance is:

$$Z_i = R + j\omega L_i = \frac{E_z}{I_z} = \frac{J_z(d/2)}{\sigma I_z} \tag{3.20}$$

where:

$$I_z = \int_0^{2\pi}\int_0^{kd/2} J_z(r)\ r\ dr\ d\phi \tag{3.21}$$

$$I_z = 2\pi A\, k \frac{d}{4} J_1(kd/2) \quad . \tag{3.22}$$

$J_1(x)$ is the first kind, first order Bessel function. The insertion of equation 3.18 evaluated at r = d/2, since the source will be applied or connected to the outside of the wire, gives the final result of the internal impedance of a cylindrical conductor:

$$Z_i = R_{dc} \frac{kd}{4} \frac{J_0(kd/2)}{J_1(kd/2)} \tag{3.23}$$

where:

R_{dc} is the D.C. resistance in ohms per unit length and is given by equation 3.24.

$$R_{dc} = \frac{4}{\sigma\pi d^2} \tag{3.24}$$

$$J_0(x) = \sum_{m=0}^{\infty} \frac{(-1)^m}{(m!)^2} \left(\frac{x}{2}\right)^{2m} \tag{3.25}$$

$$J_1(x) = \frac{x}{2}\left[\sum_{m=0}^{\infty} \frac{(-1)^m}{(m+1)!} \left(\frac{x}{2}\right)^{2m}\right] \quad . \tag{3.26}$$

The real part of Z_i is the A.C. resistance and its imaginary part corresponds to the internal reactance of the solid cylindrical conductor. A very good approximation can be used at frequencies higher than 6 MHz. The approximation is within 5% when $(\omega\mu\sigma)^{1/2} \frac{d}{2} > 7$ which corresponds to the practical conductors used in power systems to frequencies higher than 6 MHz. For high frequencies, the internal impedance is given by:

$$Z_i = \left(\frac{\omega\mu}{2\sigma}\right)^{1/2} \frac{1}{\pi d} (1+j) \quad . \tag{3.27}$$

That is the A.C. resistance and internal reactance are equal in

magnitude at high frequencies.

A subroutine algorithm called 'SKIN' is developed to evaluate the A.C. resistance and the internal reactance at any frequency.

D. Calculation of the Self and Mutual Inductances

The impedance matrix can be obtained from Carson's equations, published in 1926. From these equations, various factors influencing these impedances can be evaluated. Carson's equations are based on an earth of uniform conductivity, semi-infinite in extent, terminated by a plane parallel to the conductors. It is also assumed a common ground return for the calculation of the mutual impedances between any two conductors.

Later on, in 1933, Wagner and Evans [44] discussed this problem and offered a physical interpretation of Carson's original work. In 1948, Clarke [45] gave a good and simpler analytical representation of the impedances. Lately in the modern literature [6, 41, 46], Anderson presented a much simpler expression of the series impedance of the transmission line with ground return wire neglecting skin effect. These equations are:

$$Z_{ii} = (R_i + R_d) + j\omega k \ln \frac{D_e}{D_{si}} \tag{3.28}$$

$$Z_{ij} = R_d + j\omega k \ln \frac{D_e}{D_{si}} \tag{3.29}$$

where:

Z_{ii} is the self impedance of conductor i in ohms per unit length and is the diagonal term of the impedance matrix.

Z_{ij} is the mutual impedance between conductor i and conductor j in ohms per unit length and is the off-diagonal term of the impedance matrix.

R_i series line resistance of conductor i in ohms per unit length.

D_{si} is the self geometric mean radius of conductor i and for cylindrical conductor

$$D_{si} = 0.779\ (d/2) \quad . \tag{3.30}$$

D_{ij} is the distance between conductor i and conductor j.

k is a constant which depends on the user's units and its values are given in reference [46].

R_d is the earth resistance in ohms per unit length and is given by:

$$R_d = 9.869\ 10^{-4}\ f\ (\Omega/km) \quad . \tag{3.31}$$

D_e is a function derived in reference [46] based on Wagner and Evan's work. It characterizes the ground return and is equal to

$$D_e = 2160 \sqrt{\frac{\rho}{f}}\ \text{(feet)} \quad . \tag{3.32}$$

f is the frequency in Hz.

ρ is the earth resistivity in ohm unit length.

The equations 3.28 and 3.29 do not account for the skin effect. It was shown that skin effect is a function of frequency. Since we are dealing with very high frequencies to study the EMI, skin effect will be included as follows:

$$Z_{ii} = (R_i + R_d) + j(X_{ii} + X_i) \tag{3.33}$$

$$Z_{ij} = R_d + j\, X_{ij} \tag{3.34}$$

where:

R_i and R_d are defined previously.

X_{ii} is the self reactance of the conductor i in ohms per unit length and is given by:

$$X_{ii} = \omega k \ln \frac{D_e}{D_{si}} \tag{3.35}$$

X_i is the internal reactance of the conductor i in ohms per unit length to account for skin effect and is given by:

$$X_i = \mathrm{Im}(Z_i) \quad . \tag{3.36}$$

X_{ij} is the mutual reactance between conductor i and conductor j in ohms per unit length and is given by:

$$X_{ij} = \omega k \ln \frac{D_e}{D_{ij}} \quad . \tag{3.37}$$

The total self and mutual inductances are respectively defined by

$$L_{ii} = (X_{ii} + X_i)/\omega \tag{3.38}$$

$$L_{ij} = X_{ij}/\omega \quad . \tag{3.39}$$

The effect of ground wires on the impedance matrix can be incorporated in a similar way as previously discussed in the calculation of the potential coefficient matrix. For instance, let "p" be the subscript

for phase quantities and let "g" be the subscript for the ground wires; the new impedance matrix, $\hat{Z}_p$, after Kron-reduction is then given by:

$$[\hat{Z}_p] = [Z_p - Z_{pg} Z_g^{-1} Z_{gq}] \quad . \tag{3.40}$$

E. Summary

The electrical transmission line parameters have been qualitatively determined. The frequency dependence of the resistances as well as the inductances of the transmission line have been taken into consideration through the skin effect calculation.

A computer subroutine called 'PARM' has been developed to calculate the series impedances as well as the shunt admittances of the transmission line. The 'PARM' subroutine calls the 'SKIN' subroutine to include the frequency dependence of the transmission line parameters.

Based on the availability of the electrical line parameters information, the excitation function and consequently the corona currents and voltages will be determined in the forthcoming chapters.

IV. CORONA EXCITATION FUNCTION DETERMINATION

A. Introduction

The EMI of high voltage transmission line depends on a number of parameters. Some are related to geometrical characteristics such as (1) the dimensions of the line, (2) its position in the space, and (3) the electric gradient at the surface of the conductors. These parameters can be accurately determined. They also can be used for analytical or empirical evaluation of the EMI. On the other hand, some parameters such as the surface state of the conductors, climatic conditions, environmental pollution are of statistical aspects and they are far harder to estimate and even practically impossible to measure for the case of the state of the surface of conductors [47, 48].

However, under heavy rain, a large number of experiments illustrate the stability and the reproducibility of the interference level [6, 21, 22]. Some empirical laws, based on the results of cage and line tests on a large variety of bundle configuration, allow the prediction of the generation function [6, 21, 22, 49].

The link between the single phase to the three phase corona performance can be performed through the generation function defined initially by Adams [7, 8]. However, a simpler and perhaps a more intuitive approach is based on the work of Gary [50].

After summarizing the present state of knowledge of corona modeling, corona excitation function Γ will be defined and evaluated as a function of conductor diameter, number of subconductors per bundle, frequency. The excitation function determination will be based on the two latest

empirical methods found in the literature.

B. Gary's Model [50]

The properties of the excitation function and the reason behind its use to determine the EMI level of a conductor or a bundle have been well-developed and outlined, initially in the Adams work in 1956 and then in a more intuitive and simpler approach by Gary in 1970.

The mathematical analysis of the mechanisms involved during the formation of a streamer shows that the current injected by this streamer into the conductor depends on the capacitance of the system [21, 50]. Therefore, the same streamer does not generate the same current when the conductor is placed in a cage as when it is placed on the line. However, Gary shows that this excitation function is, indeed, independent of the capacitance of the system. But it does depend only on the physical characteristics of the corona source.

In the development of this model, it was assumed that the corona discharge process is approximated by a planar streamer comprising a line charge, q_0, which moves in one radial direction, ρ.

If i(t) represents the current injected per unit length of the conductor under the effect of streamers, $\gamma(t)$, the generation function and C the capacitance of the system configuration, the preceding properties are expressed by:

$$i(t) = \frac{C}{2\pi\varepsilon_0}\,\gamma(t) \tag{4.1}$$

where

$$\gamma(t) \cong \frac{q_0}{\rho}\,\frac{d\rho}{dt} \quad . \tag{4.2}$$

q_0 is the space charge in Coulombs per unit length.

$\frac{d\rho}{dt}$ is the velocity of the space charge.

ρ is the position of this charge relative to the conductor.

This impulsive form of the generation function is due to the internal characteristics of the electrical field within the zone of the ionized air in the neighborhood of the conductor. Due to the repeated pseudo periodicity and randomness, however, of these impulses, the Fourier spectrum of a single impulse can be replaced by its spectral density $G(\omega)$. Without going into the details of stationary random signals, it is understood that the spectral density defines an energy. According to the Parseval's theorem, the RMS value of the pseudo-periodic signal, $g(\omega)$, contained within an infinitely small frequency interval $d\omega$ is related to the spectral density $G(\omega)$ by:

$$dg^2(\omega) = G^2(\omega)\ d\omega \tag{4.3}$$

or, consequently, if the original signal passes through a measuring device tuned to the frequency ω_0 and with a quadratic equivalent bandwidth of B Hz, the RMS value of the measured signal is

$$g(\omega_0) = G(\omega_0)\ \sqrt{B} \quad . \tag{4.4}$$

For the uniformly distributed corona case and under the assumption of uncorrelated and random process, the resultant RMS value is

$$\Gamma = \sqrt{B}\ \sqrt{\sum_{i=1}^{\infty} G_i^2(\omega)} \quad . \tag{4.5}$$

This quantity is termed, by Adams, the spectral density excitation

function or just the excitation function as defined by Gary.

The RMS value of the injected HF corona current, measured at frequency ω_0 and with B Hz bandwidth, per unit length of the conductor is given by:

$$I = \frac{C}{2\pi\varepsilon_0} \Gamma. \tag{4.6}$$

Gary's work was extended to multiphase transmission lines with single or bundle conductors. The equation proves to be still valid but in generalized matrix form.

$$[I] = \frac{1}{2\pi\varepsilon_0} [C][\Gamma] \quad . \tag{4.7}$$

It is, therefore, the excitation function which must be considered as the really specific measure of the cause of interference. Γ is expressed in μA per $m^{-1/2}$. The corresponding logarithmic expression is generally preferred:

$$\Gamma \text{ (dB)} = 10 \log_{10} (\Gamma/1 \ \mu A m^{-1/2}) \quad . \tag{4.8}$$

At this point, it should be noted that the magnitude that can be measured is the current I and not the excitation function Γ. In a general case, Γ represents an intermediary parameter in the calculation of the EMI and has to be derived from experimental measurements of HF corona currents and the capacitance of the system.

The purpose of the next two sections is to provide two ways of determining the excitation function which will form the background for the transmission line corona currents and voltages determination.

C. Gary's and Moreau's Determination of the Excitation Function [21]

1. Heavy rain excitation function

In order to separate the influence of the three main parameters, which are the maximum gradient, the radius and the number of subconductors, Gary and Moreau conducted different experiments and developed the following empirical formula:

$$\Gamma_{HR} = \Gamma_0(g, r) + (11.5 + \log_{10} N^2)r - B(N) \qquad (4.9)$$

where:

Γ_{HR} is the heavy rain excitation function in decibels.

g is the maximum gradients in kilovolts per centimeter.

r is the subconductor radius in centimeters.

$\Gamma_0(g,r)$ is the heavy rain excitation function in decibels for N=1 and is given by Fig. 4.1.

B(N) represents the principal correction due to the number of subconductors and is determined experimentally to be:

Number of subconductor / Correction Factor	N	1	2	3	4	6	8
B(N)	dB	0	5	7	8	9	9.5

All excitation functions were determined for a frequency of 0.5 MHz.

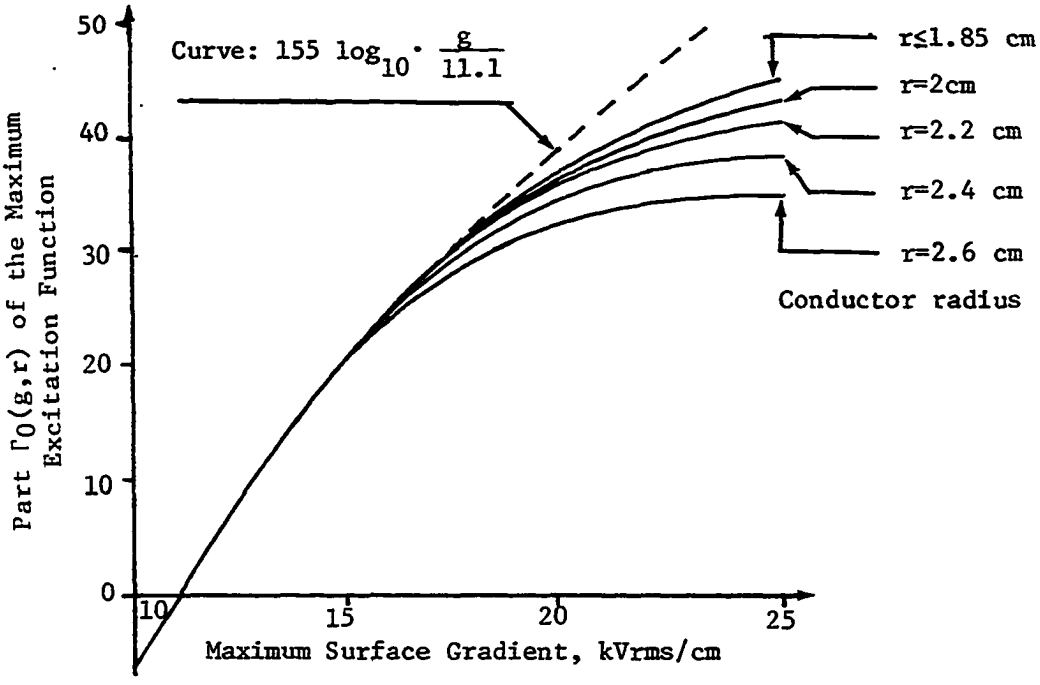

Fig. 4.1. Chart for determination of excitation functions under heavy rain [21]

For other sets of frequencies, some adjustment should be undertaken in the evaluation of Γ_{HR}.

2. Dry weather excitation function

In this climatic condition, it is difficult to evaluate qualitative parameters for calculating the EMI level. This is mainly due to the fluctuations in the seasonal and intrinsic surface state of the conductor. However, by using the analysis of a multitude of histograms [6, 16, 21], statistical studies made it possible to establish rules for making the following simple estimates. Let Γ_{HR} and Γ_{DW} be the maximum level in heavy rain and in dry weather, respectively.

For bad surface state, that is, greasy conductors or very polluted:

$$\Gamma_{DW} = \Gamma_{HR} - 14 \text{ dB} \quad . \tag{4.10}$$

For normal surface state, that is, conductors reasonably clean and aged:

$$\Gamma_{DW} = \Gamma_{HR} - 17\text{dB} \quad . \tag{4.11}$$

For very good surface state, that is, clean conductors nonpolluted region:

$$\Gamma_{DW} = \Gamma_{HR} - 20 \text{ dB} \quad . \tag{4.12}$$

D. EPRI-EHV Book Evaluation of the Excitation Function [6]

1. Heavy rain excitation function

As was previously stated, the most reproducible test data are obtained from heavy rain [21, 23, 49]. Besides, heavy rain EMI data have

a practical significance, since generally EMI levels are highest and interference to broadcast reception is greatest when the rain rate is highest [6]. An empirical law based on tests of a large number and variety of bundle configurations has been developed in [6] as follows:

$$\Gamma_{HR} = 78 - \frac{580}{g} + 38 \log_{10} \frac{d}{3.8} + K(N) \qquad (4.13)$$

where:

Γ_{HR} is the heavy rain excitation function in decibels.

g is the maximum gradient in kilovolts per centimeter.

d is the diameter of the subconductor in centimeters.

K(N) is a correction factor dependent on the number, N, of the subconductors and is given by:

$$K(N) = 7 \text{ dB} \quad \text{For } N\ 1$$

$$K(N) = 2 \text{ dB} \quad \text{For } N=2$$

$$K(N) = 0 \text{ dB} \quad \text{For } N \geq 3 \quad .$$

In the development of this empirical equation (4.13), the influence of bundle diameter was proven to be so small and therefore can be neglected.

2. Foul weather excitation function

Based on some statistical studies, the following empirical formula, for the foul weather excitation function, appears to be adequate.

$$\Gamma_{FW} = \Gamma_{HR} + C_{\omega} \qquad (4.14)$$

where:

Γ_{FW} is the foul weather excitation function in decibels.

Γ_{HR} is the heavy rain excitation function in decibels.

C_ω is a correction factor in decibels given by:

$$C_\omega = \frac{1.055}{0.826 - E_r} \qquad \text{For } 0.9 \leq E_r \leq 1.0 \qquad (4.15)$$

$$C_\omega = \frac{24.625(E_r - 1.231)}{E_r} \qquad \text{For } 1.0 < E_r < 1.2 \qquad (4.16)$$

$$C_\omega = 11.016 \frac{(E_r - 1.287)}{E_r} \qquad \text{For } 1.2 \leq E_r \leq 1.4 \qquad (4.17)$$

E_r is defined to be the ratio of the operating maximum gradient, E, to the '6 dB gradient', E_C.

$$E_r = \frac{E}{E_C} \quad . \qquad (4.18)$$

The so-called '6 dB gradient' is defined to be the gradient for which the wet conductor excitation of a particular conductor configuration is 6 dB below its heavy rain excitation. This '6 dB gradient' can be accounted for by the following empirical relation:

$$E_C = \frac{12.18\ d}{d - 0.843} \qquad \text{For } N \leq 4 \qquad (4.19)$$

$$E_C = \frac{12.18\ d}{d - 0.843} - 0.3(N - 4) \qquad \text{For } N > 4 \qquad (4.20)$$

where

d is the subconductor diameter in centimeters.

N is the number of subconductors per bundle.

3. Fair weather excitation function

Based on the IEEE/CIGRE Survey [48] and the limited data of the EPRI-EHV book [6] tests, an average value of 22 dB difference in excitation between the heavy rain and average fair weather is suggested for design studies, so that:

$$\Gamma_{fW} = \Gamma_{HR} - 22 \text{ dB} \tag{4.21}$$

where:

Γ_{fW} is the fair weather excitation function in decibels.

In all these tests and experiments, the excitation function was evaluated on a 5 kHz bandwidth meter, at quasi peak measurements at 1 MHz.

A subroutine called 'EXFUN' has been developed in this study to calculate the excitation function given the line configuration and the voltage level of the line.

E. Surface Gradient Calculation

As was explained in the previous sections, one of the dominant parameters affecting the EMI level of a transmission line and specifically the magnitude of the excitation function is the electric field at the surface of the conductors.

1. Single wire above ground

For instance, consider a wire suspended at a height h above a perfect ground, Fig. 2.2, and a voltage is applied to it. The wire will acquire a charge Q per unit length. The surface gradient is

calculated from Gauss's theorem using the superposition principle due to the image of the wire. The expression for the surface gradient at the bottom of the wire is given by:

$$E = \alpha \frac{Q}{d} \left[1 + \frac{2d}{4h-d}\right] \tag{4.22}$$

where:

Q is the line charge in coulombs per unit length.

d is the diameter of the conductor in meters.

h is the height from the conductor to ground in meters.

$$\alpha = \frac{1}{\pi \varepsilon_0} \cong 36 \times 10^9 \quad (F/m)^{-1} \quad . \tag{4.23}$$

Equation 4.22 reduces to equation 2.22 if d << h, then

$$E \cong \alpha \frac{Q}{d} \tag{4.24}$$

for single round conductor line, far from ground or other phases. Since

$$Q = CV \tag{4.25}$$

where:

C is the capacitance of the line in Farads per unit length.

V is the phase to ground voltage in volts.

Then, equation 4.24 becomes

$$E = \alpha \frac{CV}{d} \quad . \tag{4.26}$$

Equation 4.26 holds only for smooth round conductors.

The field near the conductors may be very close to the breakdown field strength of the dielectric which is in this case the air. However, the field away from the conductors may be only a very small fraction of it. This is due to the inverse distance dependence of the electric field.

The breakdown field strength in air is 30 kV/cm at standard temperature and pressure. However, its actual value depends on the atmospheric conditions whose empirical formula was given by equation 2.18, which is:

$$E_c = 30\ m\ \delta\left(1 + \frac{0.426}{\sqrt{\delta d}}\right) \quad (kV/cm) \qquad . \qquad (4.27)$$

To prevent corona at a given high voltage level, the designer must increase the conductor radius even if the extra size is not needed for current capacity. The other alternative is to change the system capacitance.

2. Bundle conductors above ground

To reduce the surface gradients in an efficient way is by reducing the capacitance of the system. This idea can be accomplished through the use of bundle conductors.

By definition, a 'bundle conductor' is composed of a certain number of subconductors for each phase, in parallel, to share the charge and current distribution. Under Stevenson's assumption [51], the total charge and current of a bundle is distributed equally on the N subconductors, the average surface gradient of a subconductor is given by:

$$E = \alpha \frac{Q}{N} \frac{1}{d} \qquad (4.28)$$

where:

E is the average surface gradient of a subconductor in kilovolt per centimeter.

Q is the subconductor charge in coulombs per unit length.

N is the number of subconductors per bundle.

d is the subconductor diameter in centimeters.

α is defined by equation 4.23.

A bundle is characterized by the following parameters:

(1) Subconductor diameter d in cm.

(2) Number of subconductors per bundle N.

(3) Pitch-circle radius which is the circle passing through the centers of all subconductors per bundle R in centimeters.

(4) Distance between two adjacent subconductors which is, for the symmetrical bundle case, given by:

$$S = 2\ R \sin\ (\pi/N) \tag{4.29}$$

(5) Equivalent radius of the bundle R_{eq} in centimeters.

The equivalent radius is the radius of an imaginary cylindrical conductor having the same capacitances as the real bundles with respect to all other neighboring conductors. For the symmetrical bundle case, R_{eq} is given by:

$$R_{eq} = R\ \sqrt[N]{\frac{Nd}{2R}} \quad . \tag{4.30}$$

Due to the mutual shield effect, the actual gradient is higher towards the exterior and smaller towards the interior of the bundle.

Thus, the values around the periphery may be obtained accordingly by the following expression.

$$E_{\theta} = E[1 + (N-1)\frac{d}{2R}\cos\theta] \qquad (4.31)$$

where the maximum corresponds to $\theta = 0$

$$E_{max} = E(1 + (n-1)\frac{d}{2R}) \quad . \qquad (4.32)$$

The geometrical representation of a symmetrical bundle is shown in Fig. 4.2.

3. Gradient for a single circuit three phase line

The method of calculating gradients is well-known and depends on electrostatic methods, mainly Gauss's theorem. An exact method must be used due to the great sensitivity of the EMI to this parameter. In general, as it was mentioned before, the average gradient on the surface of a conductor with diameter d is calculated by means of the Gauss's theorem.

$$[E] = \alpha\frac{[Q]}{d} \quad . \qquad (4.33)$$

In the case of a three phase transmission line, surface charges Q are linked to the potentials V of conductors by the matrix form equation (4.34)

$$[Q] = [C][V] \quad . \qquad (4.34)$$

If the phase voltage sequences are defined by 1, a^2 a (where a is the

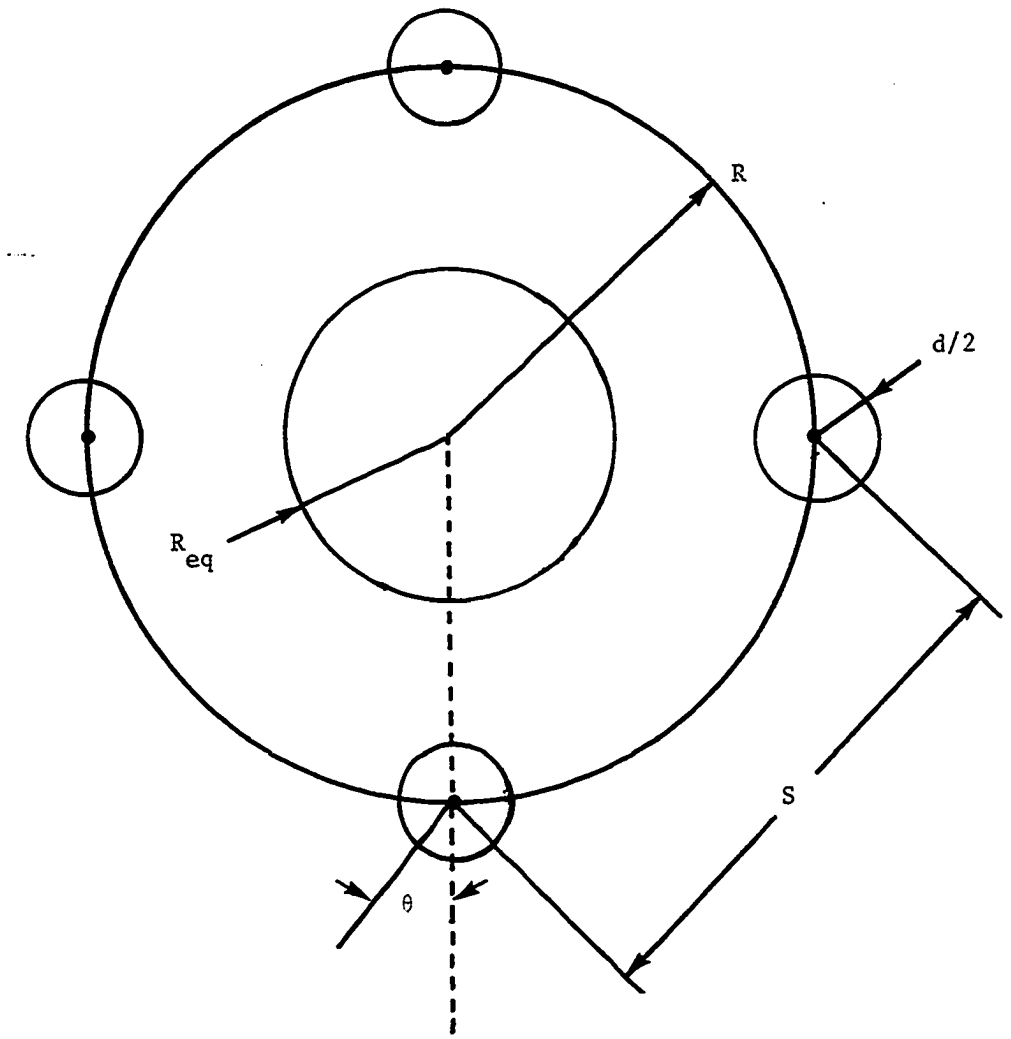

Fig. 4.2. Geometrical representation of a symmetrical bundle (N = 4)

Fortescue or symmetrical component operator) the three phase to ground balanced voltages will be:

$$\begin{bmatrix} V_a \\ V_b \\ V_c \end{bmatrix} = \begin{bmatrix} 1 \\ a^2 \\ a \end{bmatrix} V = \begin{bmatrix} 1 \\ -\frac{1}{2} - j\frac{\sqrt{3}}{2} \\ -\frac{1}{2} + j\frac{\sqrt{3}}{2} \end{bmatrix} V \qquad (4.35)$$

Due to the phase differences between conductors, the charge on a conductor, and as a result, its surface gradient does not necessarily reach a maximum at the same time as the voltage of the conductor itself. The substitution of equation 4.34 into equation 4.33 will yield:

$$[E] = \alpha[C]\frac{[V]}{d} \quad . \qquad (4.36)$$

4. Multiple circuit transmission lines

Frequently, it happens that several three phase systems are carried out by the same towers. In such a case, the precise calculation of the gradients requires, as in the previous cases, the derivation of the capacitance matrix. However, the inversion of the potential coefficients matrix becomes impractical without the use of digital computers. For the multiphase circuit, the relative positions of the phases in each circuit affect the charges on the conductors and consequently their gradients. It is important that these effects be accounted for when calculating, for instance, the gradients of a double circuit line.

For example, the horizontal flat configuration of two circuits indexed by 1, a, a^2 and 1, a, a^2 will result in higher gradients than

the arrangement 1, a, a^2 and a^2, a, 1.

5. Transmission lines with "earth" wires

The calculations for this case are exactly the same as the previous sections. The existence of these ground wires can simply be taken into consideration in the formation of the potential coefficient [P] matrix as well as in the formation of the impedance [Z] matrix. On the other hand, in the one-column voltage matrix, their potentials will evidently be considered zero for grounded systems.

The presence of ground wires naturally increases the dimension of the matrices. However, using Kron-reduction method, this order can be reduced to that of a line without earth wires. This was developed in a previous chapter. In most literature, however, the effect of the earth or ground wires is considered to be very small. They increase the gradients of the phase conductors by up to 3%. It is practically sufficient to disregard their presence, in calculating the gradients, and to compensate by increasing the latter by about 2%.

F. Summary

The properties of the excitation function and its model are presented according to the latest corona model found in the literature. Further, the determination of the excitation function is provided based on the two most used empirical formulas found in the literature. By examining these empirical formulas, one can conclude that the surface gradient is the dominant parameter. Therefore, the calculation of the surface gradient, for different transmission line cases, was developed.

A subroutine called 'EXFUN' has been generated to evaluate the excitation function.

The calculation of the corona currents and corona voltages in the next chapter will be based on the availability of the excitation function information. More specifically, this information will be incorporated in the boundary conditions.

V. CORONA CURRENTS AND CORONA VOLTAGES CALCULATION

A. Introduction

In investigating EMI arising from power transmission lines, Adams introduced the use of matrix algebra methods in the analysis of the distribution corona currents in asymmetrical systems of conductors. In his analysis, he assumed a zero resistance and an infinitely conducting earth plane with earth wires.

In Moreau's and Gary's work, the symmetrical modes of Clarke were used in the development of the corona currents. This is valid only for totally transposed transmission lines with no frequency dependence in the electrical parameters of the line.

One year later, it was found [52] that, for continuously transposed transmission lines, the line modes all have the same parameters which are relatively independent of the frequency. However, the ground mode involves currents returning through the earth and its parameters are highly frequency dependent. Based on H. Karenbauer's work, Dommel [53], in his electromagnetic transients studies, developed a simple transformation matrix which is independent of the actual line parameters for the completely transposed, lossless transmission lines.

The main purpose of this analysis is to determine the magnitude and phase of the corona currents and voltages. This will be performed for transposed and untransposed transmission lines under the influence of a single corona source per phase and a uniformly distributed corona source over the multiphase transmission line. The frequency dependence of the

line parameters will be taken into consideration.

Due to the linearity of the transmission line equations with frequency dependence, the superposition principle still applies. Laplace and Fourier transformations provide a rigorous solution of the problem. Conceptually, the time varying corona currents and corona voltages are transformed into the frequency domain to display their frequency spectrum. Then, for any frequency, the appropriate parameters are used and the response can be found accordingly for either a single corona source per phase or a uniformly distributed corona over all the multiphase transmission line.

The method of calculation of corona currents and voltages is based on the use of the similarity transformation or modal analysis. Wedepohl initiated the use of matrix methods to the solution of traveling-wave phenomena in polyphase systems [25]. Wedepohl's work was specific to the untransposed transmission lines. In the transposed line case, two models are developed namely the equivalent model and the physical or ABCD model. It has been found that these two models give the same results.

In the next section, the transmission line equations will be formulated. Then, a thorough analysis for their solutions, given a specific boundary condition, will be implemented.

B. Equations Formulation

For any polyphase transmission lines, the phase currents and line to ground voltages are related at any point on the line by the

transmission line equations. In time domain, these equations are:

$$-\frac{\partial}{\partial z}[V_p] = [R_p][I_p] + L_p \frac{\partial}{\partial t}[I_p] \tag{5.1}$$

$$-\frac{\partial}{\partial z}[I_p] = [G_p][V_p] + [C_p] \frac{\partial}{\partial t}[V_p] \tag{5.2}$$

where:

$[V_p]$ is an nxn line to ground voltage matrix whose elements V_{pij} are defined to be the line to ground (phase) voltage in phase i due to corona source in phase j.

$[I_p]$ is an nxn phase current matrix whose elements I_{pij} are defined to be the phase current in phase i due to corona source in phase j.

$[R_p]$ is a diagonal nxn frequency dependent matrix characterizing the resistances of the conductors including the Carson's ground return.

$[L_p]$ is a full nxn frequency dependent matrix which characterizes the self and mutual inductances of the line including the earth effect.

$[C_p]$ is a full nxn frequency independent matrix whose elements are the self and mutual capacitances of the line.

$[G_p]$ is a diagonal nxn frequency independent matrix whose elements are the conductances of the line. It usually is too small (10^{-6} - 10 ℧) and can be neglected especially at high frequencies.

The "p" subscript stands for phase parameters.

It is worthwhile to note that in many physical polyphase transmission line, earth or ground wires are added above the phase conductors. Their effects can be evaluated and included in the above equations 5.1 and 5.2. For instance, consider the case of a polyphase transmission line with p phase conductors, m earth or ground wires including the Carson's ground return. The above transmission line equations remain the same, but they are now of (p+m)x(p+m) dimension. Since the ground wires are at zero potential, Kron-reduction method can be used and the result will be a set of equations of order pxp.

By differentiating equations 5.1 and 5.2 with respect to the spatial variable z and the substitution of the values of $\frac{\partial}{\partial z}[I_p]$ and $\frac{\partial}{\partial z}[V_p]$ in the resulting equations will yield:

$$\frac{\partial^2}{\partial z^2}[I_p] = [G_p][R_p][I_p] + ([C_p][R_p] + [G_p][L_p])\frac{\partial}{\partial t}[I_p] + [C_p][L_p]\frac{\partial^2[I_p]}{\partial t^2} \tag{5.3}$$

$$\frac{\partial^2}{\partial z^2}[V_p] = [R_p][G_p][V_p] + ([R_p][C_p] + [L_p][G_p])\frac{\partial}{\partial t}[V_p] + [L_p][C_p]\frac{\partial^2}{\partial t^2}[V_p] \tag{5.4}$$

Since in power transmission line, the value of G is insignificant and mainly frequency independent, it can be neglected and the above equations 5.3 and 5.4 can be written as:

$$\frac{\partial^2[I_p]}{\partial z^2} = [C_p]([R_p]\frac{\partial}{\partial t}[I_p] + [L_p])\frac{\partial^2}{\partial t^2}[I_p] \tag{5.5}$$

$$\frac{\partial^2}{\partial z^2}[V_p] = ([R_p\frac{\partial}{\partial t}[V_p] + [L_p])\frac{\partial^2}{\partial t^2}[V_p])\ [C_p] \quad . \tag{5.6}$$

Equations 5.3 and 5.4 represent the general partial differential of any

polyphase transmission line in time and space domain.

The introduction of the Laplace or Fourier transforms to equation 5.1 and 5.2 with zero initial conditions will yield the following frequency domain equations:

$$-\frac{d}{dz} V_p(z,s) = (R_p + s\, L_p)\, I_p(z,s) \tag{5.7}$$

$$-\frac{d}{dz} I_p(z,s) = (G_p + s\, C_p)\, V_p(z,s) \quad . \tag{5.8}$$

For notation purpose, let $Z_p(s)$ and $Y_p(s)$ be:

$$Z_p(s) = R_p + s\, L_p \tag{5.9}$$

$$Y_p(s) = G_p + s\, C_p \quad . \tag{5.10}$$

The second derivatives of equations 5.7 and 5.9 with respect to the space variable z are:

$$\frac{d^2}{dz^2} V_p(z,s) = B(s)\, V_p(z,s) \tag{5.11}$$

$$\frac{d^2}{dz^2} I_p(z,s) = B^t(s)\, I_p(z,s) \tag{5.12}$$

where:

$$B(s) = Z(s)\, Y(s) \quad . \tag{5.13}$$

By letting $s = j\omega$, the Fourier transform may be obtained.

$$\frac{d^2 V_p(z,j\omega)}{dz^2} = B(j\omega)\, V_p(z,j\omega) \tag{5.14}$$

$$\frac{d^2 I_p(z,j\omega)}{dz^2} = B^t(j\omega)\, I_p(z,j\omega) \tag{5.15}$$

where $V_p(z,j\omega)$ and $I_p(z,j\omega)$ are the steady state phasor quantities which characterize corona voltages and currents in the spatial frequency-domain. Their solution will be detailed in the coming sections.

C. Determination of the Boundary Conditions

Any set of n differential equations of order p can be solved either analytically or numerically using digital computers. In order to find a unique solution to the set of n differential equations of order p, this latter must be accompanied by an (n+p) set of initial conditions or an (n+p) set of boundary conditions or an (n+p) set of mixed boundary and initial conditions. Since the equation to be solved represents a boundary value problem, it is necessary to define and determine the required boundary conditions for this specific problem.

From Gary's model, corona currents are related to the excitation function, previously defined by:

$$[I_p(o,j\omega) = \alpha_1[C_p][\Gamma] \tag{5.16}$$

where:

$[C_p]$ is the capacitance matrix of the line (Farad per unit length)

$$\alpha_1 = \alpha/2 = 10^9 \times 18 \quad (F/m)^{-1} \quad .$$

$[\Gamma]$ is the excitation function matrix in $\mu A\ m^{-1/2}$.

$$[\Gamma] = \begin{bmatrix} \Gamma(1) & 0 & 0 \\ 0 & \Gamma(2) & 0 \\ 0 & 0 & \Gamma(3) \end{bmatrix} \tag{5.17}$$

$\Gamma(i)$ is the excitation function in phase i.

For an infinitely long transmission line, corona voltages are proportional to corona currents at any point on the line. The constant of proportionality, for a given frequency and a specific configuration of the line, is called the characteristic or surge impedance in most power system literature. Then,

$$[V_p(o,j\omega)] = [Z_{sp}(j\omega)][I_p(o,j\omega)] \tag{5.18}$$

where

$[Z_{sp}(j\omega)]$ is the surge impedance matrix. It is found to be [25]

$$[Z_{sp}(j\omega)] = ([Y_p^{-1}][Z_p])^{-1/2} \quad . \tag{5.19}$$

$[Z_p]$ is the phase impedance matrix in ohms per unit length.

$[Y_p]$ is the phase admittance matrix in ohms per unit length or as approximated by the EPRI-EHV book [6] and others [6, 7, 21].

$$[Z_{sp}] \cong 60\ \alpha_1\ [C_p]^{-1} \quad . \tag{5.20}$$

It is worthwhile to note that we run the EMI program with both equations 5.19 and 5.20. The results came out to be very close within less than 1 dB difference in the EMI value.

D. Direct Modal Analysis

1. Introduction

The transmission line equations 5.14 and 5.15 could be used for both transposed and untransposed lines. However, for the transposed

line represented by an equivalent line model, the solution takes a special form because of the multiplicity of order two in the eigenvalues.

For multiphase transmission line analysis, the use of symmetrical components is most of the time appropriate. Although symmetrical components are widely used in power systems analysis, they are of impractical use in this problem. At these high frequencies, the asymmetry of the line cannot be neglected. Therefore, the general eigenvalue or modal analysis is adequate for this purpose through the use of the similarity transformations. Using this technique, a lossy line consisting of n conductors and ground return has n eigenvalues or modes of propagation. Each of these modes consists of a particular voltage and current composition, velocity and attenuation constant at any given frequency.

2. Similarity transformation

The main advantage of this technique is the use of a transformation method which, when applied to coupled systems, will decouple them. For this specific study, phase quantities are going to be transformed into modal quantities.

Let S and T be the desired transformations to decouple the phase voltages and phase currents, respectively.

$$[V_p] = [S][V] \tag{5.21}$$

$$[I_p] = [T][I] \tag{5.22}$$

where:

[V] is the modal voltage matrix.

[I] is the modal current matrix.

[S] is voltage similarity transformation.

[T] is current similarity transformation.

The substitution of equations 5.21 and 5.22 into equations 5.14 and 5.15 will yield:

$$\frac{d^2[V]}{dz^2} = [\gamma_v^2]\, V \tag{5.23}$$

$$\frac{d^2[I]}{dz^2} = [\gamma_i^2]\, I \tag{5.24}$$

where:

$[\gamma_v^2]$ is a diagonal matrix whose diagonal elements are the eigenvalue of $[B_p] = [Z_p][Y_p]$. It is defined by:

$$[\gamma_v^2] = [S^{-1}][B_p][S] \quad . \tag{5.25}$$

$[\gamma_i^2]$ is a diagonal matrix whose diagonal elements are the eigenvalue of $[B_p]^t = [Y_p][Z_p]$. It is defined by:

$$[\gamma_i^2] = [T^{-1}][B_p]^t[T] \quad . \tag{5.26}$$

However, from matrix theory, we can state that:

$$[\gamma_i^2] = [\gamma_v^2] \quad . \tag{5.27}$$

Because of the symmetry of the matrices $[Y_p]$ and $[Z_p]$,

$$[B_p] = [Z_p][Y_p] = ([Y_p][Z_p])^t = ([B_p]^t)^t = [B_p] \quad . \tag{5.28}$$

From matrix theory, if [A] is a square matrix and $[A]^t$ is its transpose, then [A] and $[A]^t$ have the same eigenvalues but different eigenvectors [54]. That is the reason to select [T] and [S] similarity transformations differently. Wedepohl [25] showed that these transformations are related by a certain diagonal matrix, [D]:

$$[T]^t[S] = D \quad . \tag{5.29}$$

The solution to the matriciel wave equations (5.23 and 5.24) is the traveling wave modal voltages and currents at distance z from the source. Two cases will be considered in this research, namely wave equations for single corona source per phase and those for uniformly distributed corona source for the untransposed and transposed transmission lines.

E. Solution for a Single Corona Source Case

Although the single corona source case may not be of practical use, it can be studied and used as a basis for the more practical one which is the uniformly distributed corona source.

1. Untransposed line model

If the multiphase transmission line is subject only to a single corona source per phase, the solution of the wave equations in modal form is:

$$[V] = [e^{-\gamma z}][V^-] + [e^{\gamma z}](V^+] \tag{5.30}$$

$$[I] = [e^{-\gamma z}][I^-] + [e^{\gamma z}][I^+] \quad . \tag{5.31}$$

Differentiation with respect to z to these equations (5.30 and 5.31) will yield:

$$[\gamma]\{[-e^{-\gamma z}][V^-] + [e^{\gamma z}][V^+]\} = [Z][I] \tag{5.32}$$

$$[\gamma]\{[-e^{-\gamma z}][I^-] + [e^{\gamma z}][I^+]\} = [Y][V] \tag{5.33}$$

the corresponding boundary conditions are given by:

$$[V(0)] = [V^-] + [V^+] \tag{5.34}$$

$$[I(0)] = [I^-] + [I^+] \tag{5.35}$$

$$[\gamma]\{[-V^-] + [V^+]\} = [Z][I(0)] \tag{5.36}$$

$$[\gamma]\{[I^-] + [I^+]\} = [Y][V(0)] \quad . \tag{5.37}$$

Solving for $[V^-]$, $[V^+]$, $[I^-]$ and $[I]^+$ from equations 5.34 to 5.37, we get:

$$[V^+] = \frac{1}{2}\{-[\gamma]^{-1}[Z][I(0)] + [V(0)]\} \tag{5.38}$$

$$[I^+] = \frac{1}{2}\{-[\gamma]^{-1}[Y][V(0)] + [I(0)]\} \tag{5.39}$$

$$[V^-] = \frac{1}{2}\{[\gamma]^{-1}[Z][I(0)] + [V(0)]\} \tag{5.40}$$

$$[I^-] = \frac{1}{2}\{[\gamma]^{-1}[Y][V(0)] + [I(0)]\} \quad . \tag{5.41}$$

For a practically long transmission line, the reflected waves can be neglected; that is:

$$[V^+] = 0 \tag{5.42}$$

$$[I^+] = 0 \quad . \tag{5.43}$$

Beyond this stage, a line may be considered practically infinite if the measuring point is 8 kilometers or more from the termination or abrupt change in direction. The contribution of the field strength sources more than 8 kilometers away is practically nil [6]. Therefore, since most, if not all, EHV and UHV transmission lines are at least 30 kilometers long, the infinitely long transmission line assumption holds and can be used. Equations 5.38 to 5.41 would then be:

$$[V^+] = 0 \tag{5.44}$$

$$[I^+] = 0 \tag{5.45}$$

$$[V^-] = [\gamma]^{-1}[Z][I(0)] \tag{5.46}$$

$$[I^-] = [\gamma]^{-1}[Y][V(0)] \quad . \tag{5.47}$$

For notation purpose, let $[Z_{sm}]$ and $[Y_{sm}]$ be the modal surge impedance and admittance matrix given by:

$$[Z_{sm}] = [\gamma]^{-1}[Z] \tag{5.48}$$

$$[Y_{sm}] = [\gamma]^{-1}[Y] \quad . \tag{5.49}$$

The traveling wave equations (5.30 and 5.31) would then be:

$$[V] = [e^{-\gamma z}][Z_{sm}][I(0)] \tag{5.50}$$

$$[I] = [e^{-\gamma z}][Y_{sm}][V(0)] \quad . \tag{5.51}$$

Transforming back, equations 5.50 and 5.51 to the phase voltages and phase currents, we end up with:

$$[V_p] = [S][e^{-\gamma z}][Z_{sm}][I(0)] \tag{5.52}$$

$$[I_p] = [T][e^{-\gamma z}][Y_{sm}][V(0)] \tag{5.53}$$

or

$$[V_p] = [S][e^{-\gamma z}][S]^{-1}[Z_{sp}][I_p(0)] \tag{5.54}$$

$$[I_p] = [T][e^{-\gamma z}][T]^{-1}[Y_{sp}][V_p(0)] \tag{5.55}$$

where:

$[Z_{sp}]$ is the phase surge impedance which is given by:

$$[Z_{sp}] = [S][Z_{sm}][T]^{-1} \quad . \tag{5.56}$$

$[Y_{sp}]$ is the phase surge admittance which is given by:

$$[Y_{sp}] = [T][Y_{sm}][S]^{-1} \quad . \tag{5.57}$$

For notation purpose, let's define:

$$[\Lambda] = [e^{-\gamma z}] = \begin{bmatrix} \Lambda(1) & 0 & 0 \\ 0 & \Lambda(2) & 0 \\ 0 & 0 & \Lambda(3) \end{bmatrix} \tag{5.58}$$

where:

$$\Lambda(i) = e^{-\gamma_i z} \quad . \tag{5.59}$$

Therefore, equations 5.54 and 5.55 can be written as:

$$[V_p] = [S][\Lambda][S]^{-1}[V_p(0)] \tag{5.60}$$

$$[I_p] = [T][\Lambda][T]^{-1}[I_p(0)] \quad . \tag{5.61}$$

These equations (5.60 and 5.61) are only valid under the infinitely long transmission line assumption where the reflected wave is considered

to be practically nil.

For the single corona source, the RI phase currents and the RI phase voltages are of an exponential decaying form.

The equivalent corona currents and voltages per phase will then be determined as shown below:

Let

$$[V(0)] = [S]^{-1}[V_p(0)] \tag{5.62}$$

$$[I(0)] = [T]^{-1}[I_p(0)] \tag{5.63}$$

where:

$$V_{ij}(0) = S(i,1)V_{p1j}(0) + S(i,2)V_{p2j}(0) + S(i,3)V_{p3j}(0) \tag{5.64}$$

$$I_{ij}(0) = T(i,1)I_{p1j}(0) + T(i,2)I_{p2j}(0) + T(i,3)V_{p3j}(0) \; . \tag{5.65}$$

Then, the partial corona currents and voltages at any point z along the line are respectively given by:

$$I_{pij}(z) = t(i,1)I_{1j}(0)\Lambda(1) + t(i,2)I_{2j}(0)\Lambda(2) + t(i,3)I_{3j}(0) \quad (3) \tag{5.66}$$

$$V_{pij}(z) = s(i,1)V_{ij}(0)\Lambda(1) + s(i,2)V_{2j}(0)\Lambda(2) + s(i,3)V_{3j}(0) \quad (3) \tag{5.67}$$

where:

t(i,j) are the elements of matrix [T].

T(i,j) are the elements of matrix $[T]^{-1}$.

s(i,j) are the elements of matrix [S].

S(i,j) are the elements of matrix $[S]^{-1}$.

$I_{ij}(0)$ are the elements of matrix [I(0)].

$V_{ij}(0)$ are the elements of matrix [V(0)].

Λ_i are the elements of matrix [Λ].

The equivalent corona currents and voltages per phase are given by:

$$I_{p1}(z) = I_{p11}(z) + I_{p12}(z) + I_{p13}(z) \tag{5.68}$$

$$I_{p2}(z) = I_{p21}(z) + I_{p22}(z) + I_{p23}(z) \tag{5.69}$$

$$I_{p3}(z) = I_{p31}(z) + I_{p32}(z) + I_{p33}(z) \tag{5.70}$$

and similarly for the equivalent corona voltages:

$$V_{p1}(z) = V_{p11}(z) + V_{p12}(z) + V_{p13}(z) \tag{5.71}$$

$$V_{p2}(z) = V_{p21}(z) + V_{p22}(z) + V_{p23}(z) \tag{5.72}$$

$$V_{p3}(z) = V_{p31}(z) + V_{p32}(z) + V_{p33}(z) \tag{5.73}$$

or simply, in terms of the transformation matrices elements:

$$I_{pk}(z) = W(k,1)e^{-\gamma 1 z} + W(k,2)\ e^{-\gamma 2 z} + W(k,3)\ e^{-\gamma 3 z} \tag{5.74}$$

$$V_{pk}(z) = U(k,1)\ e^{-\gamma 1 z} + U(k,2)\ e^{-\gamma 2 z} + U(k,3)\ e^{-\gamma 3 z} \tag{5.75}$$

where:

$$W(k,m) = t(k,m)(I_{m1}(0) + I_{m2}(0) + I_{m3}(0)) \tag{5.76}$$

$$U(k,m) = s(k,m)(V_{m1}(0) + V_{m2}(0) + V_{m3}(0)) \tag{5.77}$$

Some complex functions occur at W(k,m) and U(k,m) that depend upon frequency, line parameters, line configuration, weather conditions and boundary conditions.

2. Transposed transmission line: Equivalent model

For the untransposed transmission line case, the three modes of propagation do not all have the same parameters. Therefore, the currents

and voltages on the lines will become unbalanced.

Balance of the three phases can be restored by exchanging the positions of the conductors at regular intervals. Thus, each conductor occupies the original position of every other conductor over an equal distance. Such a rotation of conductor positions is called transposition. The complete transposition cycle is shown in Fig. 5.1. By observing Fig. 5.1, it can be stated that transposition is a physical rotation of the conductors, arranged so that each conductor is moved to occupy the next position in a regular sequence such as a-b-c, b-c-a, c-a-b etc.

The equivalent model of the transposed line consists in averaging the impedances and admittances of the transmission line. Thus, the new impedance matrix and new admittance matrix will be given by:

$$[Z_p] = \begin{bmatrix} Z_s & Z_{m1} & Z_{m2} \\ Z_{m1} & Z_s & Z_{m3} \\ Z_{m2} & Z_{m3} & Z_s \end{bmatrix} \tag{5.78}$$

$$[Y_p] = \begin{bmatrix} Y_s & Y_{m1} & Y_{m2} \\ Y_{m1} & Y_s & Y_{m3} \\ Y_{m2} & Y_{m3} & Y_s \end{bmatrix} \tag{5.79}$$

It is clear that for identical conductors, the self impedance and self-admittances are given by:

$$Z_s = Z_{p11} = Z_{p22} = Z_{p33} \tag{5.80}$$

$$Y_s = Y_{p11} = Y_{p22} = Y_{p33} \quad . \tag{5.81}$$

Similarly, the mutual impedance and admittance terms are:

$$Z_{m1} = f(1)Z_{p12} + f(2)Z_{p23} + f(3)Z_{p13} \tag{5.82}$$

$$Z_{m2} = f(1)Z_{p13} + f(2)Z_{p12} + f(3)Z_{p23} \tag{5.83}$$

$$Z_{m3} = f(1)Z_{p23} + f(2)Z_{p13} + f(3)Z_{p12} \tag{5.84}$$

$$Y_{m1} = f(1)Y_{p12} + f(2)Y_{p23} + f(3)Y_{p13} \tag{5.85}$$

$$Y_{m2} = f(1)Y_{p13} + f(2)Y_{p12} + f(3)Y_{p23} \tag{5.86}$$

$$Y_{m3} = f(1)Y_{p23} + f(2)Y_{p13} + f(3)Y_{p12} \tag{5.87}$$

where:

f(k) is the fraction of the total line length in section k and is given by:

$$f(k) = \frac{\ell(k)}{\ell} \quad . \tag{5.88}$$

k is the line section identifier.

$\ell(k)$ is the length of line section k.

ℓ is the total length of the line.

For a completely transposed, that is:

$$f(1) = f(2) = f(3) = 1/3 \quad . \tag{5.89}$$

Then, from equations 5.82 to 5.87, we get:

$$Z_{m1} = Z_{m2} = Z_{m3} = Z_m \tag{5.90}$$

$$Y_{m1} = Y_{m2} = Y_{m3} = Y_m \quad . \tag{5.91}$$

Therefore, the impedance and admittance matrix, for a completely transposed line and under the equivalent model assumptions, will then become:

$$[Z_p] = \begin{bmatrix} Z_s & Z_m & Z_m \\ Z_m & Z_s & Z_m \\ Z_m & Z_m & Z_s \end{bmatrix} \tag{5.92}$$

$$[Y_p] = \begin{bmatrix} Y_s & Y_m & Y_m \\ Y_m & Y_s & Y_m \\ Y_m & Y_m & Y_s \end{bmatrix} \tag{5.93}$$

The transmission line equations will then be given by:

$$\frac{d^2[V_p]}{dz^2} = [Z_p][Y_p][V_p] \tag{5.94}$$

$$\frac{d^2[I_p]}{dz^2} = [Y_p][Z_p][I_p] \quad . \tag{5.95}$$

Let's define a new matrix $[B_q]$ as follows:

$$[B_q] = [Z_p][Y_p] \quad . \tag{5.96}$$

Then

$$[B_q]^t = [Y_p][Z_p] \tag{5.97}$$

The elements of the matrix $[B_q]$ are:

$$B_s = Z_s Y_s + 2Z_m Y_m \tag{5.98}$$

$$B_m = Z_s Y_m + Z_m Y_s + Z_m Y_m \quad . \tag{5.99}$$

To find the normal or uncoupled modes, we seek to find a new set of variables [V] and [I]. These new variables would then be related by linear transformations to the phase variables $[V_p]$ and $[I_p]$. [V] and [I] satisfy an equation similar to that presented in equations 5.23 and 5.24:

$$\frac{d^2[I]}{dz^2} = [\gamma_i^2][I] \tag{5.100}$$

$$\frac{d^2[V]}{dz^2} = [\gamma_v^2][V] \tag{5.101}$$

where

$$[\gamma_v^2] = [S_q^{-1}][B_q][S_q] = [\gamma_i^2] \tag{5.102}$$

$$[\gamma_i^2] = [T_q^{-1}][B_q]^t[T_q] = [\gamma_v^2] \tag{5.103}$$

or in slightly different form:

$$[B_q]^t[T_q] = [T_q][\gamma_i^2] \tag{5.104}$$

$$[B_q][S_q] = [S_q][\gamma_v^2] \quad . \tag{5.105}$$

These matrix relations represent a set of linear equations in the elements of the matrices involved. This set of equations can have a solution only if the determinant of the coefficients of the elements of [T] or [S] in the set of equations 5.104 or 5.105 vanish. Let's use equation 5.105, for instance.

$$\det\{[B_q] - [\gamma_v^2]\} = 0 \quad . \tag{5.106}$$

This determinant is equal to:

$$(B_s - B_m - \gamma_v^2)\{(B_s - \gamma_v^2)(B_s + B_m - \gamma_v^2) - 2\,B_m^2\} = 0 \quad . \tag{5.107}$$

This equation results in the following roots:

$$\gamma_1^2 = \gamma_3^2 = B_s - B_m \tag{5.108}$$

$$\gamma_2^2 = B_s + 2\,B_m \quad . \tag{5.109}$$

We conclude that there are only two propagation constants to this system, namely:

$$\gamma_1 = \gamma_3 = \sqrt{B_s - B_m} \tag{5.110}$$

$$\gamma_2 = \sqrt{B_s + 2\,B_m} \quad . \tag{5.111}$$

Since two eigenvalues are the same ($\gamma_1 = \gamma_3$), the solutions would then take the following form:

$$[V_p(z)] = [S_q][\Lambda_q][S_q]^{-1}[V_p(0)] \tag{5.112}$$

$$[I_p(z)] = [T_q][\Lambda_q][T_q]^{-1}[V_p(0)] \tag{5.113}$$

where:

$[S_q]$ is the new voltage similarity transformation.

$[T_q]$ is the new current similarity transformation.

$$[\Lambda_q] = \begin{bmatrix} \Lambda(1) & 0 & 0 \\ 0 & \Lambda(2) & 0 \\ 0 & 0 & z\Lambda(3) \end{bmatrix} \tag{5.114}$$

$$\Lambda(i) = e^{-\gamma_i z} \quad . \tag{5.115}$$

Similar to the untransposed case, the equivalent corona currents and voltages per phase can be shown to be:

$$I_{qk}(z) = (W_q(k,1) + zW_q(k,3))\Lambda(1) + W_q(k,3)\Lambda(2) \tag{5.116}$$

$$V_{qk}(z) = (U_q(k,1) + zU_q(k,3))\Lambda(1) + U_q(k,3)\Lambda(2) \quad . \tag{5.117}$$

For the single corona source per phase, the EMI phase currents and the EMI phase voltages are predominantly of an exponential decaying form under this specific equivalent model.

3. Transposed transmission line: Physical model

While the averaging of the line parameters for the transposed case is common practice, it is not completely consistent. It was assumed that the charge per unit length and the current on a conductor are the same in every part of the transposition cycle.

A better way to do averaging is in terms of the physical model or the ABCD parameters for each line section. This physical model is our target in this section. Let's sectionalize the line and determine the corona currents and voltages solutions in each section with the corresponding matched boundary conditions. Referring to Fig. 5.1, the first section is governed by the following boundary value problem over the

interval $-\frac{\ell}{2} \leq z \leq -\frac{\ell}{6}$.

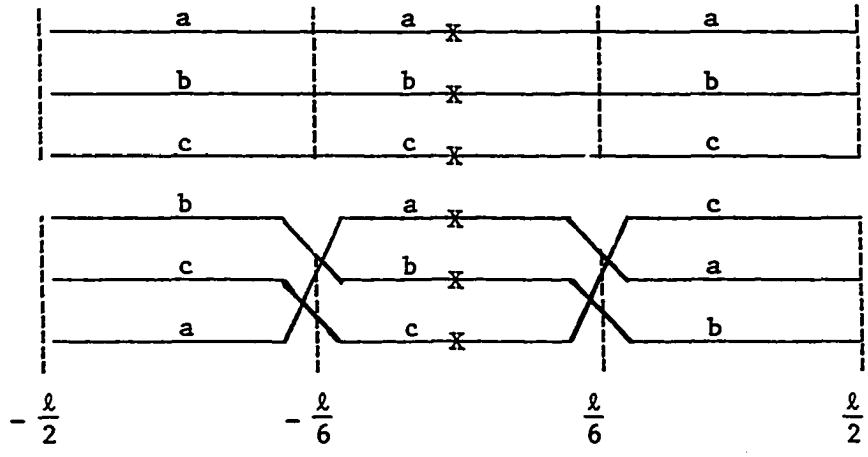

Fig. 5.1. Single circuit untransposed and transposed transmission lines subject to a single corona source per phase

$$\frac{d^2[I_{1p}]}{dz^2} = [B_p]^t[I_{1p}] \tag{5.118}$$

$$\frac{d^2[V_{1p}]}{dz^2} = [B_p][V_{1p}] \tag{5.119}$$

subject to:

$$[I_{1p}(-\tfrac{\ell}{6})] = R[I_{2p}(-\tfrac{\ell}{6})] \tag{5.120}$$

$$[V_{1p}(-\tfrac{\ell}{6})] = R[V_{2p}(-\tfrac{\ell}{6})] \quad . \tag{5.121}$$

Borrowing the result from the untransposed case, we get:

$$[I_{1p}] = [T][\Lambda_1][T^{-1}][I_{1p}(-\tfrac{\ell}{6})] \tag{5.122}$$

where:

$$[\Lambda_1] = \begin{bmatrix} e^{+\gamma_1 z} & 0 & 0 \\ 0 & e^{+\gamma_2 z} & 0 \\ 0 & 0 & e^{+\gamma_3 z} \end{bmatrix} \tag{5.123}$$

In passing through the first transposition between section one and section two from the left, the conductors are seen to change positions. In a model concept, let a, b, c be considered as referring to geometric positions in space. In this sense, the voltages and currents on either side of the transposition can be equated with the introduction of the rotation matrix R as in equations 5.120 and 5.121. The rotation matrix is given by:

$$R = \begin{bmatrix} 0 & 1 & 0 \\ 0 & 0 & 1 \\ 1 & 0 & 0 \end{bmatrix} \tag{5.124}$$

and its inverse is given by:

$$[R]^{-1} = \begin{bmatrix} 0 & 0 & 1 \\ 1 & 0 & 0 \\ 0 & 1 & 0 \end{bmatrix} \tag{5.125}$$

Therefore, the second section obeys the following boundary value problem:

$$\frac{d^2[I_{2p}]}{dz^2} = [B]^t[I_{2p}] \tag{5.125}$$

$$\frac{d^2[V_{2p}]}{dz^2} = [B][V_{2p}] \tag{5.126}$$

subject to:

$$[I_{2p}(0)] = \alpha[C_p][\Gamma] \tag{5.127}$$

$$[V_{2p}(0)] = [Z_{sp}][I_{2p}(0)] \quad . \tag{5.128}$$

The solution to this boundary value problem is given by:

$$[I_{2p}^{-}] = [T][\Lambda_1][T]^{-1}[I_{1p}(0)] \tag{5.129}$$

for the interval $-\frac{\ell}{6} \leq z \leq 0$ and

$$[I_{2p}^{+}] = [T][\Lambda][T]^{-1}[I_{1p}(0)] \tag{5.130}$$

for the interval $0 \leq z \leq \frac{\ell}{6}$, where $[\Lambda]$ is defined in equation 5.58.

In a similar way, the transition between the second and the third sections is governed by:

$$[I_{3p}(\tfrac{\ell}{6}) = [R]^{-1}[I_{2p}^{+}(\tfrac{\ell}{6})] \tag{5.131}$$

$$[V_{3p}(\tfrac{\ell}{6})] = [R]^{-1}[V_{2p}^{+}(\tfrac{\ell}{6})] \quad . \tag{5.132}$$

These equations, coupled with equations 5.133 and 5.134, enable the calculated corona currents and voltages in the third section over the interval $\frac{\ell}{6} \leq z \leq \frac{\ell}{2}$.

$$\frac{d^2[I_{3p}]}{dz^2} = [B]^t[I_{3p}] \tag{5.133}$$

$$\frac{d^2[V_{3p}]}{dz^2} = [B][V_{3p}] \quad . \tag{5.134}$$

The equivalent corona currents per phase can be shown to be of the form:

$$I_{1pk}(z) = W_1(k,1)\ e^{+\gamma 1^3} + W_1(k,2)\ e^{+\gamma 2z} + W_1(k,3)e^{+\gamma 3^z} \tag{5.135}$$

for the interval $-\frac{\ell}{2} \leq z \leq -\frac{\ell}{6}$.

$$I^{-}_{2pk}(z) = W_2(k,1)\ e^{+\gamma 1 z} + W_2(k,2)e^{+\gamma 2 z} + W_2(k,3)\ e^{+\gamma 3 z} \qquad (5.136)$$

for the interval $-\frac{\ell}{6} \leq z \leq 0$.

$$I^{+}_{2pk}(z) = W_3(k,1)\ e^{-\gamma 1 z} + W_3(k,2)\ e^{-\gamma 2 z} + W_3(k,3)\ e^{-\gamma 3 z} \qquad (5.137)$$

for the interval $0 \leq z \leq \frac{\ell}{6}$.

$$I_{3pk}(z) = W_4(k,1)\ e^{-\gamma 1 z} + W_4(k,2)\ e^{-\gamma 2 z} + W_4(k,3)\ e^{-\gamma 3 z} \qquad (5.138)$$

for the interval $\frac{\ell}{6} \leq z \leq \frac{\ell}{2}$.

Similar expressions hold true for the equivalent corona voltages except that the $W_m(k,j)$ coefficients in equations 5.135 to 5.138 would be substituted by the terms $U_m(k,j)$.

The coefficients $W_m(k,j)$ are given by:

$$W_1(k,m) = t(k,m)\ \{\sum_{i=1}^{3} e^{-\gamma i \ell/6}\ [T(m,1)W_2(2,i) + T(m,2)W_2(3,i) + T(m,3)W_3(1,i)]\} \qquad (5.139)$$

$$W_2(k,m) = t(k,m)\ \{T(m,1)I_{1p}(0) + T(m,2)I_{2p}(0) + T(m,3)I_{3p}(0)\}\ . \qquad (5.140)$$

$$W_3(k,m) = W_2(k,m) \qquad (5.141)$$

$$W_4(k,m) = t(k,m)\{\sum\ e^{-\gamma i \ell/6}\ [T(m,1)W_3(3,i) + T(m,2)W_3(1,i) + T(m,3)W_3(2,i)]\}\ . \qquad (5.142)$$

The coefficients $U_n(k,m)$ are of the same form as the $W_n(k,m)$ except that the $t(k,m)$ and $T(k,m)$ terms are substituted by the $s(k,m)$ and $S(k,m)$, respectively. Also the $I_{kp}(0)$ and $W_n(k,m)$ factors are replaced

by the $V_{kp}(0)$ and $U_n(k,m)$, respectively.

Finally, the corona currents and voltages are known at any point z on the line subject to a single corona source in the middle of the line.

F. Solution for a Uniformly Distributed Corona Source Case

Practically, corona is uniformly distributed along most of the transmission lines. The development of this analysis will be mainly based on the single corona source and the use of the superposition principle.

Due to the randomness of corona sources, the total corona current, $I_{tk}(z)$, per phase at any point in space along z, is given by:

$$I_t(k) = \sqrt{2 \int_0^\infty I_k^2(z)dz} \tag{5.143}$$

where $I_k(z)$ is the EMI current in phase k determined from the single corona source per phase case.

1. Untransposed line model

The substitution of equation 5.74 into 5.143 and then the integration of the latter will yield:

$$I_t(k) = \sqrt{2}\ \{ \sum_{i=1}^{3} \sum_{j=1}^{3} [\frac{W(k,i)W(k,j)}{\gamma(i) + \gamma(j)}]\}^{1/2} \quad . \tag{5.144}$$

In a similar way, the total EMI voltage per phase would be:

$$V_t(k) = \sqrt{2}\ \{ \sum_{i=1}^{3} \sum_{j=1}^{3} [\frac{U(k,i)U(k,j)}{\gamma(i) + \gamma(j)}]\}^{1/2} \quad . \tag{5.145}$$

It should be pointed out that the transmission line corona currents and corona voltages for this case are also uniformly distributed. Therefore,

they are space independent.

2. Transposed line: Equivalent model

The total corona currents per phase can be found by substituting equation 5.116 into equation 5.143. From equation 5.116, $I_k^2(z)$ is of the form:

$$I_k^2(z) = \{2 \sum_{p=1}^{3} \sum_{m=1}^{3} [W_q(k,p)W_q(k,m)\Lambda_q(p)\Lambda_q(m)]\}^{1/2} \tag{5.146}$$

where:

$$\Lambda_q(1)\Lambda_q(1) = z^2 e^{-2\gamma_1 q} \tag{5.147}$$

$$\Lambda_q(1)\Lambda_q(2) = z e^{-(\gamma_1+\gamma_2)z} \tag{5.148}$$

$$\Lambda_q(2)\Lambda_q(2) = e^{-2\gamma_2 z} \tag{5.149}$$

$$\Lambda_q(2)\Lambda_q(3) = e^{-(\gamma_2+\gamma_1)z} \tag{5.150}$$

$$\Lambda_q(3)\Lambda_q(3) = e^{-2\gamma_1 z} \quad . \tag{5.151}$$

For real a>0, we can obtain the following results:

$$\int_0^\infty e^{-az}\, dz = 1/a \tag{5.152}$$

$$\int_0^\infty z e^{-az}\, dz = 1/a^2 \tag{5.153}$$

$$\int_0^\infty z^2 e^{-az}\, dz = 2/a^3 \quad . \tag{5.154}$$

Applying these results to the integration of equation 5.146 substituted into equation 5.143 will yield:

$$I_t(k) = \sqrt{2}\ \{\frac{W_q(k,1)W_q(k,2)}{4(\gamma(1))^3} + \frac{2W_q(k,1)W_q(k,2)}{(\gamma(1)+\gamma(2))^2} + \frac{W_q(k,2)W_q(k,2)}{2\gamma(2)}$$
$$+ \frac{2W_q(k,2)W_q(k,3)}{(\gamma(2)+\gamma(1))} + \frac{W_q(k,1)W_q(k,3)}{4(\gamma(1))^2} + \frac{W_q(k,3)W_q(k,3)}{2\gamma(3)}\ \}^{1/2} . \quad (5.155)$$

The total corona voltages, $V_t(k)$, would be exactly of the same form as the total corona currents, I_{tk}, shown in equation 5.155 except that the $W_q(k,J)$ coefficients would be sbustituted by the $U_q(k,J)$ coefficients. Another alternative is to calculate the total corona voltages using the phase surge impedance, Z_{sp}, concept.

$$[V_t] = \begin{bmatrix} V_{t1} \\ V_{t2} \\ V_{t3} \end{bmatrix} = [Z_{sp}][I_t] = [Z_{sp}] \begin{bmatrix} I_{t1} \\ I_{t2} \\ I_{t3} \end{bmatrix} . \quad (5.156)$$

Fig. 5.2 represents the untransposed and transposed lines under the uniformly distributed corona source conditions.

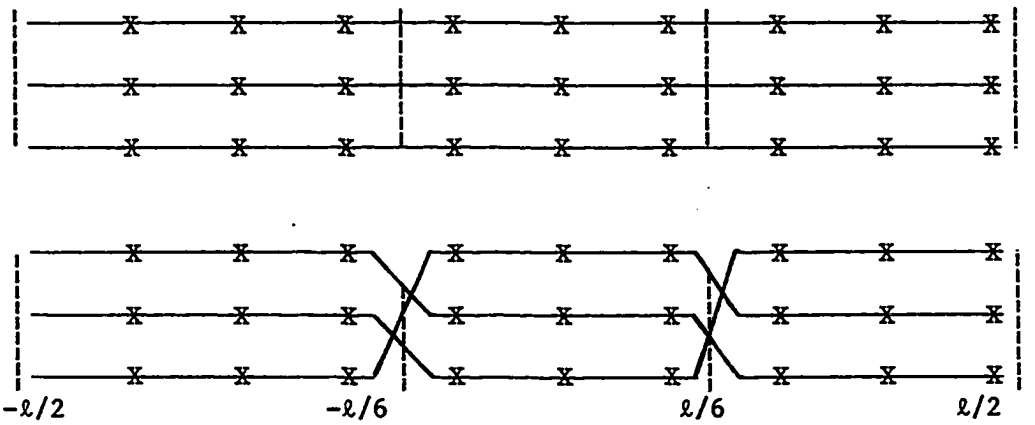

Fig. 5.2. Single circuit untransposed and transposed transmission line subject to a uniformly distributed corona source over all the phases

3. Transposed line: Physical model

The total corona currents, at any point z on the line, for the uniformly distributed corona source is given by:

$$I_t(k) = \sqrt{\int_{-\ell/2}^{\ell/2} I_k^2(z)\, dz} \quad . \tag{5.157}$$

Under the physical model conditions, equation 5.157 can be written into the following form:

$$I_t(k) = \{\int_{-\ell/2}^{-\ell/6} I_{1pk}^2(z)dz + \int_{-\ell/6}^{0} (I_{2pk}^-(z))^2 dz + \int_{0}^{\ell/6} (I_{2pk}^+(z))^2 dz + \int_{\ell/6}^{\ell/2} I_{3pk}^2(z)dz\}^{1/2} \quad . \tag{5.158}$$

The first integral can be shown to be:

$$A_1 = \sum_{\alpha=1}^{3} \sum_{\beta=1}^{3} \{\frac{W_1(k,\alpha)W_1(k,\beta)}{(\gamma_\alpha + \gamma_\beta)}[e^{-(\gamma_\alpha+\gamma_\beta)\ell/6} - e^{-(\gamma_\alpha+\gamma_\beta)\ell/2}]\} \tag{5.159}$$

Similarly, the second integral is given by:

$$A_2 = \sum_{\alpha=1}^{3} \sum_{\beta=1}^{3} \{\frac{W_2(k,\alpha)W_2(k,\beta)}{(\gamma_\alpha + \gamma_\beta)}[1-e^{-(\gamma_\alpha+\gamma_\beta)\ell/6}]\} \quad . \tag{5.160}$$

The third integral would be:

$$A_3 = \sum_{\alpha=1}^{3} \sum_{\beta=1}^{3} \{\frac{W_3(k,\alpha)W_3(k,\beta)}{-(\gamma_\alpha + \gamma_\beta)}[e^{-(\gamma_\alpha+\gamma_\beta)\ell/6} - 1]\} \quad . \tag{5.161}$$

The last integral is of the form:

$$A_4 = \sum_{\alpha=1}^{3} \sum_{\beta=1}^{3} \{\frac{W_4(k,\alpha)W_4(k,\beta)}{-(\gamma_\alpha + \gamma_\beta)}[e^{-(\gamma_\alpha+\gamma_\beta)\ell/2} - e^{-(\gamma_\alpha+\gamma_\beta)\ell/6}]\} \tag{5.162}$$

For the infinitely long transmission line, ℓ gets close to infinity; therefore,

$$L_1 = \lim_{\ell\to\infty} A_1 = 0 \tag{5.163}$$

$$L_2 = \lim_{\ell\to\infty} A_2 = \sum_{\alpha=1}^{3}\sum_{\beta=1}^{3} \frac{W_2(k,\alpha)W_2(k,\beta)}{(\gamma_\alpha + \gamma_\beta)} \tag{5.164}$$

$$L_3 = \lim_{\ell\to\infty} A_3 = \sum_{\alpha=1}^{3}\sum_{\beta=1}^{3} \frac{W_3(k,\alpha)W_3(k,\beta)}{(\gamma_\alpha + \gamma_\beta)} \tag{5.165}$$

$$L_4 = \lim_{\ell\to\infty} A_4 = 0 \tag{5.166}$$

Therefore, the total corona current in each phase is given by

$$I_t(k) = (L_3 + L_2)^{1/2} \quad . \tag{5.167}$$

But, since $W_3(k,m) = W_2(k,m)$ from equation 5.141, equation 5.167 would then be:

$$I_t(k) = \sqrt{2}\{\sum_{\alpha=1}^{3}\sum_{\beta=1}^{3} \frac{W_2(k,\alpha)W_2(k,\beta)}{\gamma_\alpha + \gamma_\beta}\}^{1/2} \quad . \tag{5.168}$$

Comparing this quantity with that given in equation 5.144, we conclude that the total corona current per phase for the transposed line simulated by the physical model is equivalent to that total corona current per phase calculated for the untransposed transmission under the uniformly distributed corona source condition.

Similarly, it can be shown that the total corona voltages are given by:

$$V_t(k) = \sqrt{2}\ \{\sum_{\alpha=1}^{3}\sum_{\beta=1}^{3} \frac{U_2(k,\alpha)U_2(k,\beta)}{\gamma_\alpha + \gamma_\beta}\}^{1/2} \quad . \tag{5.169}$$

G. Summary

The modal analysis method has been successful in the determination of corona currents and corona voltages from transposed and untransposed transmission lines. This was possible for the single corona source per phase as well as for the uniformly distributed corona source all over the phases.

Corona currents and corona voltages from the untransposed line and the transposed line represented by the physical model were found analytically to be the same under the uniformly distributed corona source case. Consequently, the EMI level is expected to be the same for both transposed and untransposed lines.

However, corona currents and corona voltages from transposed line simulated by an equivalent model have different form than those determined from the physical model.

A subroutine called 'CORONA' has been elaborated to determine corona currents and corona voltages. 'CORONA' subroutine acquires 'EXFUN' subroutine.

The calculation of the EMI requires the knowledge of the corona currents or corona voltages. This will depend on the method used to evaluate the EMI.

VI. ELECTROMAGNETIC INTERFERENCE FIELD CALCULATION

A. Introduction

At the present time, the quasi static method is used to determine the electromagnetic interference field (EMI). This method has been applied since the line geometry and the distance from the source to the observation or measuring point are generally small compared to the wavelength, λ.

$$\lambda = \frac{\nu}{f} \tag{6.1}$$

where:

λ is the wavelength in (meter).

ν is the wave velocity, $\nu = 3 \times 10^8$ (m/s) for the air.

f is the frequency in Hz.

The quasi static method has been shown to be practically valid for frequencies less than 10 MHz.

Radio noise analysis is usually performed in three steps: (1) generation, (2) propagation, and (3) radiation. The generation process has been already dealt with in Chapter IV through the use of the excitation function. Once corona generation takes place, radio noise energy must travel from its source to the public's receiver. The travel can be accomplished or achieved through propagation of noise as an electromagnetic wave along conductors and then radiation from conductors into the atmosphere. It should be pointed out that at low frequencies, the noise is coupled electromagnetically to the receiver's antenna. At these low frequencies, the noise energy can also be conducted from the

source along the lines, through transformers and/or system neutrals to the receiver power supply.

Although conduction and induction are more important at lower frequencies, radiation becomes more efficient at higher frequencies. Therefore, for higher frequencies, the field noise must be determined by an exact solution of the complex field wave equation. This can be performed by solving a form of Maxwell's equation.

B. Main Characteristics of the Noise Field

Radio noise generated by line corona is the result of many frequency components which make up the corona pulse, the line configuration, the spatial distribution of corona, climatic conditions and the surface state of the conductors.

Within the limit of the quasi static method, the noise energy is induced or partially radiated from the sources. The variations in the intensity or field strength of the radiated noise are usually studied in terms of (1) the spectrum frequency, (2) the lateral survey or profile, and (3) the seasonal noise level distribution. It should be noted, however, that the study of these parameters is mainly based on the assumption that these parameters are mutually independent.

1. Seasonal noise level distribution

EMI generation varies daily and seasonally due to variations in climatic weather conditions such as temperature, pressure, humidity, wind velocity, precipitation frequency and amounts, etc. As weather conditions change, line corona generation changes and consequently EMI

noise changes.

The systematic study of these EMI noise fluctuations necessitates the permanent recording of the field under the line over at least one year. This recording should be done at a fixed distance from the line and with a fixed measuring frequency. Numerous researchers, in many countries, have carried out such measurements [6, 10, 12, 13, 16, 18, 21, 22]. These studies have resolved the climatic conditions into two categories, namely (1) foul weather and (2) fair and dry weather. These can be used as references to define standard noise levels.

In this study of the EMI, the weather parameters have been incorporated in the evaluation of the excitation function in Chapter IV.

2. Noise field frequency spectrum

The spectrum gives the variation of the noise power measured at a given point in the vicinity of a transmission line, as a function of frequency. The noise field is produced by the high frequency current flowing in the conductors. In the range of broadcasting frequencies, the spectrum behaves quite independently of the conductor diameter. This result has been verified by means of experimental tests [22, 55]. On the other hand, it has been shown that the complex signal spectrum which results from the superposition of many stationary random pulses is of the same form as that of the single pulse. This implies that the shape of the spectrum is relatively independent of the shape and number of pulses and also of the surface state of the conductors. Many experiments, in the U.S.A. and abroad, have shown that the spectrum of an interference field does not depend in practice either on lateral

distances from the line or atmospheric conditions [6, 32, 55]. Furthermore, it is roughly the same for all transmission lines.

The other phenomenon involved in the frequency spectrum is the attenuation of propagation. This latter increases with frequency and earth resistivity. This effect reduces the interference noise level with the increase in the frequency. This frequency dependence of the interference level has been incorporated in the calculation of corona currents and corona voltages through the frequency dependence of the electrical transmission line parameters R, L, G, C.

The literature provides some standard spectra which are usually given in relative values. The reference point is taken as either 1 MHz in the U.S.A. or 0.5 MHz in Europe. The 1 MHz frequency was selected because it is near the center of the AM radio stations. It was also stated, in Chapter IV, that the excitation function measurements were established for either a 1 MHz frequency in the U.S.A. or a 0.5 MHz frequency in Europe. Therefore, when EMI corrections at frequencies comparable to 1 MHz are desirable, corrections may be made to account for the differences through the noise field frequency spectrum.

3. Radio noise lateral profile

The EMI lateral survey is the variation of the noise field as a function of the distance from the line. This variation is characterized by a rapid decrease. The profile is determined over a distance not exceeding 200 meters from the center of the HV line. Beyond this point, the RI effect of the lines usually becomes negligible. In practice, the measurement becomes inaccurate beyond 100 meters because

the distance starts to be comparable to the RF wavelength. The measuring or calculating frequency chosen is usually 0.5 MHz (CISPR-Standard) or 1 MHz (ANSI-Standard).

Numerous measurements carried out in the U.S.A. and abroad have enabled a good experimental knowledge of the phenomenon. These experimental results have been confirmed by theoretical calculations within the limits of the quasi static method. Some lateral profiles were proposed for all types of line, from 220 kV to 765 kV. Also, some empirical formulas were proposed to simulate the attenuation law of the noise field as a function of the distance D between the observation point and the outer conductor [47]:

$$E = E_0 \left(\frac{D_0}{D}\right)^k \tag{6.2}$$

where the coefficient k lies between 1.4 and 1.9 according to the line configuration and the resistivity of the soil. This empirical law can be used in the determination of the right of way subject to the interference. However, some more accurate analysis can be used to enable profiles to be plotted as functions of classes of line voltage and configuration. The first method deals with the static field. However, a second method will be introduced to overcome the limitations of the quasi static method.

C. EMI Calculation by the Quasi-Static Method

1. Introduction and assumptions

At the present time, the quasi-static method is widely used to determine the EMI field. The EMI analysis in this section is also

based on static electric fields. The A.C. transmission lines produce so-called quasi-static fields within certain frequency limitations. This method has been applied since the maximum geometrical distances of the lines are small compared to the wavelength, defined by equation 6.1. This means that the distance is small enough that the time required for the fields to propagate from the line to the location is negligible compared to its period. The quasi-static method has been shown to be valid for frequencies less than 10 MHz. The assumptions, for which this method is based on, are:

- No free charge is present.
- The permittivity ε is constant everywhere.
- The method is not valid for fields below the earth's surface.
- The earth is a perfect conductor.
- The lines are perfectly horizontal over a flat plane.
- The earth's resistivity is constant.

2. Electric field computation

The static interference field can be determined by applying Gauss's theorem. If the conducting earth is represented by an image of the conductor carrying a charge equal and opposite to the charge of the conductor, the horizontal and vertical components of the electric field strength, at any point in the space, can be shown to be given by:

$$E_v(k) = E_c(k) \cos(\theta_c(k)) + E_i(k) \cos(\theta_i(k)) \qquad (6.3)$$

$$E_h(k) = -E_c(k) \sin(\theta_c(k)) + E_i(k) \sin(\theta_i(k)) \qquad (6.4)$$

where:

v is the subscript for the vertical component.

h is the subscript for the horizontal component.

c is the subscript standing for the conductor.

i is the subscript standing for the image.

$E_c(k)$ is the electric field due to the physical conductor in phase k only.

$E_i(k)$ is the electric field due to the image of the conductor in phase k only.

$E_v(k)$ is the vertical component due to phase k and its images.

$E_h(k)$ is the horizontal component due to phase k and its images.

$$\text{Cos}(\theta_c(k)) = \frac{(h(k) - y(k))}{d_c(k)} \tag{6.5}$$

$$\text{Cos}(\theta_i(k)) = \frac{(h(k) + y(k))}{d_i(k)} \tag{6.6}$$

$$\text{Sin}(\theta_c(k)) = \frac{x(k)}{d_c(k)} \tag{6.7}$$

$$\text{Sin}(\theta_i(k)) = \frac{x(k)}{d_i(k)} \tag{6.8}$$

$$d_c(k) = \sqrt{(h(k) - y(k))^2 + (x(k))^2} \tag{6.9}$$

$$d_i(k) = \sqrt{(h(k) + y(k))^2 + (x(k))^2} \tag{6.10}$$

where h, y, x, d_i, d_c, θ_i, θ_c are geometrical parameters described in Fig. 6.1, for an arbitrary phase k. The electrical fields $E_c(k)$ and $E_i(k)$ are given by:

$$E_c(k) = \alpha_1 \frac{Q(k)}{d_c(k)} \tag{6.11}$$

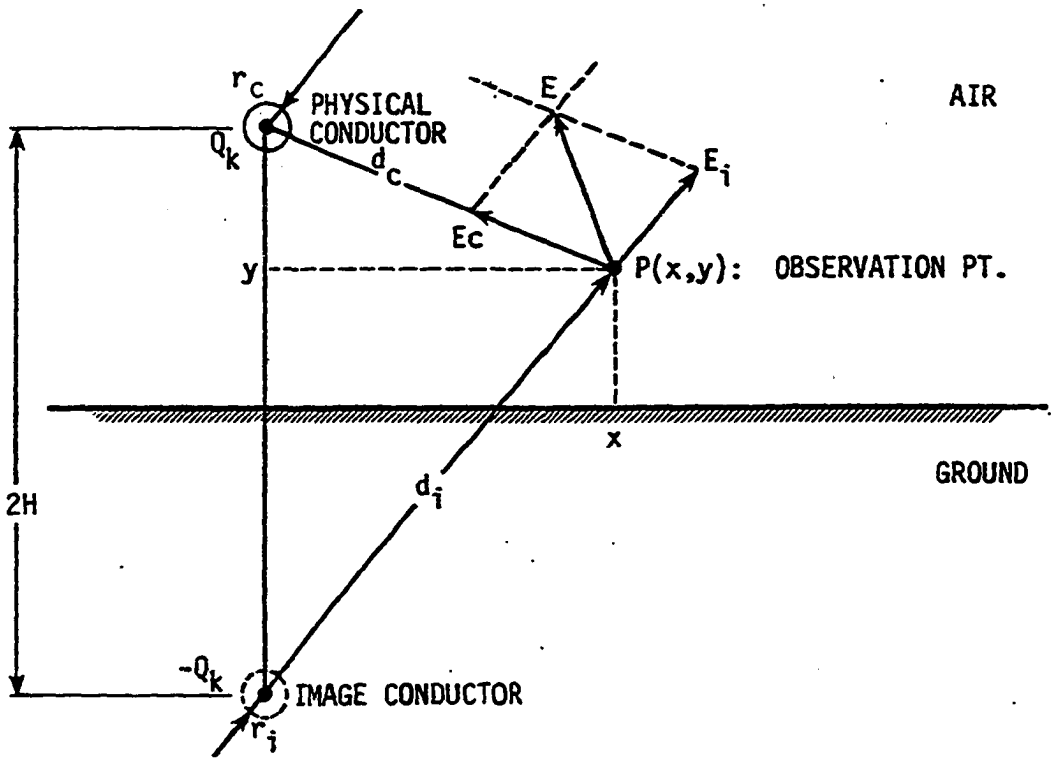

Fig. 6.1. Geometry for calculation of the electric field strength at any point P (x.y)

$$E_i(k) = -\alpha_1 \frac{Q(k)}{d_i(k)} \quad . \tag{6.12}$$

The substitution of equations 6.5 to 6.12 into 6.3 and 6.4 would yield the EMI horizontal and vertical components to be:

$$E_v(k) = \alpha_1 Q(k) \left[\frac{(h(k) - y(k))}{d_c^2(k)} + \frac{(h(k) + y(k))}{d_i^2(k)}\right] \tag{6.13}$$

$$E_h(k) = \alpha_1 Q(k) \left[\frac{1}{d_i^2(k)} - \frac{1}{d_c^2(k)}\right] \times (k) \quad . \tag{6.14}$$

The general relation used to calculate the line charges carried out by the conductors of a multiphase line is the following matrix equation:

$$[Q] = [C][V] \tag{6.15}$$

where:

[Q] is a one column matrix of charges on the conductors.

[V] is a one column corona voltage whose elements are given in Chapter V by equation 5.145 for the untransposed and equations 5.156 or 5.169 for the transposed case under the uniformly distributed corona source condition.

[C] is the capacitance matrix. It is given by:

$$[C] = [P]^{-1} \quad .$$

[P] is the potential coefficient matrix whose elements are given in Chapter III.

The elements of the matrix [P] were obtained in Chapter III by direct application of the theory of images where the ground, considered

at zero potential, is replaced by the image of the conductors with respect to the ground plane.

It should be pointed out that for

$$d_i(k) = d_c(k) \quad , \tag{6.16}$$

the horizontal component $E_h(k)$ becomes zero. The total ground level EMI field from each plane, under this specific condition, would be

$$E(k) = E_v(k) \quad . \tag{6.17}$$

In general, the total static EMI field per phase, at any spatial point above ground, is:

$$E(k) = \sqrt{(E_v(k))^2 + (E_h(k))^2} \quad . \tag{6.18}$$

From equation 6.15, the per phase charges per unit length can be computed:

$$Q(k) = C(k,1)\ V(1) + C(k,2)\ V(2) + C(k,3)\ V(3) \quad . \tag{6.19}$$

The knowledge of the capacitances and that of the corona voltages would enable the calculation of the EMI field per phase, at any point in the space, for the untransposed transmission line as well as for the transposed ones. Once the EMI field per phase is computed, the total EMI field from the multiphase transmission line would then be given by the square law:

$$E = \sqrt{\sum_{k=1}^{p} (E(k))^2} \quad . \tag{6.20}$$

Equation 6.20 is valid under the assumption that corona sources are random and therefore their effects are uncorrelated.

Considering the quasi static method, U.S. standards state that the EMI lateral survey is measured or calculated at 1 MHz. The wavelengths of traveling waves near this frequency are generally large compared to the line geometry and the distance from the measuring point.

When frequencies are relatively comparable to 1 MHz, corrections may be made to account for the differences [6, 22]. These corrections are based on the noise field frequency spectrum. A computer algorithm was developed to compute the static EMI field at any frequency. However, for higher frequencies, this method would no longer be applicable. A new method is needed to overcome the limitations of the quasi static method. Such a method will be introduced and developed in the next section.

D. EMI Calculation by the Radiation Method

The radiation method has been introduced to overcome the limitations of the quasi static method. The radiation method extends and validates the study of the EMI field spectrum to FM broadcast band and television frequencies. It is based primarily on the solution of Maxwell's equations.

1. Field equation formulation

The interaction of charges and currents on conductors in space is governed by the well-known Maxwell-Lorentz equations which define the electromagnetic field. These equations are basically expressed by

[43, 56-58]:

$$\nabla \times \overline{E} + \frac{\partial \overline{B}}{\partial t} = 0 \tag{6.21}$$

$$\nabla \times \overline{H} - \frac{\partial \overline{D}}{\partial t} = \overline{J} \tag{6.22}$$

$$\nabla \cdot \overline{D} = \rho \tag{6.23}$$

$$\nabla \cdot \overline{B} = 0 \tag{6.24}$$

where:

$\overline{E}$ is the electric field intensity vector.

$\overline{B}$ is the magnetic flux density vector.

$\overline{D}$ is the electric flux density vector.

$\overline{H}$ is the magnetic field intensity vector.

$\overline{J}$ is the source or impressed current density vector.

ρ is the charge density.

The charge density ρ and the current density vector $\overline{J}$ are related by the equation of continuity or conservation of charge.

$$\nabla \cdot \overline{J} + \frac{\partial}{\partial t} \rho = 0 \quad . \tag{6.25}$$

Equations 6.21 to 6.25 are not sufficient to determine the electromagnetic fields. They have to be supplemented by some constitutive equations. The constitutive laws show how the field is related to the properties of the medium. For this study, the medium is air. In fact, the simplest constitutive equations occur in free space, where:

$$\overline{D} = \varepsilon_0 \overline{E} \tag{6.26}$$

$$\overline{B} = \mu_0 \overline{H} \tag{6.27}$$

where μ_0 and ε_0 are called, respectively, the permeability constant and the permittivity constant of the air. They are related by:

$$v = \sqrt{\frac{1}{\mu_0 \varepsilon_0}} \tag{6.28}$$

where v is the speed of light. In the SI system which will be employed here, the above constants are:

$$\mu_0 = 4\pi\ 10^{-7} \qquad \text{Henry/meter} \tag{6.29}$$

$$\varepsilon_0 = \left(\frac{1}{36\pi}\right)\ 10^{-9} \qquad \text{Farad/meter} \tag{6.30}$$

$$v = 3\ 10^{8} \qquad \text{meter/second} \ . \tag{6.31}$$

For a conductor case, Ohm's law holds in the form:

$$\overline{J} = \sigma\, \overline{E} \tag{6.32}$$

where σ is known as the conductivity in Siemens/meter.

Fields which are produced by currents and charges whose variation with the time, t, are simple harmonic functions are of considerable importance in practice. If ε, μ and σ are independent of the time, Maxwell's equations and the constitutive laws are linear. Thus, the superposition principle may be applied, if necessary. It, therefore, is possible to write:

$$\overline{E} = \overline{E}_H\, e^{j\omega t} \tag{6.33}$$

$$\overline{H} = \overline{H}_H\, e^{j\omega t} \ . \tag{6.34}$$

Accordingly, Maxwell's equations for harmonic fields, $\bar{E}_H$ and $\bar{H}_H$, subject to equations 6.26 and 6.27, can be written as:

$$\nabla \times \bar{E}_H + j\omega\mu \bar{H}_H = 0 \tag{6.35}$$

$$\nabla \times \bar{H}_H - j\omega\epsilon \bar{E}_H = \bar{J}_H \tag{6.36}$$

$$\nabla \cdot (\epsilon \bar{E}_H) = \rho_H \tag{6.37}$$

$$\nabla \cdot (\mu \bar{H}_H) = 0 \tag{6.38}$$

$$\nabla \cdot \bar{J}_H + j\omega\rho_H = 0 \quad . \tag{6.39}$$

It is worthwhile to notice that the time dependence has been eliminated through the use of equations 6.33 and 6.34. Equations 6.35 to 6.39 are the Maxwell's equation in the frequency domain. Those equations would have been derived easily through the use of Fourier transform applied to equations 6.21 to 6.25.

For $\omega \neq 0$, the divergence of equation 6.35 yields 6.38 and the divergence of equation 6.36 gives 6.37 when equation 6.39 is taken into account. Therefore, for harmonic fields, which are non-static, it is sufficient to employ equations 6.35 and 6.36 in addition to equation 6.39.

The relevant boundary conditions at interface between a conductor (subscript c) and the air (subscript a) are expressed in terms of the tangential and normal components of the electric and magnetic fields. These boundaries are:

$$\hat{n}_c \times \bar{E}_c + \hat{n}_a \times \bar{E}_a = 0 \tag{6.40}$$

$$\hat{n}_c \times \bar{H}_c + \hat{n}_a \times \bar{H}_a = +\bar{J}_s \quad . \tag{6.41}$$

$$\hat{n}_c \cdot \bar{D}_c + \hat{n}_a \cdot \bar{D}_a = +\rho_s \tag{6.42}$$

$$\hat{n}_c \cdot \bar{B}_c + \hat{n}_a \cdot \bar{B}_a = 0 \tag{6.43}$$

where:

$\hat{n}_i$ is the unit vector outward normal to region i.

$\bar{J}_s$ is the density of surface current in amperes per meter on the conductor.

ρ_s is the density of surface charge in coulombs per square meter on the conductor.

In this study, medium c is a perfect conductor; therefore:

$$\bar{E}_c = 0 \tag{6.44}$$

$$\bar{B}_c = 0 \quad . \tag{6.45}$$

Then equations 6.40 to 6.43 simplify to:

$$\hat{n}_a \times \bar{E}_a = 0 \tag{6.46}$$

$$\hat{n}_a \times \bar{B}_a = +\mu_0 \bar{J}_s \tag{6.47}$$

$$\hat{n}_a \cdot \bar{E}_a = +\frac{\rho_s}{\varepsilon_0} \tag{6.48}$$

$$\hat{n}_a \cdot \bar{B}_a = 0 \quad . \tag{6.49}$$

At a boundary which separates one medium from another, the parameters μ, ε and σ might change sharply. Then, it is necessary to have formulas which convert the fields on the two sides of the boundary. These boundary conditions are given by equations 6.40 to 6.43 in the general case or equations 6.46 to 6.49 if one of the medium is characterized by a

perfect conductor. Those equations state that:

(1) The component of the electric field in air tangent to the surface of a perfect conductor must be zero.

(2) The tangential magnetic field in air, at the surface of a perfect conductor, is proportional to the surface density of current in the conductor.

(3) The change in the normal component of $\overline{D}$ is equal to the surface charge density.

(4) The change in the normal component of $\overline{B}$ is nil.

Under these conditions, the solution of the electromagnetic problem can be shown to be unique [59].

A convenient method of solving the vector partial differential equations 6.35 to 6.39 is with the use of the scalar and vector potentials, ϕ and $\overline{A}$. The defining relationships between the potentials and the electromagnetic field vectors are obtained with the aid of Maxwell's equations. In a homogeneous medium, equation 6.38 implies

$$\nabla \cdot \overline{H} = 0 \quad . \tag{6.50}$$

Therefore, the magnetic field intensity, $\overline{H}$, can be chosen as follows:

$$\overline{H} = \nabla \times \overline{A} \tag{6.51}$$

where $\overline{A}$ is the magnetic vector potential.

If equation 6.51 is substituted in equation 6.35, it follows that:

$$\nabla \times (\overline{E} + j\omega\mu\, \overline{A}) = 0 \quad . \tag{6.52}$$

This equation (6.52) implies that one can define a scalar potential ϕ as:

$$\nabla\phi = - [\bar{E} + j\omega\mu \bar{A}] \quad . \tag{6.53}$$

The substitution of equation 6.51 and 6.53 into the remaining Maxwell's equations leads a mixed vector equation for $\bar{A}$ and ϕ.

$$\nabla \times \nabla \times \bar{A} - \zeta \bar{A} = \bar{J} - j\omega\varepsilon\nabla\phi \tag{6.54}$$

where:

ζ is called the wave number and is given by:

$$\zeta^2 = \omega^2\mu\varepsilon \ . \tag{6.55}$$

It is also related to the wavelength λ by:

$$\zeta = \frac{2\pi}{\lambda} \quad . \tag{6.56}$$

Equation 6.54 can be written in the following form:

$$\nabla(\nabla\cdot\bar{A}) - \nabla^2\bar{A} - \zeta^2\bar{A} = \bar{J} - j\omega\varepsilon \nabla\phi \ . \tag{6.57}$$

The variables $\bar{A}$ and ϕ can be separated if we use the Lorentz gauge condition, which is:

$$\nabla\cdot\bar{A} = -j\omega\varepsilon\phi \quad . \tag{6.58}$$

The resulting vector Helmholtz equations for $\bar{A}$ and ϕ in air are:

$$\nabla^2\bar{A} + \zeta^2\bar{A} = -\bar{J} \tag{6.59}$$

$$\nabla^2\phi + \zeta^2\phi = 0 \quad . \tag{6.60}$$

The solutions of equations 6.59 and 6.60 give $\bar{A}$ and ϕ. Consequently, the electric field $\bar{E}$ and the magnetic field $\bar{H}$ will be determined easily from:

$$\bar{H} = \nabla \times \bar{A} \tag{6.61}$$

$$\bar{E} = -j\omega\mu\bar{A} + (j\omega\varepsilon)^{-1} \nabla(\nabla\cdot\bar{A}) \quad . \tag{6.62}$$

The magnetic vector potential $\bar{A}$ was introduced mainly for two reasons: (1) the rectangular components of $\bar{A}$ correspond to those of the source $\bar{J}$, and (2) the magnetic vector potential need not be divergenceless.

2. General solution to the Helmholtz wave equation

Since transmission lines are composed of conductors aligned in the z-direction in space, it is sufficient to use the axial component of the magnetic vector $\bar{A}$.

$$\bar{A} = A_z \hat{a}_z \tag{6.63}$$

where:

$\hat{a}_z$ is the unit vector in the z-direction.

A_z is the z-component of $\bar{A}$.

Then, the vector complex wave equation (6.59) will be reduced to a scalar form:

$$\nabla^2 A_z + \zeta^2 A_z = - J_z \quad . \tag{6.64}$$

Particular integrals of equations 6.60 and 6.64 are directly derivable with the use of the free space Green's function. The solutions, in an

integral form, for A_z and ϕ, in the infinitely long transmission line case whose diameter, d, is small compared to the wavelength would be:

$$A_{zk} = \frac{1}{4\pi} \int_{-\infty}^{\infty} I_k(z') \frac{e^{-j\zeta R(z')}}{R(z')} \, dz' \tag{6.65}$$

$$\phi_k = \frac{1}{4\pi} \int_{-\infty}^{\infty} Q_k(z') \frac{e^{-j\zeta R(z')}}{R(z')} \, dz' \tag{6.66}$$

where:

$I_k(z)$ is the RI corona current in phase k.

$Q_k(z)$ is the charge per unit length in phase k

with

$$\Sigma = \pi \frac{d^2}{4} \tag{6.67}$$

defined as the area of the cross-section, the current is given by

$$I_k(z) = \int_{\Sigma} J_z d\Sigma + \pi d \, J_s \tag{6.68}$$

and the charge per unit length is:

$$Q_k(z) = \pi d \, \rho_s \tag{6.69}$$

where:

J_s is the total axial current.

$J_z = 0$, for a perfect conductor.

ρ_s is the total surface charge density.

$R(z')$ is the distance from the source point to the point of observation and is given by:

$$R(z') = \sqrt{(\rho - \rho')^2 + (z - z')^2} \tag{6.70}$$

(ρ', ϕ', z') and (ρ, ϕ, z) are respectively the source cylindrical coordinates and the observation cylindrical coordinates. Fig. 6.2 defines explicitly these coordinates.

For a perfect conductor, $J_z = 0$ and the one-dimensional Lorentz gauge condition (equation 6.58) becomes

$$\frac{dA_z}{dz} = -j\omega\varepsilon\phi \quad . \tag{6.71}$$

The continuity equation (6.39) expresses the condition of conservation of change. It is of the form:

$$\frac{dI}{dz} = -j\omega q \quad . \tag{6.72}$$

Then, finally, the electric field $\overline{E}$ and the magnetic field $\overline{H}$ for an infinitely long line are obtained from equations 6.61 and 6.62. In the cylindrical coordinates (ρ, ϕ, z), these fields are given by:

$$\overline{H} = H_\phi \, \hat{a}_\phi \tag{6.73}$$

$$\overline{E} = E_\rho \, \hat{a}_\rho + E_z \, \hat{a}_z \tag{6.74}$$

where their components are given by:

$$H_\phi = -\frac{\partial A_z}{\partial \rho} \tag{6.75}$$

$$E_\rho = -\frac{j}{\omega\varepsilon} \frac{\partial^2 A_z}{\partial \rho \partial z} \tag{6.76}$$

$$E_z = -j\omega\mu \, A_z - \frac{j}{\omega\varepsilon} \frac{\partial^2 A_z}{\partial z^2} \quad . \tag{6.77}$$

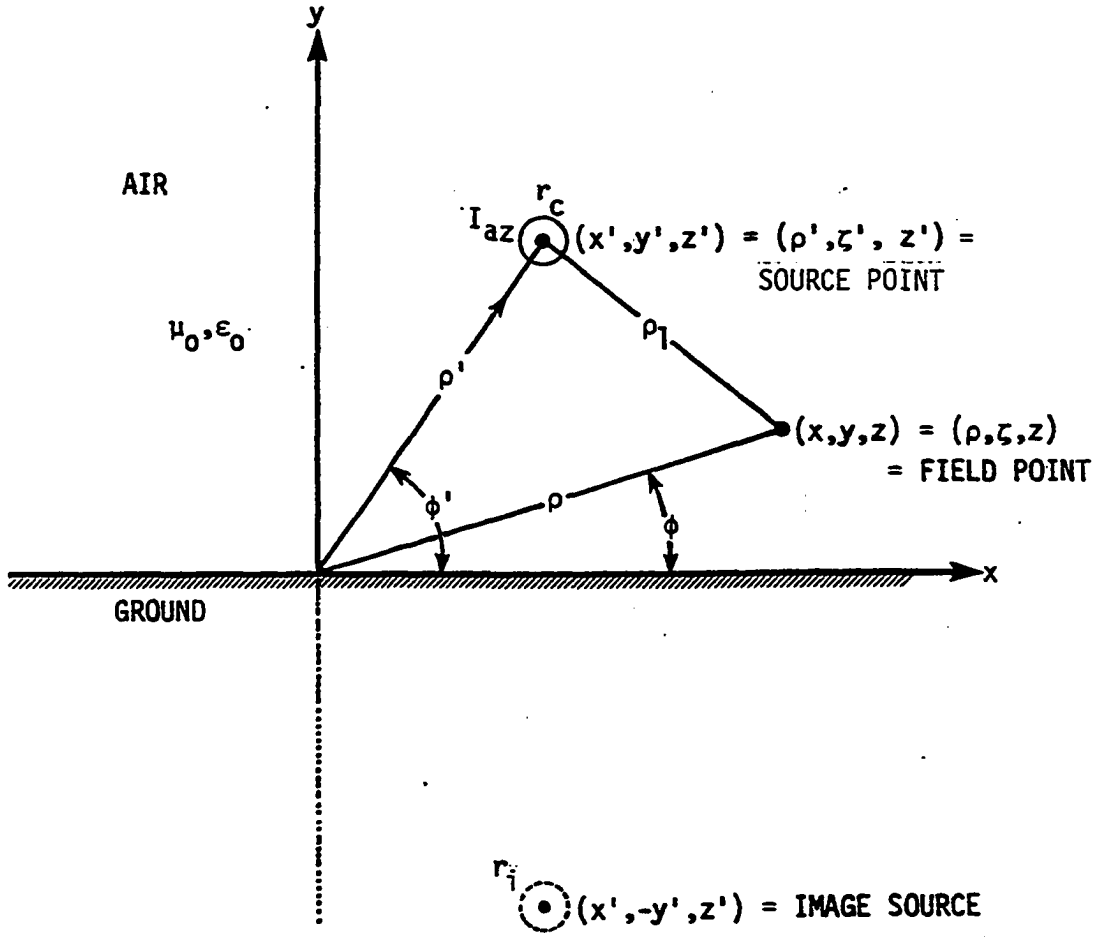

Fig. 6.2. Geometry for calculation of the interference field by radiation method

3. EMI calculation for a single corona source

For a single corona source per phase, HF corona currents over the transmission line conductors are of a decaying exponential type current. They are explicitly of the form of

$$I_k(z) = W(k,1)\ e^{-\gamma 1 z} + W(k,2)\ e^{-\gamma 2 z} + W(k,3)\ e^{-\gamma 3 z} \qquad (6.78)$$

for the untransposed transmission line and of the form of:

$$I_k(z) = (W_q(k,1) + zW_q(k,3))\ e^{-\gamma 1 z} + W_q(k,2)\ e^{-\gamma 2 z} \qquad (6.79)$$

for the completely transposed transmission line represented by the equivalent model.

By inserting these equations into equation 6.65, the z-directed magnetic vector potential can then be determined. However, due to the mathematical complication in the integration process, numerical integration techniques may be required.

The substitution of the magnetic vector vector potential into equations 6.75 to 6.77 will enable the determination of the electric and magnetic field components and consequently the electromagnetic interference field will be easily known from equations 6.73 and 6.74.

Since the single corona source is not of practical use, the interference field would not be explicitly calculated in this research.

4. EMI calculation for a uniformly distributed corona source

To determine the z-directed magnetic vector potential in the uniformly-distributed corona source over all the multiphase transmission line, either of equations 5.144 or 5.155 would be substituted for the

current into equation 6.65. It was shown that the EMI corona currents and voltages, in this specific case, are also uniformly distributed. Therefore, they are space independent. This space independency property enables the exact determination of the magnetic vector potential by direct, analytical methods.

The corona currents are explicitly of the form:

$$I_t(k) = \sqrt{2}\ \{\sum_{i=1}^{3}\sum_{j=1}^{3}[\frac{W(k,i)W(k,j)}{\gamma(i)+\gamma(j)}]\}^{1/2} \tag{6.80}$$

for the untransposed case and

$$I_t(k) = \sqrt{2}\ \{\frac{W_q(k,1)W_q(k,2)}{4(\gamma(1))^3} + \frac{2W_q(k,1)W_q(k,2)}{(\gamma(1)+\gamma(2))^2} + \frac{W_q(k,2)W_q(k,2)}{2\gamma(2)} + \frac{2W_q(k,2)W_q(k,3)}{(\gamma(2)+\gamma(1))} + \frac{W_q(k,1)W_q(k,3)}{4(\gamma(1))^2} + \frac{W_q(k,3)W_q(k,3)}{2\gamma(3)}\}^{1/2} \tag{6.81}$$

for the transposed case represented by an equivalent model, or

$$I_t(k) = \sqrt{2}\ \{\sum_{\alpha=1}^{3}\sum_{\alpha=1}^{3}\frac{W_2(k,\alpha)W_2(k,\beta)}{\gamma_\alpha+\gamma_\beta}\}^{1/2} \tag{6.82}$$

for the transposed case represented by the physical model.

The substitution of either one of the above corona currents into equation 6.65 will yield

$$A_{zk} = \frac{I_t(k)}{4\pi}[\int_{-\infty}^{\infty}\frac{e^{-j\zeta R(z')}}{R(z')}\,dz'] \quad . \tag{6.83}$$

From the table of integrals [40], with ρ_{1k} defined by 6.91, we get

$$A_{zk} = \frac{I_t(k)}{4\pi}\ [-j\pi\ H_0^{(2)}(\zeta\rho_{1k})] \tag{6.84}$$

or

$$A_{zk} = \frac{-jI_t(k)}{4} H_0^{(2)}(\zeta\rho_{1k}) \quad . \tag{6.85}$$

Thus, the determination of the magnetic vector potential, for either a transposed or an untransposed transmission line, has been accomplished with the introduction of the standard zero order Hankel function of the second kind denoted by $H_0^{(2)}(x)$.

For this practical case, the component of the electric and magnetic field per phase are:

$$E_{\rho k} = 0 \tag{6.86}$$

$$E_{\phi k} = 0 \tag{6.87}$$

$$E_{zk} = -\omega\mu\left(\frac{I_t(k)}{4}\right)H_0^{(2)}(\zeta\rho_{1k}) \tag{6.88}$$

$$H_{\rho k} = 0$$

$$H_{\phi k} = -j\left(\frac{I_t(k)}{4}\right)\zeta\, H_1^{(2)}(\zeta\rho_{1k}) \tag{6.89}$$

$$H_{zk} = 0 \tag{6.90}$$

where:

$H_1^{(2)}(\zeta\,\rho_{1k})$ is the second kind, first order Hankel function.

$$\rho_{1k} = \rho_k - \rho_k' \quad . \tag{6.91}$$

The total electromagnetic interference field will then be due to the contribution of all phases:

$$EMI = \sqrt{\sum_{i=1}^{p} (E(k))^2} \quad . \tag{6.92}$$

The small-argument and the large-argument of the second kind, zero order Hankel function are given by equations 6.93 and 6.94, respectively.

$$H_0^{(2)}(\zeta\rho) \cong 1 + j\frac{2}{\pi}\log_{10}\left(\frac{2}{1.781\ \zeta\rho}\right) \tag{6.93}$$

$$H_0^{(2)}(\zeta\rho) \cong \sqrt{\frac{2j}{\pi\zeta\rho}}\ e^{-j\zeta\rho} \quad . \tag{6.94}$$

E. Summary

In this chapter, the EMI is evaluated based on the knowledge of the corona currents or corona voltages.

The EMI was investigated by a newly developed method as well as by the use of the classical method. The classical procedure is based on the quasi-static method. However, the newly developed method is based primarily on the solution of Maxwell's equations. This newly developed method is called the radiation method. The radiation method is characterized by the calculation of the near field as well as the far field. Therefore, there are no limitations, whatsoever, with regard to the wavelengths of the traveling waves compared to the geometry of the line and the distance from the measuring point. Consequently, since there exists a relationship between the wavelength and the frequency, there will be no limitations on the frequency range as well. This implies that the radiation method extends and validates the study of the EMI spectrum to the FM radio and television range of frequencies.

Two algorithms were developed to compute the EMI level by the quasi-static method and the EMI level determined by the radiation method. The subroutines are called 'QUASI' and 'RADIA', respectively.

Fig. 6.3 exhibits the flowchart for the determination of the electromagnetic interference field.

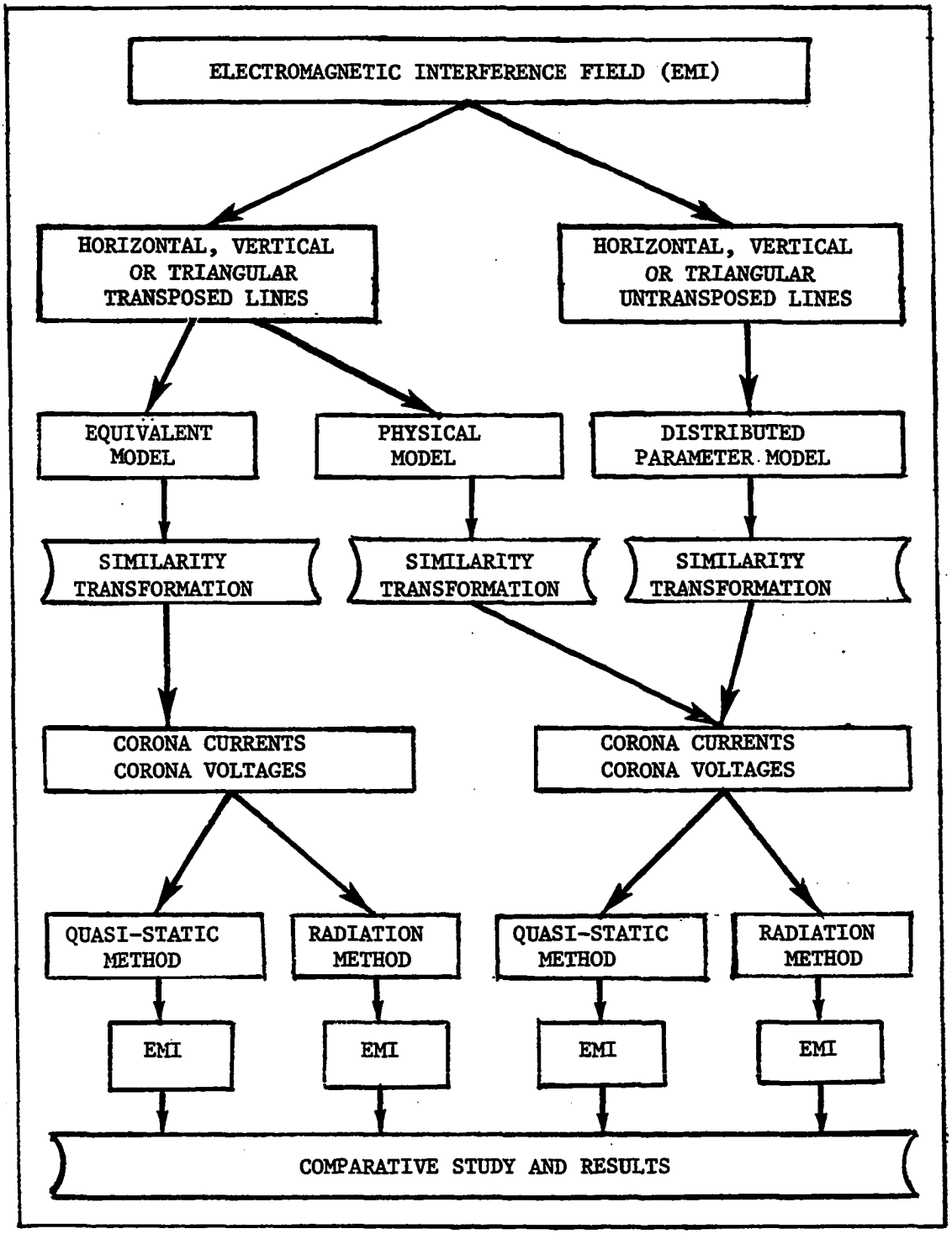

Fig. 6.3. Flowchart for the calculation of the EMI

VII. RESULTS AND CONCLUSIONS

A. Model Comparison

An analysis of the EMI for transposed and untransposed transmission lines has been presented. The untransposed line was modeled by series impedance and shunt admittance which are uniformly distributed throughout the length of the line. However, the transposed line was represented by two different models. The first model, called the equivalent model, consists of taking an average equivalent series impedance and an average equivalent shunt admittance of the three sections of the line. The second model, named the physical model, takes into consideration the physical configuration of the line by matching the boundary conditions at each section through the use of the rotation matrix.

Although the equivalent model is common practice, it is not completely consistent. But it is far simpler than the physical model. However, it should be mentioned that the physical model is a better way to do averaging for the line sections, though it is tedious. It can be best done with the use of digital computer.

Corona currents and corona voltages from untransposed line and transposed line simulated by the physical model have been shown to be analytically the same under the uniformly distributed corona source assumption. Therefore, the EMI level from the transposed line simulated by the physical model and untransposed line is going to be identically the same.

B. Results

The interference fields were computed for various transmission line configurations (Figs. 7.1 and 7.2) using the newly developed method and the classical method. An algorithm program was generated. This algorithm requires input data such asthe conductor radius, the coordinates of each conductor, the earth resistivity, the frequency and the voltage level.

It was previously mentioned that the EMI level from the transposed line, simulated by the physical model, is quantitatively the same as the EMI level from the untransposed line. Therefore, there is no need to do any comparative study based on the physical model of transposition.

However, it is worthwhile to compare the EMI level from the transposed line, represented by the equivalent model, to the EMI level from the untransposed line. This comparison will enable us to determine the validity of the equivalent model at different frequencies and for different configurations.

For the purpose of clarification, it is emphasized that transposition is going to be simulated by an equivalent model throughout this section.

Subsequent subsections in this section compare the effects of different factors on the EMI. These factors are:

(1) Configuration of the line;

(2) Transposition simulated by an equivalent model;

(3) Bundling; and

(4) Frequency.

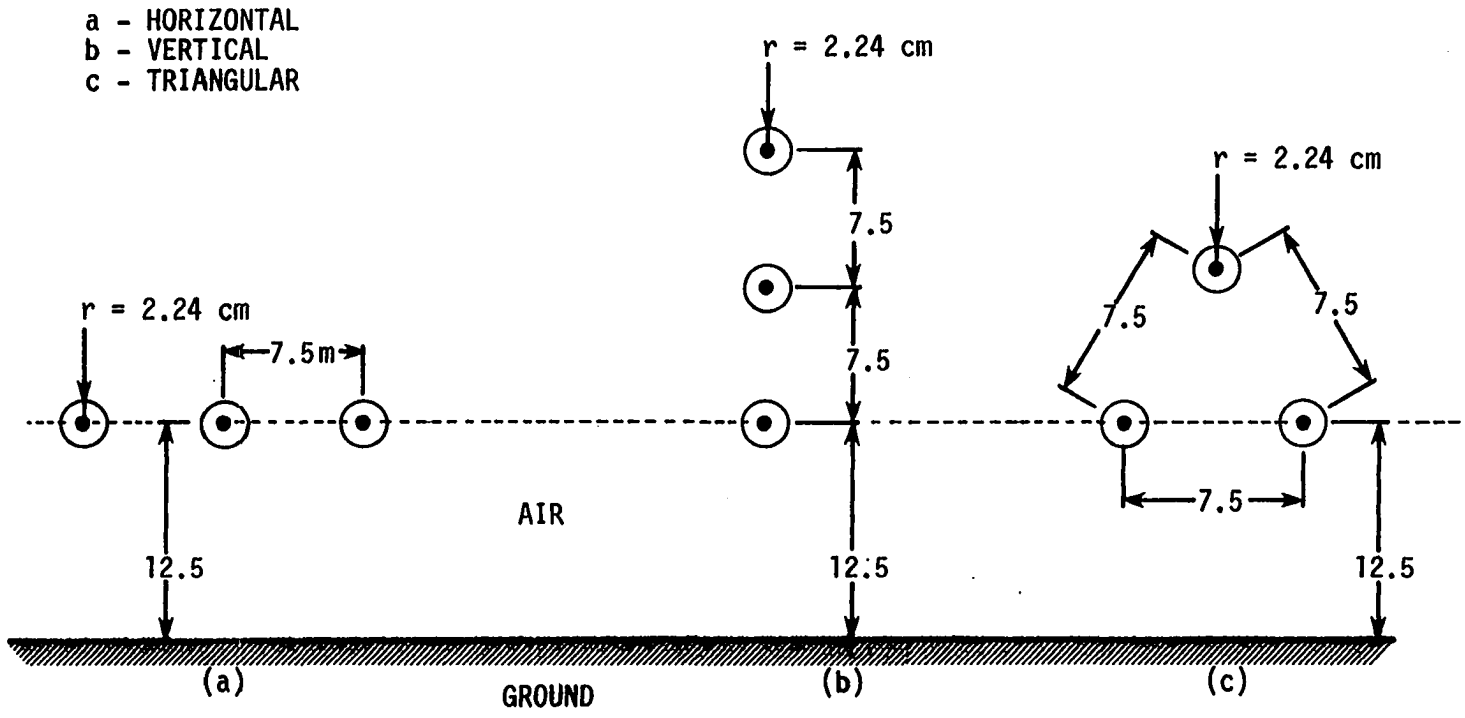

Fig. 7.1. Different geometrical configuration for 362 KV line single circuit (N = 1)

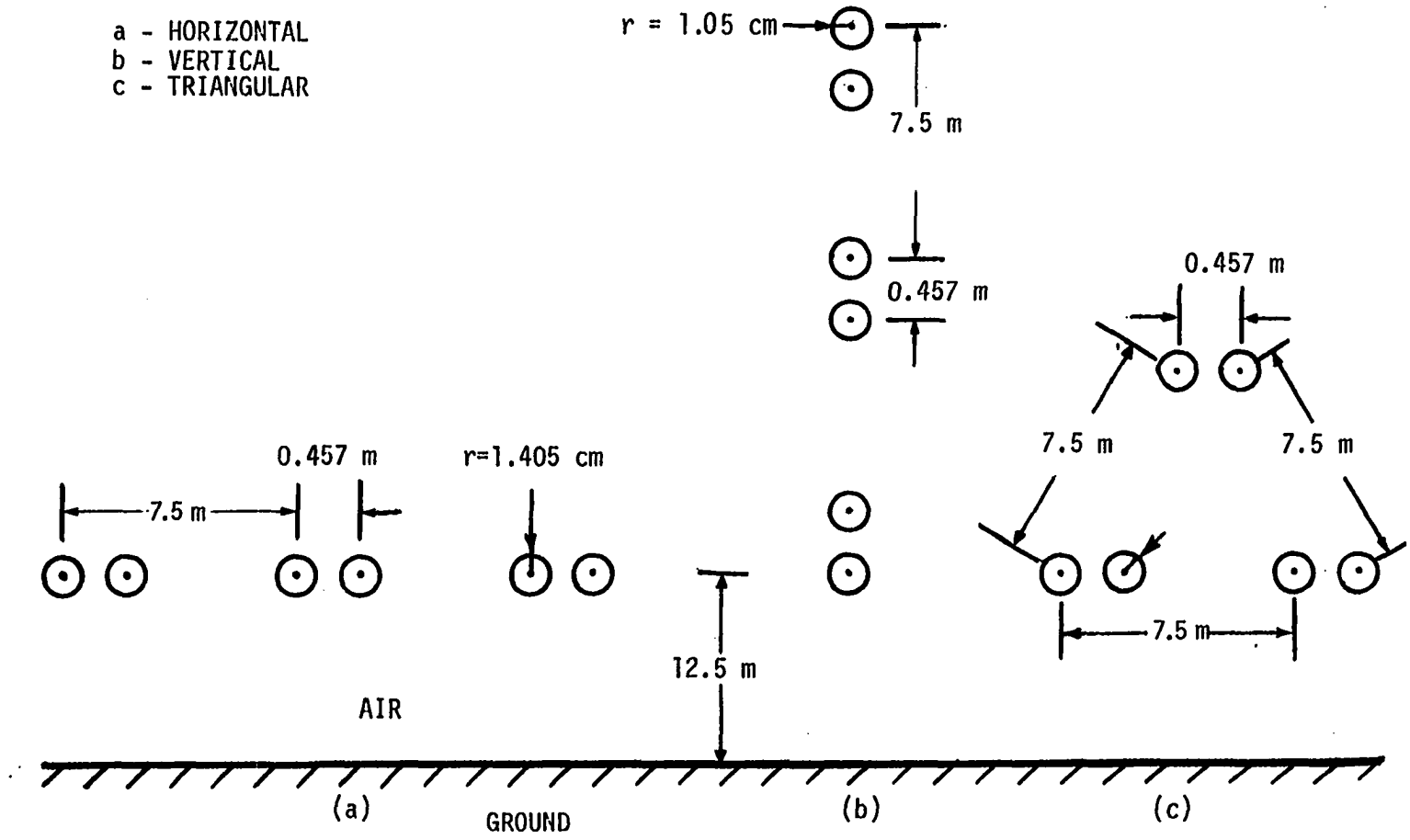

Fig. 7.2. Different geometrical configuration for 362 kV line single circuit (N = 2)

The comparative study will be done in parallel for the EMI level computed by the quasi-static method as well as that computed by the radiation method under the above consideration.

1. Effect of configuration of the line

The results for a 362-kV transmission line (Shown in Fig. 7.1) are presented in Figs. 7.3-7.6 for the untransposed case and Figs. 7.7-7.10 for the transposed case simulated by the equivalent model based on the quasi-static method. The results for the untransposed case are very close to most of the measured and calculated fields by many other authors, namely G. E. Adams in the U.S.A. and C. Gary and M. Moreau in Europe.

The general pattern of the lateral surveys computed thus far are similar in the three configurations and coincide with published results.

For the untransposed case, Fig. 7.6 displays a comparative study of the three configurations at 0.5 MHz and 5 MHz. At a distance less than 30 m from the center line, the EMI level from the horizontal configuration is found to be slightly higher than the EMI level from the other two configurations. However, for distances greater than 30 m, the EMI level from the vertical and the triangular configurations is found to be slightly higher than the EMI level in the horizontal configuration. These results are consistent with the study done by G. E. Adams and others.

Fig. 7.10 shows a comparative study of the three configurations at 0.5 MHz and 5 MHz for the transposed transmission line simulated by an equivalent model. Similar conclusions hold true as the ones derived from Fig. 7.6.

The comparative study of the three configurations for the EMI level, computed by the radiation method, from transposed and untransposed lines is exhibited in Tables 7.1-7.4. These tables show that there is no significant difference in the EMI level at low frequencies (≤5 MHz). The difference is less than two decibels. However, at high frequencies, the difference is quite fluctuating. These fluctuations are more pronounced for the transposed lines. This result implies that the equivalent model of the transposition is not suitable for this purpose at high frequencies.

2. Effect of transposition

Based on the quasi-static method, the EMI level from untransposed transmission lines and transposed transmission lines simulated by the equivalent model is practically the same in the three different configurations. More precisely, the EMI level from the transposed lines is less than one decibel lower than the EMI level computed from the transposed case. Therefore, there is no advantage in using transposed transmission lines as far as the improvement of the EMI is concerned. Figs. 7.11-7.13 show these results explicitly for the three configurations at 0.5 MHz and 5 MHz. It was stated and analytically proven that the untransposed line as well as the transposed line simulated by the physical model give exactly the same EMI level.

At low frequencies, the radiation method also shows that the EMI level computed from the transposed lines simulated by the equivalent model is very close to that computed from the untransposed lines. However, this result is no longer valid at high frequencies. Again, this

disproves the validity of the equivalent model for the transposition. Tables 7.5-7.6 exhibit the above results for the effect of transposition, simulated by an equivalent model, on the EMI level using the radiation method.

3. Effect of bundling

The results for the same 362-kV transmission line but composed of bundled conductors (N=2) are shown in Figs. 7.14-7.16 for the untransposed case and in Figs. 7.17-7.19 for the transposed, simulated by an equivalent model, case based on the quasi-static method.

The EMI level for the 362-kV line with two subconductors per phase has been found to be less than the EMI level for the 362-kV line with one conductor per phase. This result is shown in Tables 7.7-7.8 at 0.5 MHz and 5 MHz. There is on the average a 4-dB difference.

The EMI level computed by the radiation method for the 362-kV line with two subconductors per phase has also been found to be less than the EMI level for the 362-kV line with a single conductor per phase. Tables 7.9-7.10 exhibit this result for two frequencies, namely 1 MHz and 100 MHz. The difference is still about 4 dB at low frequencies. However, the difference is quite fluctuating at high frequencies.

4. Effect of frequency

Based on the quasi-static method, the EMI spectrum decreases as the frequency increases for a given lateral distance. This is totally in concordance with all published results. The reader is referred to Figs. 7.3-7.5, Figs. 7.7-7.9, Figs. 7.14-7.16, and Figs. 7.17-7.19 for the

quasi-static EMI level. However, the radiated EMI level spectrum does not follow the same pattern as the quasi-static EMI level spectrum.

It can be seen from Tables 7.11-7.22 that the radiated EMI level spectrum passes through a series of minima and maxima as the frequency increases.

Figs. 7.20-7.25 display the relationship between the radiated EMI level and the distance from the centerline at different frequencies. It is worthwhile to notice that as the frequency increases, the number of minima and maxima increases. A similar result has been found from the measurement done by the CIGRE working group 36.01 at television frequencies shown in Fig. 7.26.

C. Conclusions

An analysis of the EMI for transposed and untransposed transmission lines has been presented. Transposition has been simulated by two different models, namely the equivalent model and the physical model.

In this research, the modal or similarity transformation method was extended to include the frequency dependence of the electrical transmission line parameters as well as the resistivity of the earth. The use of this modal analysis made it possible to determine the HF corona currents and HF corona voltages due to a single corona source or to a uniformly distributed transmission line corona.

It has been analytically found that the HF corona currents and HF corona voltages from the untransposed line and transposed line represented by the physical model are the same under the uniformly distributed corona source assumption.

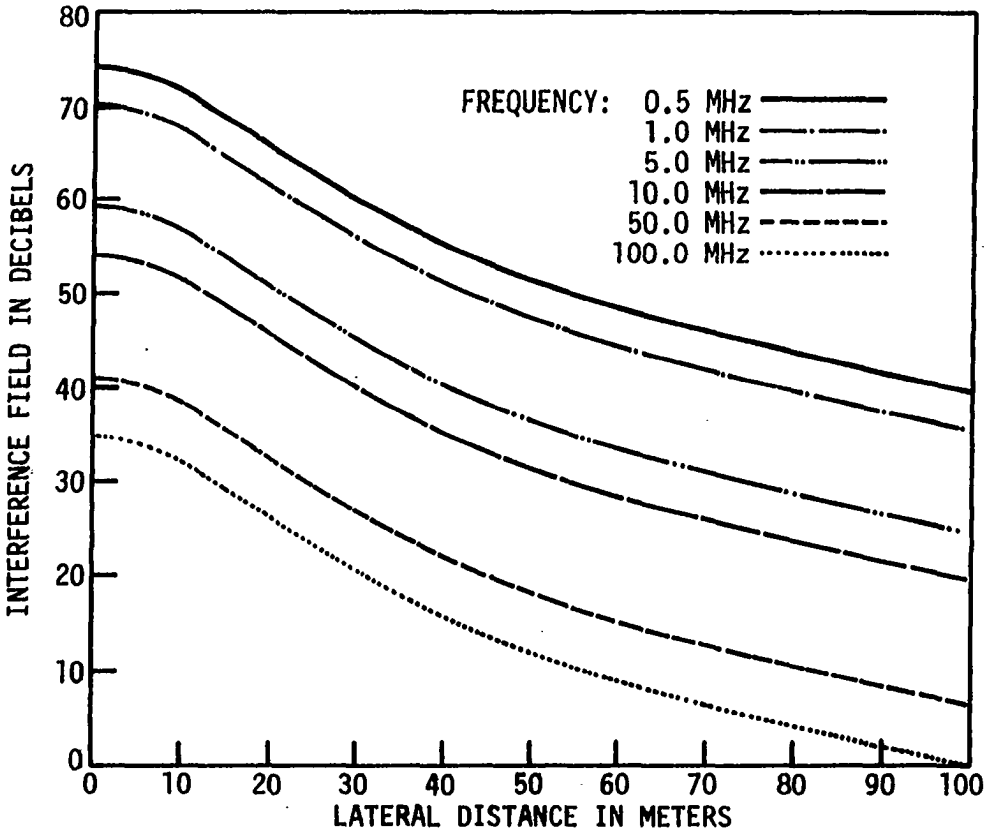

Fig. 7.3. Untransposed horizontal 362 kV line - single circuit quasi-static method (N = 1)

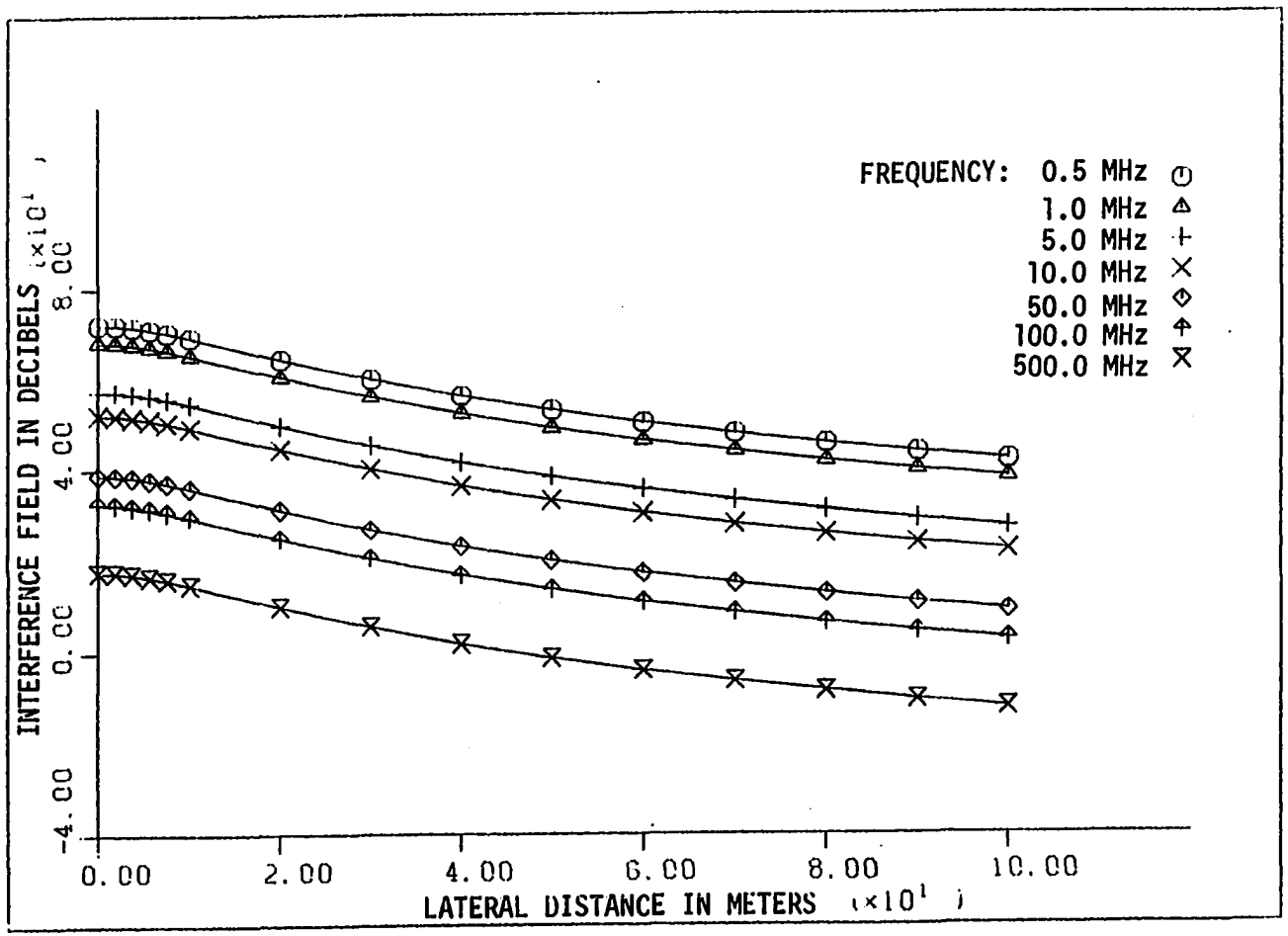

Fig. 7.4. Untransposed vertica1362 kV line - single circuit quasi-static method (N = 1)

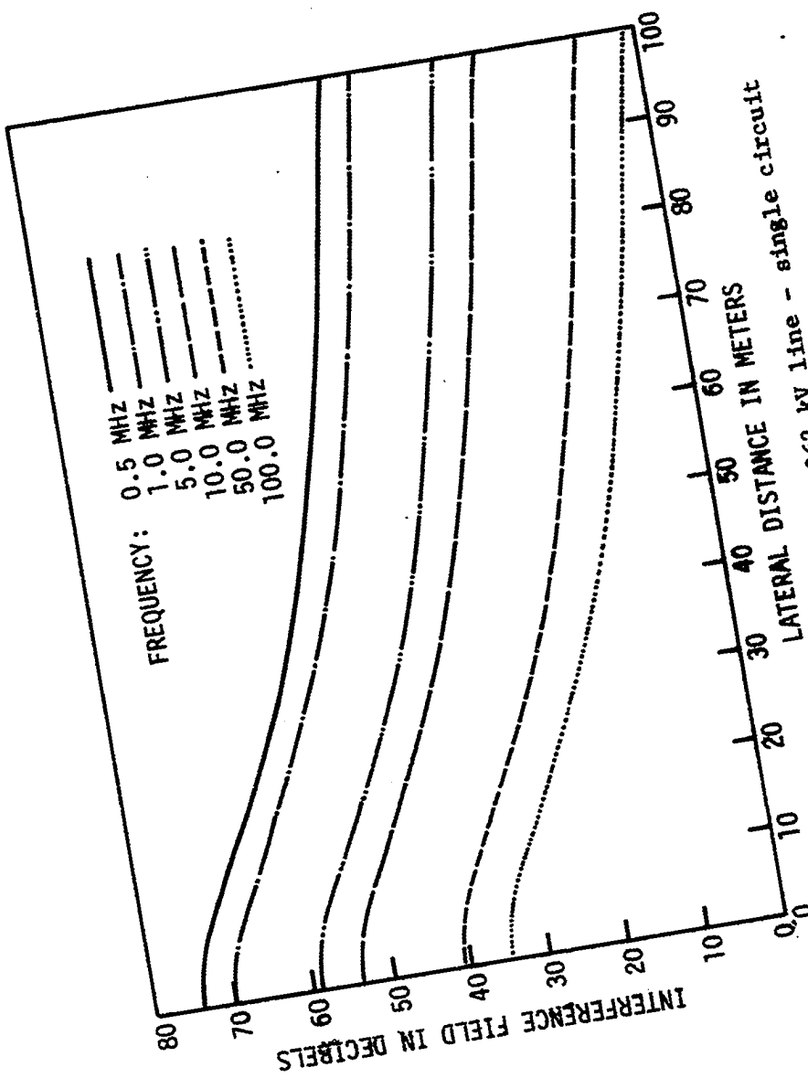

Fig. 7.5. Untransposed triangular 362 kV line - single circuit quasi-static method (N = 1)

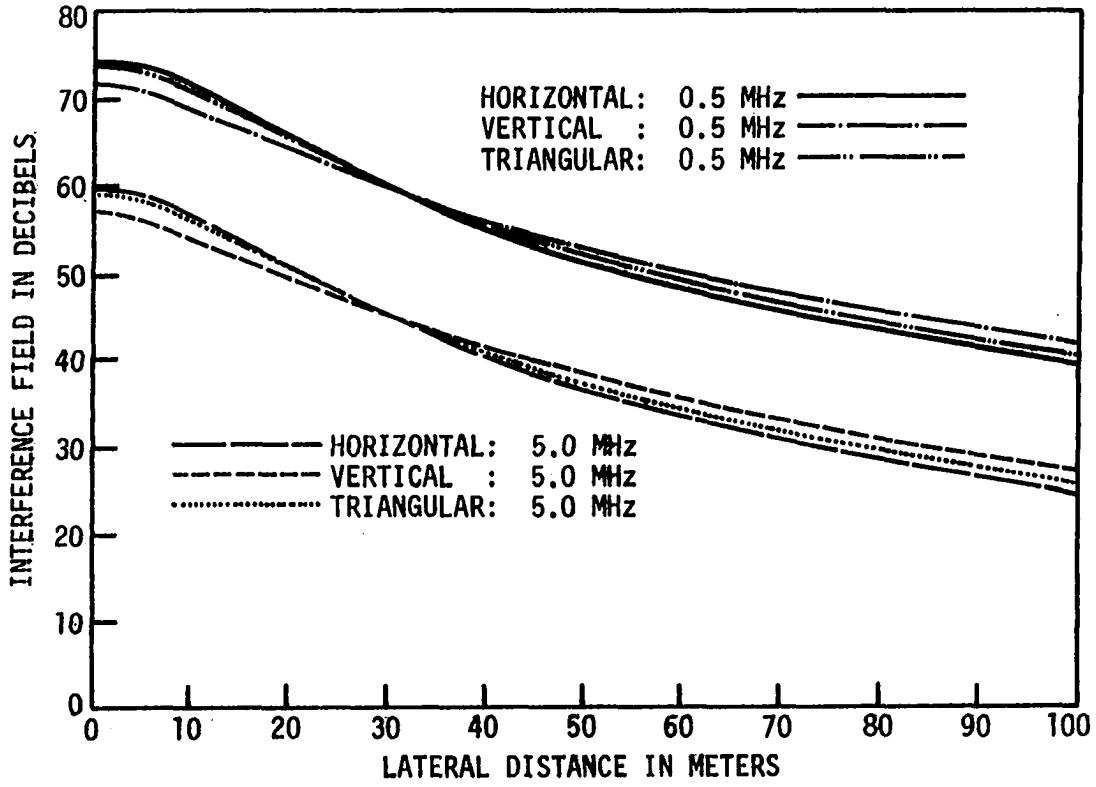

Fig. 7.6. Comparative study 362 kV untransposed - single circuit quasi-static method (N = 1)

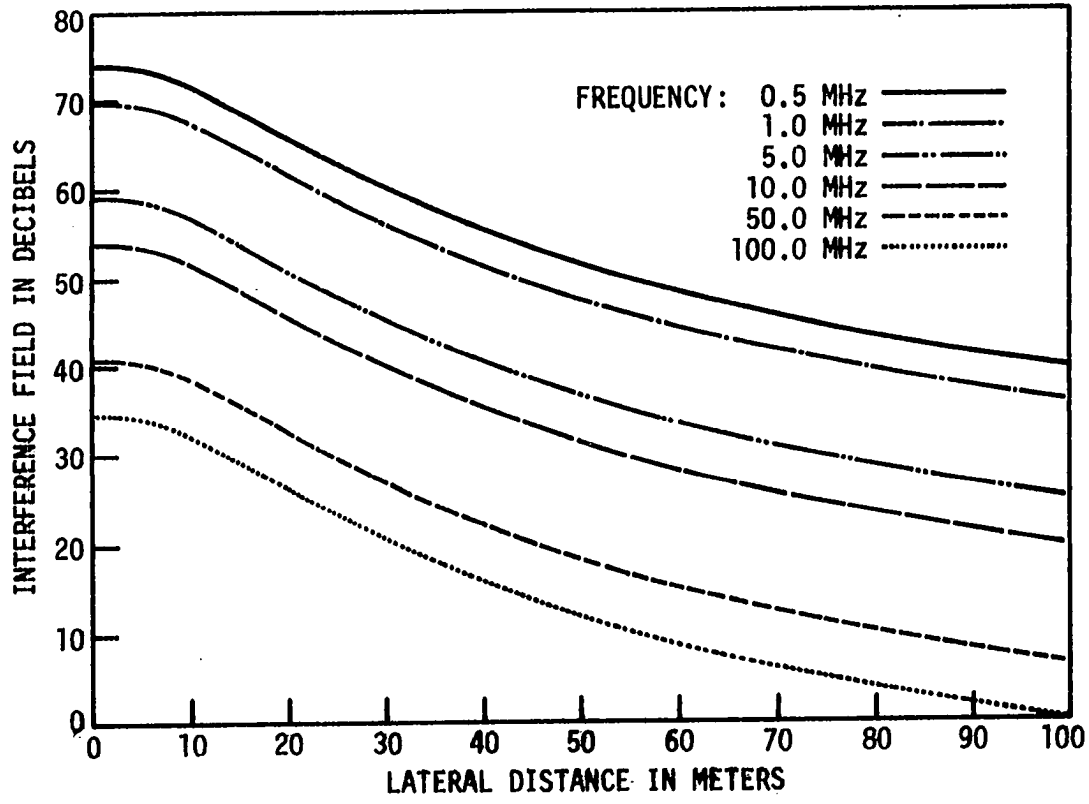

Fig. 7.7. Transposed horizontal 362 kV line - single circuit quasi-static method (N = 1, equivalent model)

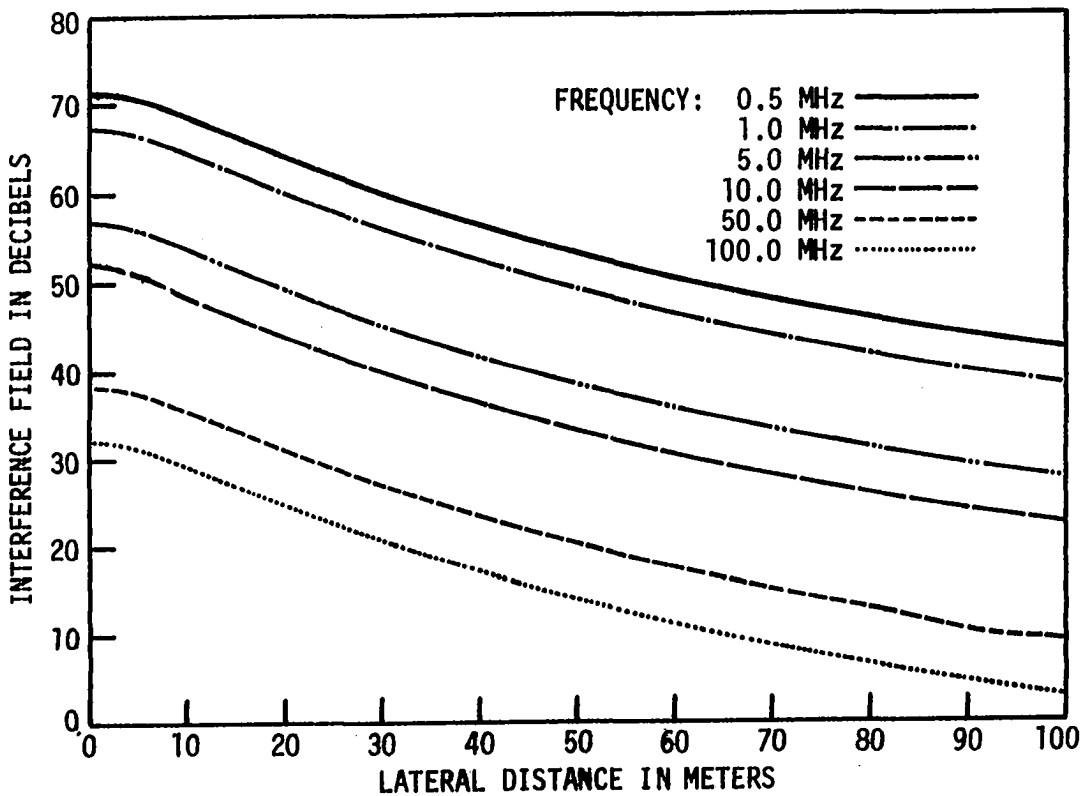

Fig. 7.8. Transposed vertical 362 kV line - single circuit quasi-static method (N = 1, equivalent model)

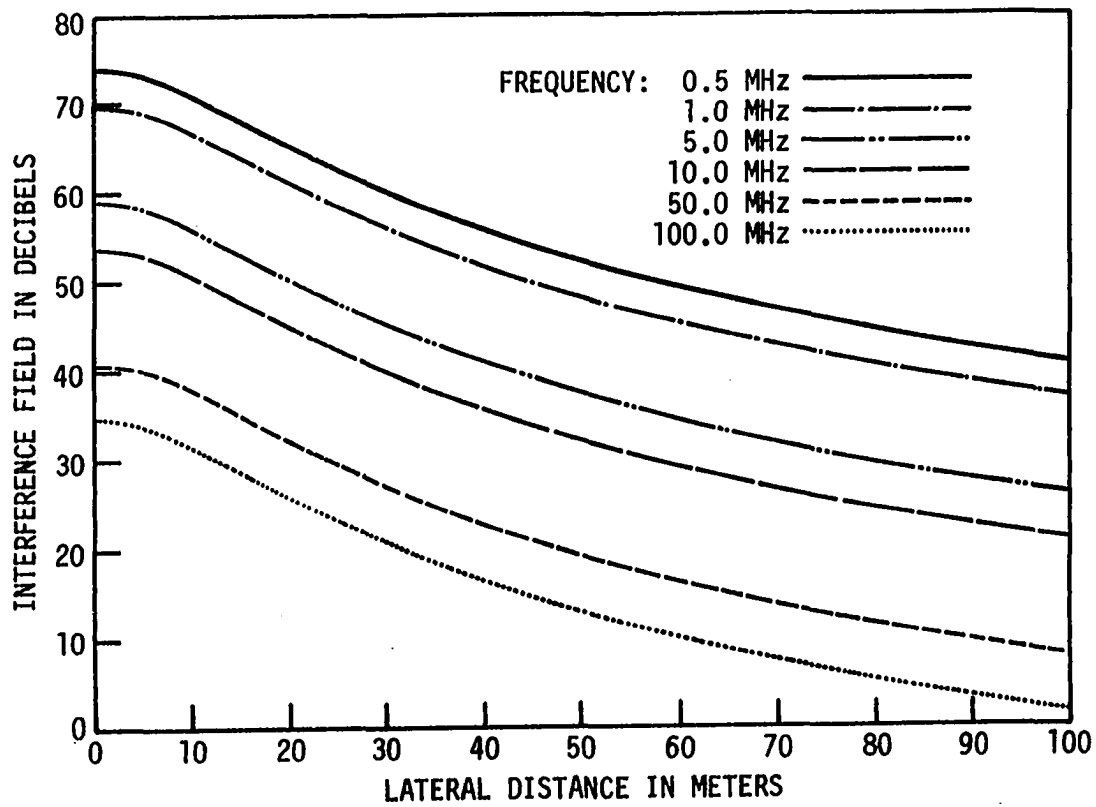

Fig. 7.9. Transposed triangular 362 kV line - single circuit quasi-static method (N = 1, equivalent model)

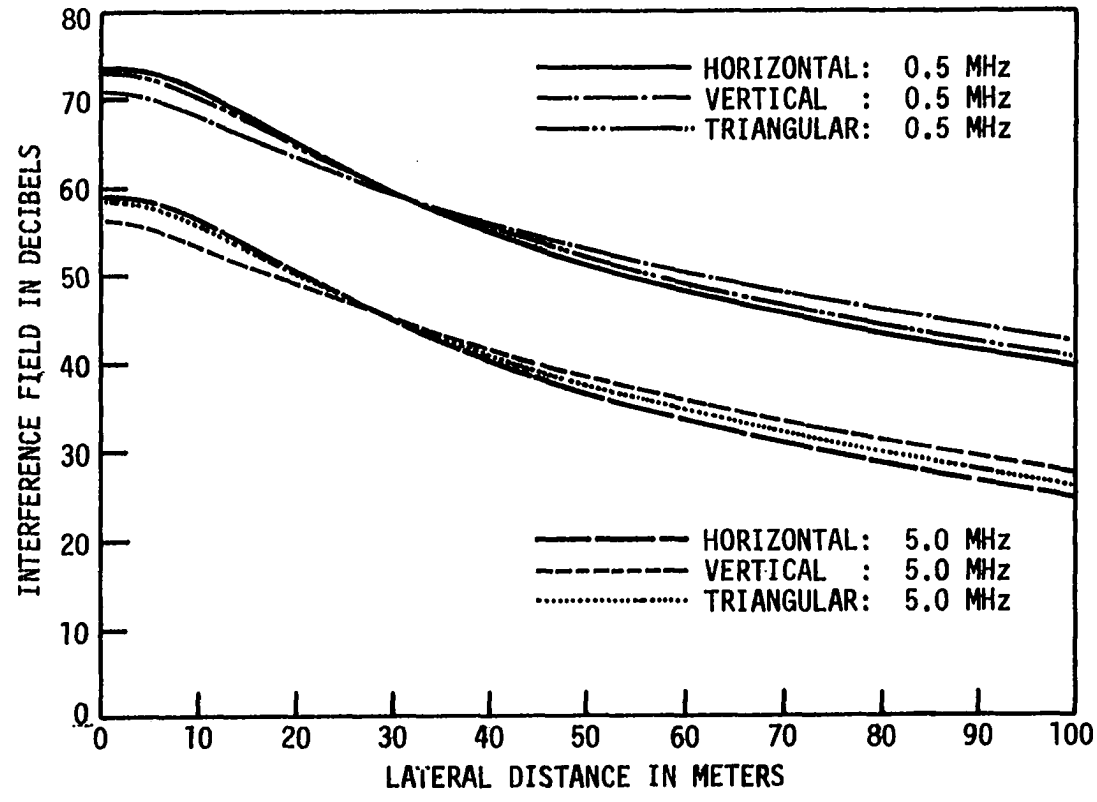

Fig. 7.10. Comparative study 362 kV transposed - single circuit quasi-static method (N = 1, equivalent model)

Table 7.1. Effect of configuration of the line on the EMI using radiation method - untransposed line (N = 1)

Lateral distance, m	EMI level in dB above 1 μV/m																	
	Horizontal						Vertical						Triangular					
	Frequency, MHz						Frequency, MHz						Frequency, MHz					
	0.5	1	5	10	100	500	0.5	1	5	10	100	500	0.5	1	5	10	100	500
0.000	65.9	66.2	54.9	60.0	42.6	33.5	64.4	64.4	39.3	51.9	39.8	26.1	65.9	65.8	51.5	59.0	42.8	34.0
1.875	65.9	66.1	54.6	59.9	35.8	39.4	64.4	64.3	40.4	51.9	38.4	26.5	65.7	65.9	51.1	59.0	42.2	32.7
3.750	65.9	66.1	53.8	59.8	43.1	28.6	64.4	64.3	43.0	51.8	22.2	24.4	65.7	65.8	49.7	59.0	41.1	25.3
5.625	65.8	66.0	52.2	59.6	34.5	39.2	64.3	64.2	45.9	51.6	34.1	35.9	65.6	65.7	46.9	59.0	47.0	37.7
7.500	65.7	65.8	49.6	59.2	37.0	31.4	64.2	64.0	48.7	50.9	37.5	32.6	65.5	65.5	41.1	58.7	35.7	24.8
10.000	65.5	65.6	42.4	58.3	43.6	23.9	64.0	63.8	51.7	48.8	42.4	33.7	65.3	65.3	35.6	57.8	38.4	37.9
20.000	64.5	64.1	55.6	36.1	43.0	21.4	63.2	62.5	58.1	51.9	27.3	25.7	64.4	63.8	57.6	44.3	33.3	33.4
30.000	63.5	62.3	58.4	50.8	22.9	32.0	62.3	60.8	57.5	50.0	28.7	34.4	63.4	62.0	59.0	54.2	36.3	28.9
40.000	62.5	60.2	51.8	44.1	24.9	29.0	61.4	58.7	45.3	54.0	43.4	29.8	62.4	59.9	50.8	51.9	35.8	15.3
50.000	61.5	57.5	49.1	41.6	31.6	29.2	60.5	56.0	53.1	20.5	43.1	23.4	61.4	57.2	51.7	42.6	35.8	16.3
60.000	60.5	54.0	55.4	46.9	22.3	29.9	59.5	52.3	56.0	52.7	35.0	26.1	60.4	53.6	56.5	52.6	32.4	31.0
70.000	59.5	48.5	50.1	39.5	32.3	21.1	58.4	46.2	47.8	50.7	23.4	23.4	59.3	47.8	50.2	47.5	23.2	25.8
80.000	58.3	33.8	46.4	40.3	28.0	11.0	57.3	23.4	49.8	40.6	30.6	15.9	58.2	30.3	48.7	44.4	28.0	18.7
90.000	57.0	43.2	53.7	44.9	28.2	4.2	56.0	43.8	54.5	52.0	19.4	31.1	56.9	44.0	54.8	51.1	28.9	28.5
100.000	55.6	49.9	48.8	37.1	31.6	-3.5	54.6	49.6	47.8	47.9	31.6	27.4	55.5	50.2	49.2	44.8	27.8	24.2

Table 7.2. Effect of configuration of the line on the EMI using radiation method - transposed line (N = 1, equivalent model)

Lateral distance, m	EMI level in dB above 1 μV/m																	
	Horizontal						Vertical						Triangular					
	Frequency, MHz						Frequency, MHz						Frequency, MHz					
	0.5	1	5	10	100	500	0.5	1	5	10	100	500	0.5	1	5	10	100	500
0.000	65.8	65.1	54.5	59.9	43.7	29.2	64.1	64.0	44.1	49.1	39.6	15.1	65.6	65.8	49.7	58.5	41.8	35.5
1.875	65.8	66.0	54.2	59.9	34.8	39.4	64.1	64.0	44.7	49.1	37.8	31.3	65.6	65.7	49.2	58.5	41.6	26.0
3.750	65.8	66.0	53.4	59.7	42.7	27.2	64.1	63.9	46.2	49.0	-2.1	11.5	65.6	65.7	47.6	58.5	40.5	28.8
5.625	65.7	65.9	51.9	59.4	37.5	38.6	64.0	63.8	48.1	48.7	37.6	34.7	65.5	65.5	44.2	58.4	47.7	35.1
7.500	65.6	65.7	49.3	59.0	32.2	29.3	63.9	63.6	50.1	47.9	31.4	33.5	65.4	65.4	35.3	58.1	29.1	30.2
10.000	65.4	65.5	42.1	58.0	44.3	21.4	63.8	63.4	52.5	45.2	40.0	31.0	65.2	65.1	40.6	57.1	40.0	37.0
20.000	64.5	64.1	55.4	38.1	42.9	23.8	63.0	62.1	57.9	51.6	29.2	23.4	64.3	63.7	57.7	46.2	19.8	33.8
30.000	63.5	62.2	58.2	50.1	30.1	33.3	62.1	60.5	56.9	48.0	11.7	34.3	63.3	61.9	58.9	53.8	37.4	30.7
40.000	62.5	60.1	51.7	42.3	32.3	29.3	61.2	58.4	43.3	53.6	42.2	24.8	62.3	59.8	50.3	52.2	36.9	25.7
50.000	61.5	57.5	48.8	41.7	31.3	28.9	60.3	55.7	53.2	32.4	43.0	23.7	61.4	57.1	51.9	41.3	37.3	4.8
60.000	60.5	53.9	55.2	45.9	31.1	29.4	59.3	51.9	55.7	52.0	36.9	29.8	60.3	53.5	56.5	52.6	34.5	28.5
70.000	59.4	48.4	50.0	37.3	31.5	13.1	58.2	45.8	47.0	50.6	30.3	22.7	59.3	47.6	49.9	48.0	20.8	26.0
80.000	58.2	33.7	46.0	40.1	32.9	13.9	57.1	18.9	49.9	38.5	31.3	23.9	58.1	29.6	48.8	43.9	31.4	-12.6
90.000	57.0	43.1	53.4	43.8	22.5	17.2	55.8	44.0	54.3	51.6	27.1	28.6	56.8	44.0	54.8	51.1	28.4	28.4
100.000	55.5	49.8	48.7	34.7	33.5	19.5	54.4	49.6	47.2	48.0	33.9	26.8	55.4	50.2	49.1	45.2	30.9	25.9

Table 7.3. Effect of configuration of the line on the EMI using radiation method - untransposed line (N = 2)

Lateral distance, m	EMI level in dB above 1 μV/m																	
	Horizontal						Vertical						Triangular					
	Frequency, MHz						Frequency, MHz						Frequency, MHz					
	0.5	1	5	10	100	500	0.5	1	5	10	100	500	0.5	1	5	10	100	500
0.000	62.4	62.7	53.2	55.8	36.4	30.3	60.8	60.9	17.9	48.9	34.9	24.8	62.2	62.4	50.3	55.4	37.2	29.4
1.875	62.4	62.7	53.0	55.8	34.0	34.7	60.8	60.8	24.3	48.9	34.1	14.9	62.2	62.4	49.9	55.4	37.5	29.7
3.750	62.3	62.6	52.3	55.8	37.1	26.3	60.7	60.8	32.4	48.9	25.0	21.7	62.1	62.4	48.9	55.5	35.6	17.7
5.625	62.2	62.5	51.1	55.7	26.6	34.5	60.7	60.7	38.2	48.8	24.0	32.6	62.0	62.2	46.9	55.5	42.3	34.0
7.500	62.1	62.4	49.1	55.4	34.2	27.1	60.6	60.5	42.4	48.3	34.5	27.2	61.9	62.1	43.3	55.4	31.6	17.8
10.000	61.9	62.1	44.3	54.8	39.6	22.0	60.4	60.3	46.6	46.6	38.2	29.8	61.7	61.8	27.9	54.8	31.7	33.8
20.000	61.0	60.7	51.2	37.2	37.1	9.0	59.6	59.0	54.4	47.7	22.4	23.6	60.8	60.4	53.6	35.4	30.2	28.5
30.000	60.0	59.0	55.1	47.5	11.0	26.6	58.7	57.4	54.5	48.0	26.8	30.0	59.8	58.7	55.8	51.3	29.0	23.3
40.000	59.0	56.9	49.5	39.7	-3.2	23.2	57.9	55.4	44.5	50.2	38.8	27.6	58.9	56.6	48.7	47.5	29.1	1.5
50.000	58.1	54.4	44.2	39.3	26.7	24.1	56.9	52.8	48.7	30.9	38.3	15.9	57.9	54.0	47.2	42.1	29.7	11.4
60.000	57.1	51.1	52.0	43.6	12.1	25.9	56.0	49.4	52.7	49.7	30.2	18.6	56.9	50.6	53.1	49.3	26.7	27.6
70.000	56.1	46.0	47.7	35.0	27.9	19.3	54.9	43.9	46.0	46.1	11.0	17.2	55.9	45.3	47.8	42.5	21.1	20.7
80.000	54.9	34.6	41.3	37.9	13.4	14.0	53.8	29.4	45.2	40.5	24.6	-14.7	54.8	32.2	43.9	42.8	19.8	17.1
90.000	53.7	37.8	50.2	41.6	26.3	12.2	52.6	38.6	51.1	48.7	0.5	27.4	53.5	38.9	51.4	47.6	25.2	23.7
100.000	52.3	45.7	46.4	32.5	24.4	9.1	51.2	45.4	45.6	42.9	24.4	22.5	52.1	46.0	46.8	39.3	19.9	18.2

Table 7.4. Effect of configuration of the line on the EMI using radiation method - transposed line (N = 2, equivalent model)

Lateral distance, m	EMI level in dB above 1 μV/m																	
	Horizontal						Vertical						Triangular					
	Frequency, MHz						Frequency, MHz						Frequency, MHz					
	0.5	1	5	10	100	500	0.5	1	5	10	100	500	0.5	1	5	10	100	500
0.000	62.3	62.6	52.8	55.7	38.2	25.1	60.5	60.4	35.0	45.8	35.1	12.2	62.0	62.2	48.7	54.7	35.7	31.1
1.875	62.2	62.6	52.5	55.7	32.2	34.7	60.4	60.4	36.1	45.8	33.6	26.5	62.0	62.2	48.3	54.7	36.7	20.9
3.750	62.2	62.5	51.9	55.6	36.8	23.7	60.4	60.3	38.6	45.8	13.5	3.0	61.9	62.1	47.1	54.8	34.7	23.7
5.625	62.1	62.4	50.6	55.4	33.5	34.0	60.3	60.2	41.6	45.7	32.7	30.4	61.9	62.0	44.7	54.8	43.3	30.3
7.500	62.0	62.3	48.7	55.1	27.4	24.7	60.2	60.1	44.4	45.2	25.7	28.5	61.8	61.9	40.1	54.6	19.7	26.1
10.000	61.9	62.0	44.0	54.4	40.7	17.3	60.1	59.9	47.5	43.2	34.5	26.5	61.6	61.6	21.9	53.9	34.7	32.7
20.000	60.9	60.6	50.9	39.0	37.2	17.3	59.3	58.7	54.0	47.0	23.2	19.3	60.7	60.2	53.7	39.0	-4.7	29.2
30.000	59.9	58.9	54.8	46.6	26.2	28.5	58.5	57.0	53.8	45.9	16.1	29.6	59.7	58.5	55.6	50.8	31.3	26.2
40.000	59.0	56.8	49.3	36.7	27.5	24.1	57.6	55.0	42.7	49.6	37.0	20.7	58.8	56.5	48.2	47.8	31.1	21.8
50.000	58.0	54.3	43.7	39.6	27.3	23.8	56.7	52.5	48.8	20.6	38.1	18.3	57.8	53.9	47.4	40.9	32.3	-10.8
60.000	57.0	51.0	51.8	42.2	25.7	24.9	55.7	48.9	52.3	48.9	32.2	25.3	56.8	50.4	53.0	49.2	30.0	24.3
70.000	56.0	45.9	47.5	30.8	27.5	8.2	54.7	43.4	45.1	46.1	25.7	17.1	55.8	45.1	47.5	43.1	18.7	20.8
80.000	54.8	34.5	40.7	37.8	27.8	9.4	53.6	27.5	45.3	38.8	27.1	19.1	54.7	31.6	44.2	42.3	26.3	-14.9
90.000	53.6	37.7	49.9	40.1	19.9	12.4	52.4	38.9	50.8	48.1	20.7	24.1	53.4	39.0	51.3	47.7	24.7	23.8
100.000	52.2	45.6	46.2	27.9	28.9	14.8	51.0	45.3	45.0	43.0	29.4	21.7	52.0	46.0	46.6	40.0	25.7	21.0

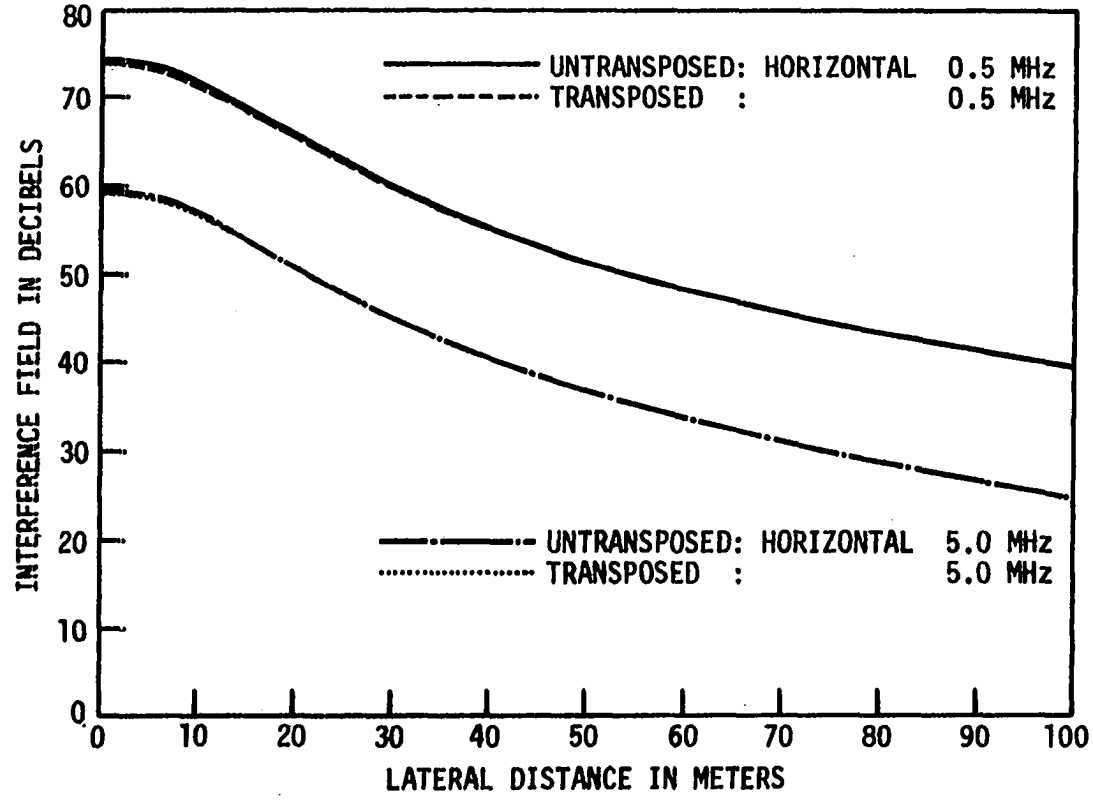

Fig. 7.11. Transposed vs. untransposed 362 kV horizontal line - quasi-static method (N = 1)

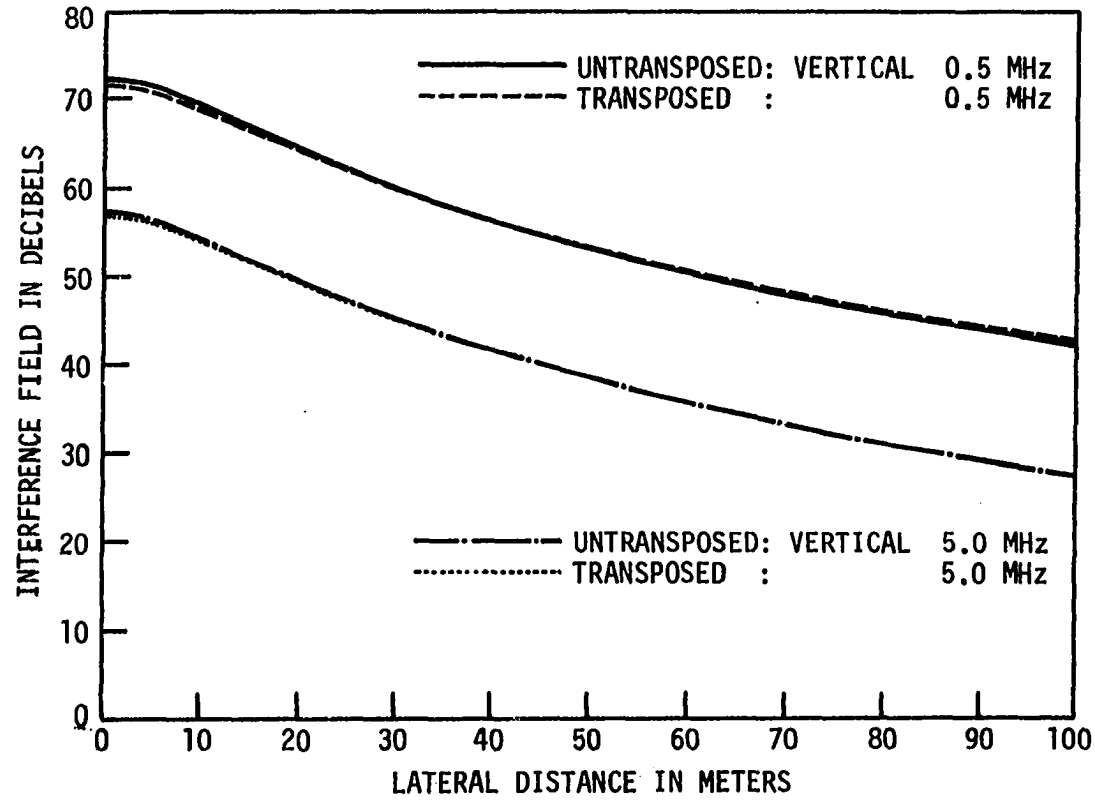

Fig. 7.12. Transposed vs. untransposed 362 kV vertical line - quasi-static method (N = 1)

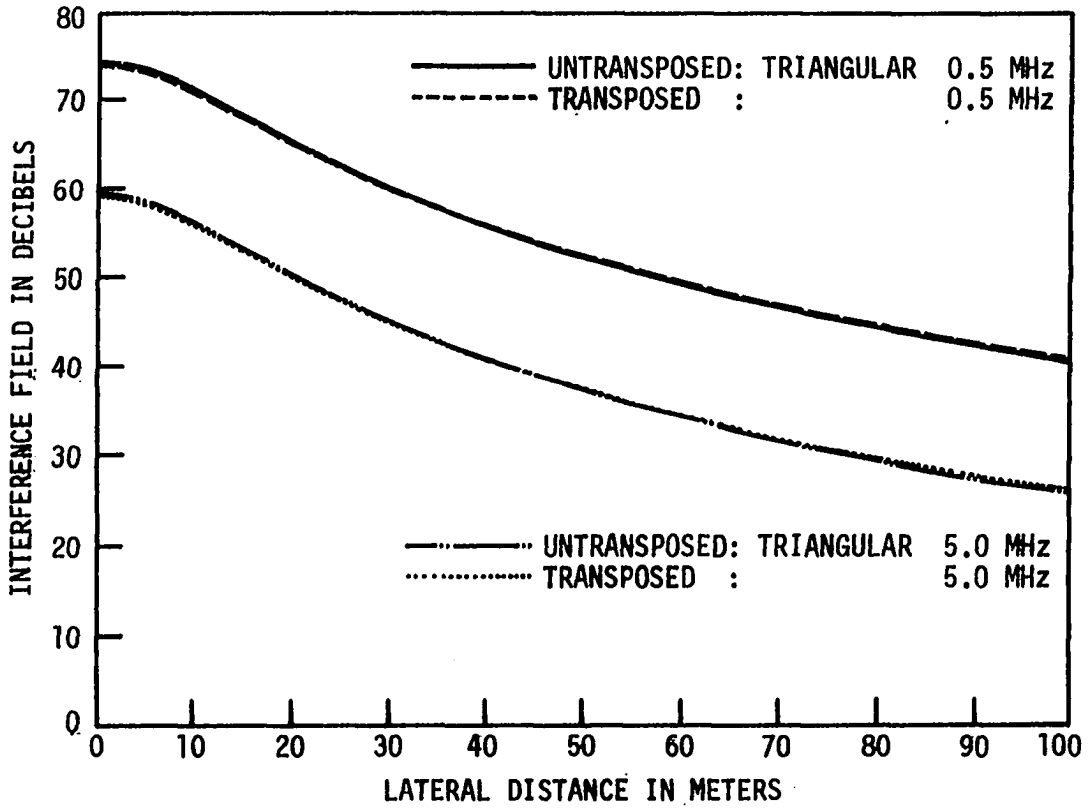

Fig. 7.13. Transposed vs. untransposed 362 kV triangular line - quasi-static method (N = 1)

Table 7.5. Effect of transposition simulated by an equivalent model on the EMI (N = 1)

Lateral distance, m	EMI level in dB above 1 μV/m											
	Horizontal				Vertical				Triangular			
	Frequency, MHz				Frequency, MHz				Frequency, MHz			
	1 MHz		100 MHz		1 MHz		100 MHz		1 MHz		100 MHz	
	Untransposed	Transposed	Untransposed	Transposed	Untransposed	Transposed	Untransposed	Transposed	Untransposed	Transposed	Untransposed	Transposed
0.000	66.2	66.1	42.6	43.7	64.4	64.0	39.8	39.6	65.9	65.8	42.8	41.8
1.875	66.1	66.0	35.8	34.8	64.3	64.0	38.4	37.8	65.9	65.7	42.2	41.6
3.750	66.1	66.0	43.1	42.7	64.3	63.9	22.2	-2.1	65.8	65.7	41.1	40.5
5.625	66.0	65.9	34.5	37.5	64.2	63.8	34.1	37.6	65.7	65.5	47.0	47.7
7.500	65.8	65.7	37.0	32.2	64.0	63.6	37.5	31.4	65.5	65.4	35.7	29.1
10.000	65.6	65.5	43.6	44.3	63.8	63.4	42.4	40.0	65.3	65.1	38.4	40.0
20.000	64.1	64.1	43.0	42.9	62.5	62.1	27.3	29.2	63.8	63.7	33.3	19.8
30.000	62.3	62.2	22.9	30.1	60.8	60.5	28.7	11.7	62.0	61.9	36.3	37.4
40.000	60.2	60.1	24.9	32.3	58.7	58.4	43.4	42.2	59.9	59.8	35.8	36.9
50.000	57.5	57.5	31.6	31.3	56.0	55.7	43.1	43.0	57.2	57.1	35.8	37.3
60.000	54.0	53.9	22.3	31.1	52.3	51.9	35.0	36.9	53.6	53.5	32.4	34.5
70.000	48.5	48.4	32.3	31.5	46.2	45.8	23.4	30.3	47.8	47.6	23.2	20.8
80.000	33.8	33.7	28.0	32.9	23.4	18.9	30.6	31.3	30.3	29.6	28.0	31.4
90.000	43.2	43.1	28.2	22.2	43.8	44.0	19.9	27.1	44.0	44.0	28.9	28.4
100.000	49.9	49.8	31.6	33.5	49.6	49.6	31.6	33.9	50.2	50.2	27.8	30.9

Table 7.6. Effect of transposition simulated by an equivalent model on the EMI (N = 2)

Lateral distance, m	EMI level in dB above 1 μV/m											
	Horizontal				Vertical				Triangular			
	Frequency, MHz				Frequency, MHz				Frequency, MHz			
	1 MHz		100 MHz		1 MHz		100 MHz		1 MHz		100 MHz	
	Untransposed	Transposed	Untransposed	Transposed	Untransposed	Transposed	Untransposed	Transposed	Untransposed	Transposed	Untransposed	Transposed
0.000	62.7	62.6	36.4	38.2	60.9	60.4	34.9	35.1	62.4	62.2	37.2	35.7
1.875	62.7	62.6	34.0	32.2	60.8	60.4	34.1	33.6	62.4	62.2	37.5	36.7
3.750	62.6	62.5	37.1	36.8	60.8	60.3	25.0	13.5	62.4	62.1	35.6	34.7
5.625	62.5	62.4	26.6	33.5	60.7	60.2	24.0	32.7	62.2	62.0	42.3	43.3
7.500	62.4	62.3	34.2	27.4	60.5	60.1	34.5	25.7	62.1	61.9	31.6	19.7
10.000	62.1	62.0	39.6	40.7	60.3	59.9	38.2	34.5	61.8	61.6	31.7	34.7
20.000	60.7	60.6	37.1	37.2	59.0	58.7	22.4	23.2	60.4	60.2	30.2	-4.7
30.000	59.0	56.9	11.0	26.2	57.4	57.0	26.8	16.1	58.7	58.5	29.0	31.3
40.000	56.9	56.8	-3.2	27.5	55.4	55.0	38.8	37.0	56.6	56.5	29.1	31.1
50.000	54.4	54.3	26.7	27.3	52.8	52.5	38.3	38.1	54.0	53.9	29.7	32.3
60.000	51.1	51.0	12.1	25.7	49.4	48.9	30.2	32.2	50.6	50.4	26.7	30.0
70.000	46.0	45.9	27.9	27.5	43.9	43.4	11.0	25.7	45.3	45.1	21.1	18.7
80.000	34.6	34.5	13.4	27.8	29.4	27.5	24.6	27.1	32.2	31.6	19.8	26.3
90.000	37.8	37.7	26.3	19.9	38.6	38.9	0.5	20.7	38.9	39.0	25.2	24.7
100.000	45.7	45.6	24.4	28.9	45.4	45.3	24.4	29.4	46.0	46.0	19.9	25.7

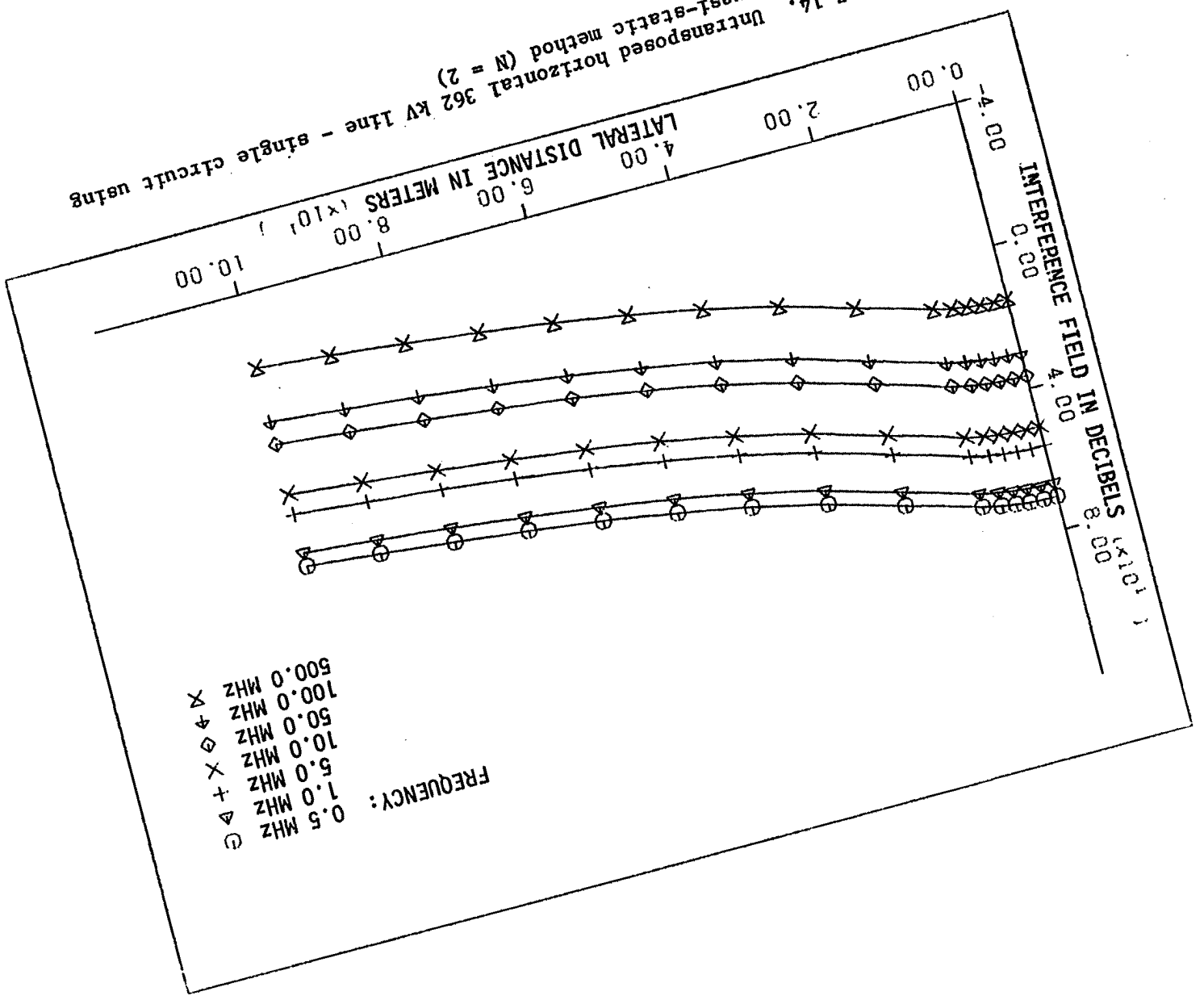

Fig. 7.14. Untransposed horizontal 362 kV line - single circuit using quasi-static method (N = 2)

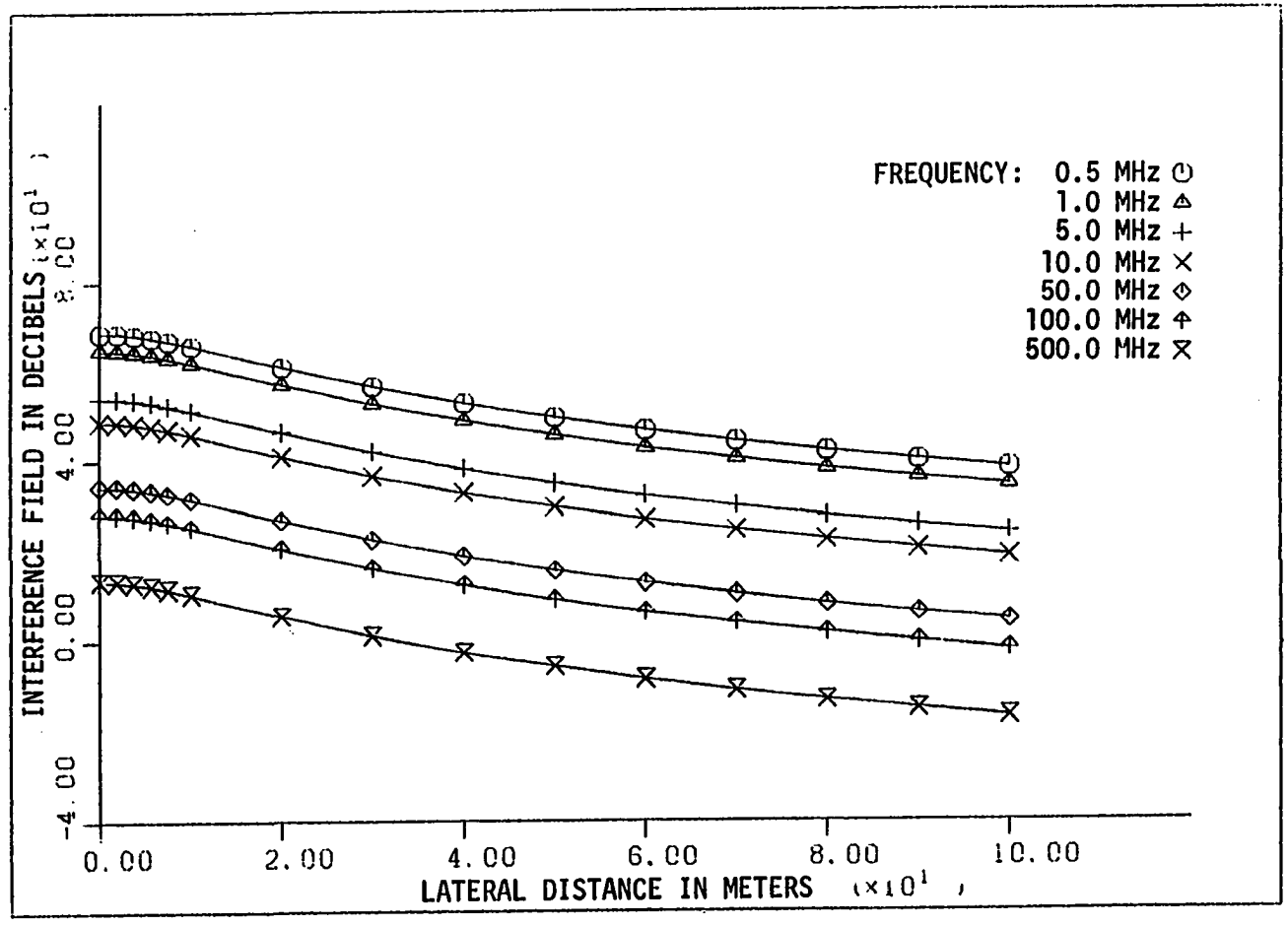

Fig. 7.15. Untransposed vertical 362 kV line - single circuit using quasi-static method (N = 2)

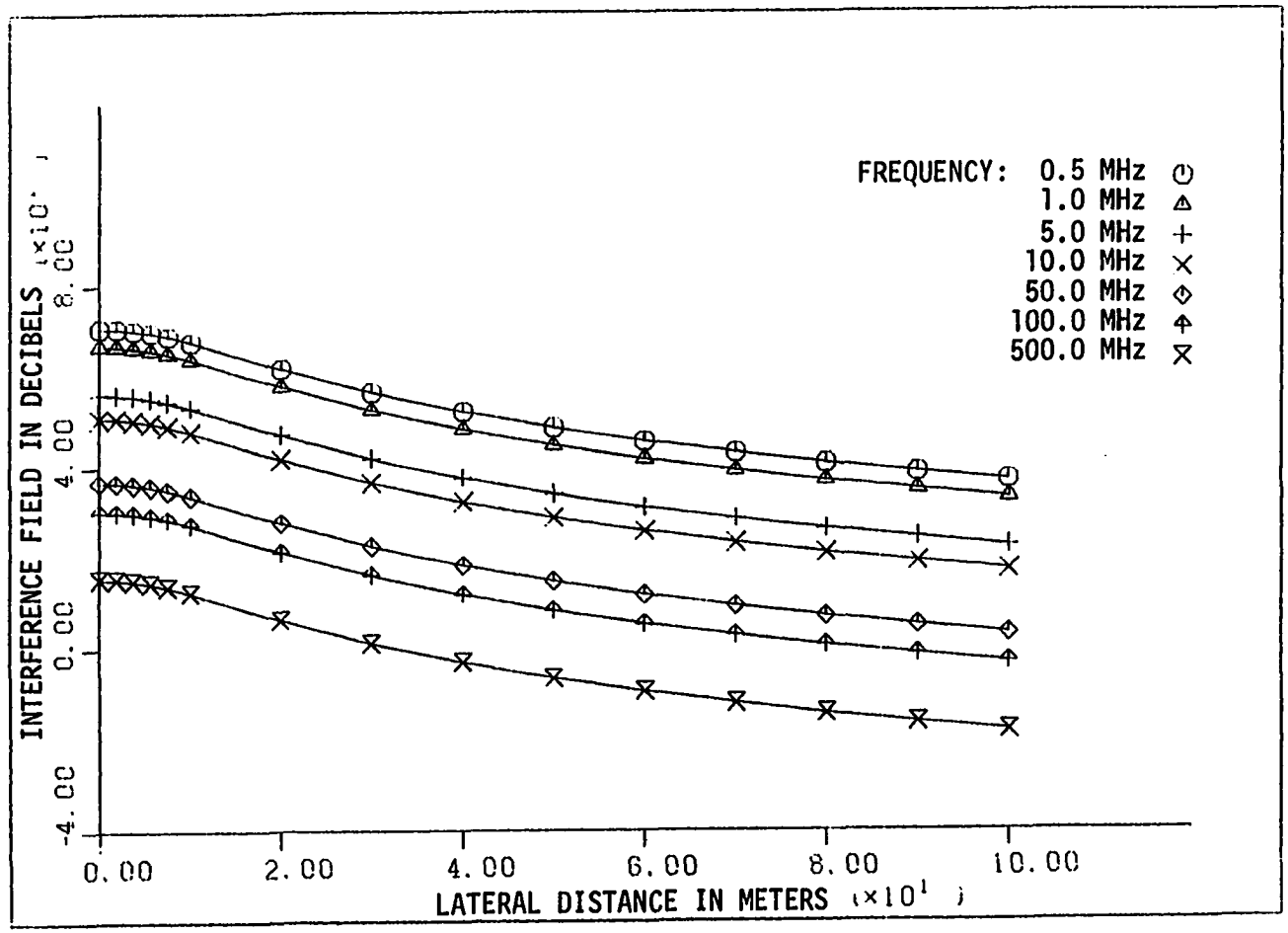

Fig. 7.16. Untransposed triangular 362 kV line - single circuit using quasi-static method (N = 2)

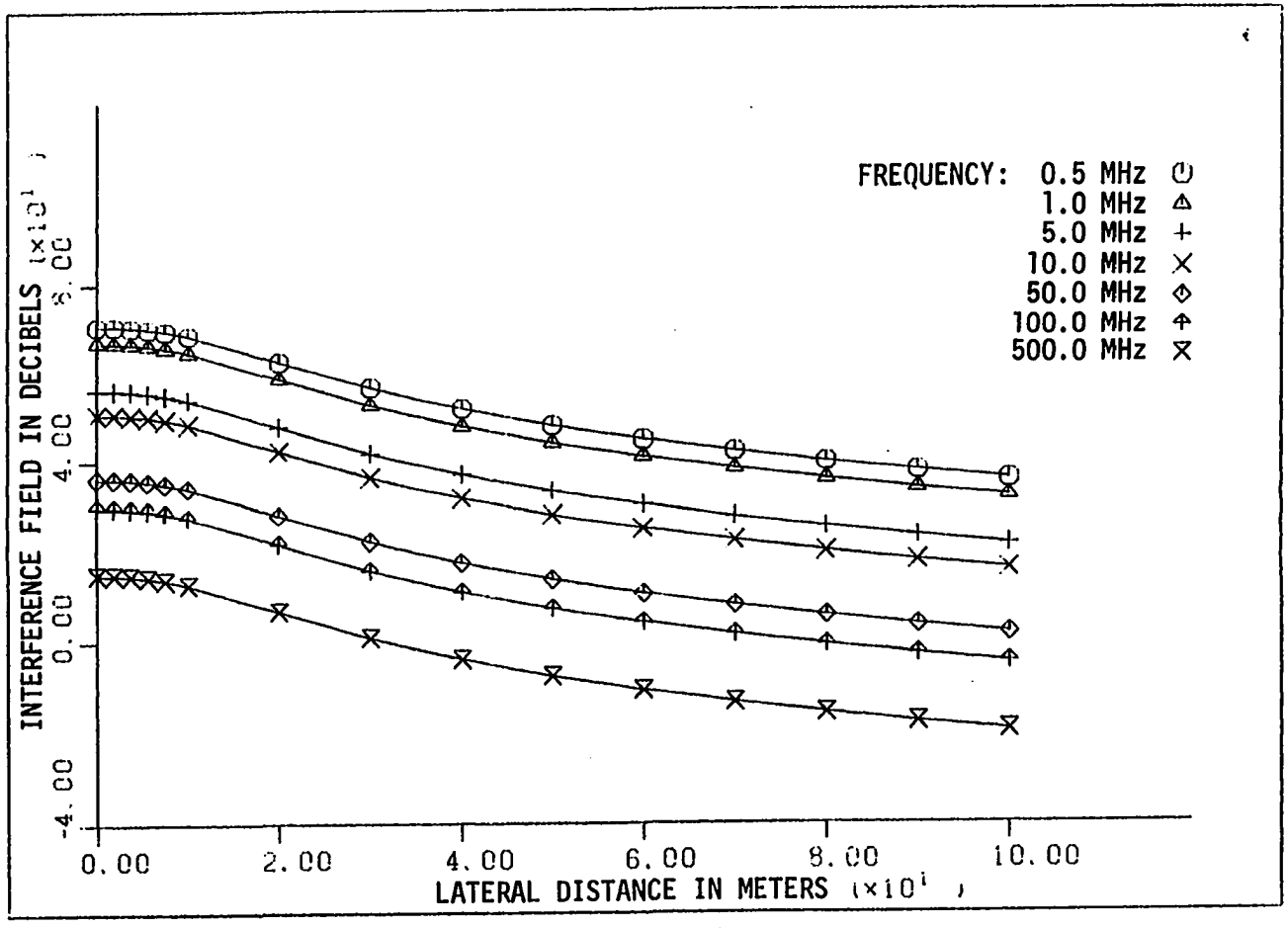

Fig. 7.17. Transposed horizontal 362 kV line - single circuit using quasi-static method (N = 2, equivalent model)

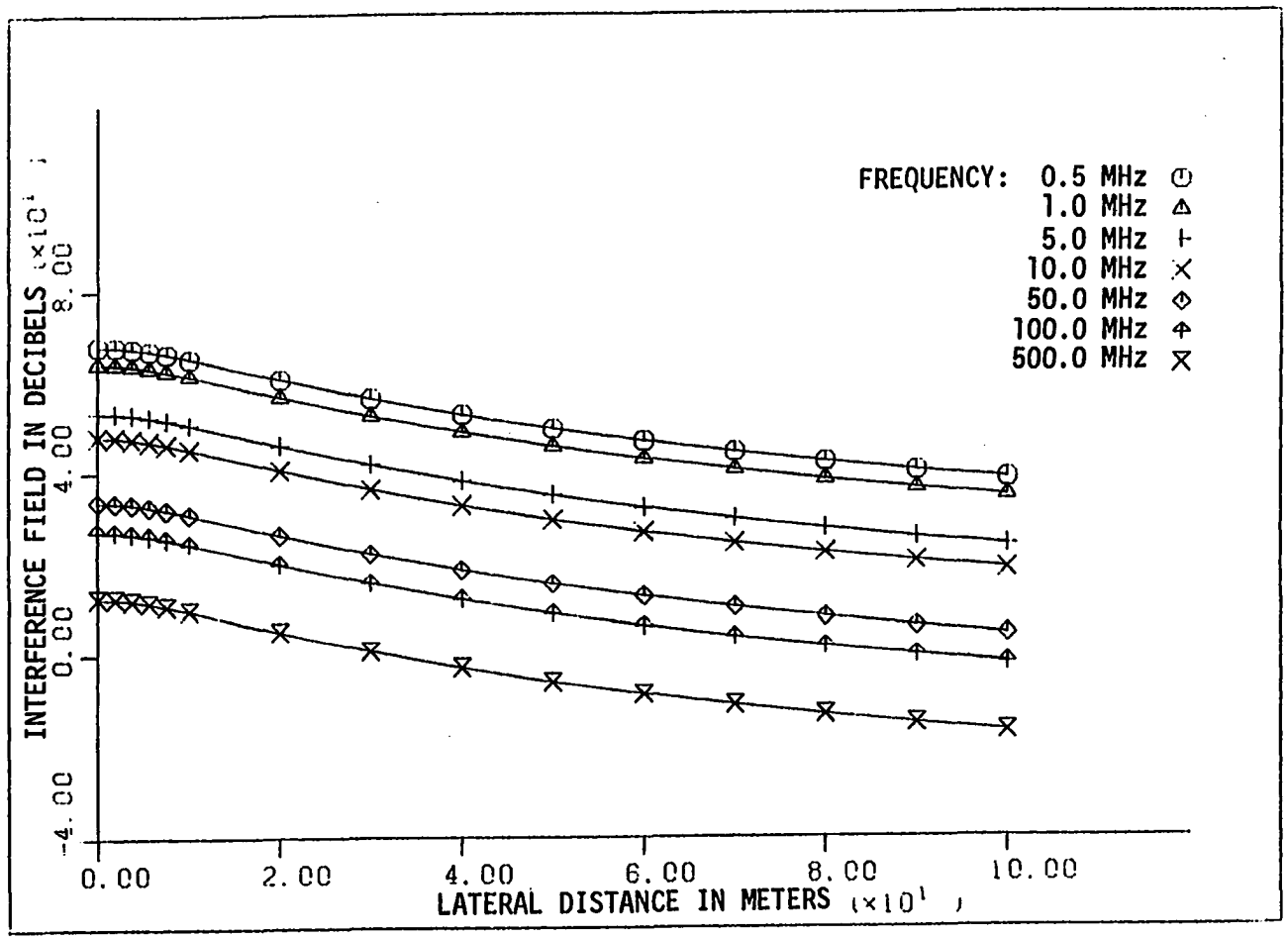

Fig. 7.18. Transposed vertical 362 kV line - single circuit using quasi-static method (N = 2, equivalent model)

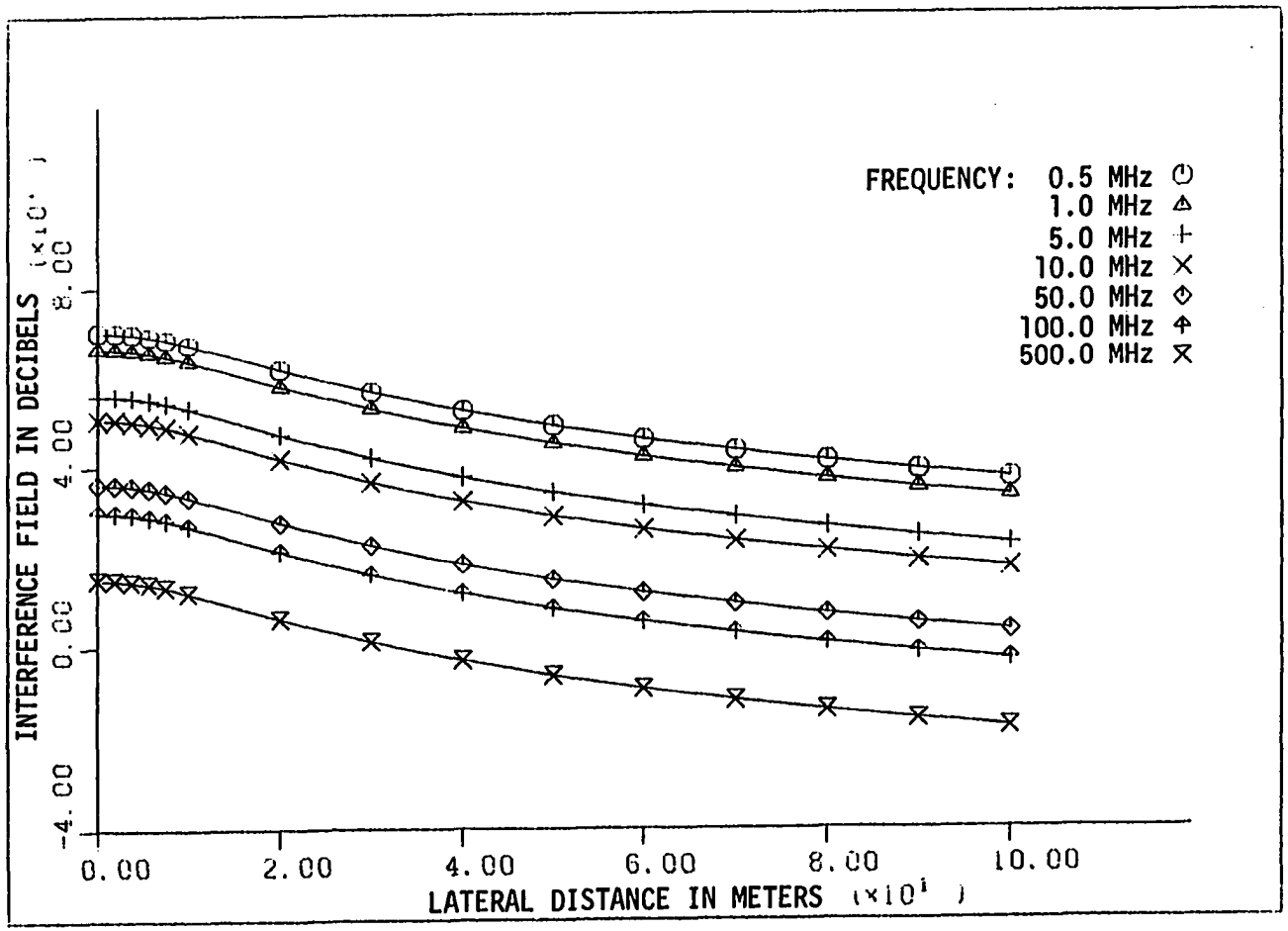

Fig. 7.19. Transposed triangular 362 kV line - single circuit using quasi-static method (N = 2, equivalent model)

Table 7.7. Effect of bundling on the EMI for a 362-kV untransposed line using quasi-static method

Lateral distance, m	EMI level in dB above 1 μV/m											
	Frequency = 0.5 MHz						Frequency = 5 MHz					
	Horizontal		Vertical		Triangular		Horizontal		Vertical		Triangular	
	N=1	N=2	N=1	N=2	N=1	N=2	N=1	N=2	N=1	N=2	N=1	N=2
0.000	74.1	70.6	72.0	68.4	74.1	70.6	59.4	56.0	57.2	53.8	59.3	56.0
1.875	74.0	70.5	71.9	68.3	74.0	70.5	59.8	56.0	57.1	53.7	49.2	55.8
3.750	73.7	70.3	71.5	67.9	73.6	70.1	59.0	55.7	56.7	53.3	58.8	55.5
5.625	73.3	69.8	70.9	67.3	73.1	69.6	58.6	55.3	56.2	52.7	58.3	54.9
7.500	72.7	69.2	70.2	66.6	72.3	68.8	58.0	54.7	55.4	52.0	57.5	54.2
10.000	71.6	68.1	69.1	65.5	71.0	67.5	56.9	53.6	54.3	50.9	56.3	52.9
20.000	65.5	62.0	64.2	60.6	65.1	61.5	50.9	47.5	49.5	46.1	50.3	47.0
30.000	59.7	56.1	59.8	56.2	59.8	56.2	45.0	41.6	45.2	41.7	45.1	41.7
40.000	55.0	51.5	56.1	52.4	55.5	51.9	40.3	37.0	41.4	38.0	40.8	37.4
50.000	51.3	47.8	52.9	49.2	52.0	48.4	36.6	33.3	38.2	34.8	37.3	33.9
60.000	48.2	44.7	50.1	46.4	49.1	45.4	33.6	30.2	35.5	32.0	34.3	30.9
70.000	45.6	42.0	47.7	44.0	46.5	42.9	30.9	27.5	33.0	29.6	31.8	28.4
80.000	43.3	39.8	45.5	41.8	44.3	40.6	28.6	25.2	30.9	27.4	29.6	26.1
90.000	41.2	37.7	43.6	39.9	42.3	38.6	26.5	23.2	29.0	25.5	27.6	24.2
100.000	39.4	35.9	41.8	38.2	40.5	36.9	24.7	21.4	27.2	23.8	25.8	22.4

Table 7.8. Effect of bundling on the EMI for a 362-kV transposed line using quasi-static method

Lateral distance, m	EMI level in dB above 1 μV/m											
	Frequency = 0.5 MHz						Frequency = 5 MHz					
	Horizontal		Vertical		Triangular		Horizontal		Vertical		Triangular	
	N=1	N=2	N=1	N=2	N=1	N=2	N=1	N=2	N=1	N=2	N=1	N=2
0.000	73.9	70.3	71.4	67.8	73.8	70.2	59.1	55.8	56.7	53.2	59.0	55.6
1.875	73.8	70.3	71.3	67.7	73.7	70.1	59.1	55.7	56.6	53.1	58.9	55.5
3.750	73.6	70.0	71.0	67.3	73.4	69.8	58.8	55.5	56.3	52.8	58.6	55.2
5.625	73.2	69.6	70.4	66.8	72.8	69.2	58.5	55.1	55.7	52.2	58.1	54.7
7.500	72.6	69.1	69.7	66.1	72.1	68.5	57.9	54.5	55.0	51.5	57.3	53.9
10.000	71.6	68.1	68.7	65.0	70.9	67.3	56.9	53.5	54.0	50.5	56.1	52.7
20.000	65.6	62.0	64.1	60.4	65.1	61.5	50.9	47.5	49.4	45.9	50.3	46.9
30.000	59.7	56.2	59.9	56.2	59.9	56.3	45.0	41.6	45.1	41.7	45.2	41.8
40.000	55.0	51.5	56.2	52.6	55.7	52.1	40.3	36.9	41.5	38.0	41.0	37.6
50.000	51.3	47.7	53.1	49.4	52.2	48.7	36.6	33.2	38.4	34.9	37.5	34.1
60.000	48.2	44.6	50.3	46.7	49.3	45.7	33.5	30.1	35.6	32.1	34.5	31.2
70.000	45.5	42.0	47.9	44.3	46.8	43.2	30.8	27.4	33.2	29.7	32.0	28.6
80.000	43.2	39.7	45.8	42.2	44.5	41.0	28.5	25.2	31.1	27.6	29.8	26.4
90.000	41.2	37.7	43.9	40.2	42.6	39.0	26.5	23.1	29.2	25.7	27.8	24.4
100.000	39.4	35.8	42.2	38.5	40.8	37.2	24.7	21.3	27.4	24.0	26.0	22.6

Table 7.9. Effect of bundling on the EMI for a 362-kV untransposed line using radiation method

Lateral distance, m	EMI level in dB 1 μV/,											
	Frequency = 1 MHz						Frequency = 100 MHz					
	Horizontal		Vertical		Triangular		Horizontal		Vertical		Triangular	
	N=1	N=2	N=1	N=2	N=1	N=2	N=1	N=2	N=1	N=2	N=1	N=2
0.000	66.2	62.7	64.4	60.9	65.9	62.4	42.6	36.4	39.8	34.9	42.8	37.2
1.875	66.1	62.7	64.3	60.8	65.9	62.4	35.8	34.0	38.4	34.1	42.2	37.5
3.750	66.1	62.6	64.3	60.8	65.8	62.4	43.1	37.1	22.2	25.0	41.1	35.6
5.625	66.0	62.5	64.2	60.7	65.7	62.2	34.5	26.6	34.1	24.0	47.0	42.3
7.500	65.8	62.4	64.0	60.5	65.5	62.1	37.0	34.2	37.5	34.5	35.7	31.6
10.000	65.6	62.1	63.8	60.3	65.3	61.8	43.6	39.6	42.4	38.2	38.4	31.7
20.000	64.1	60.7	62.5	59.0	63.8	60.4	43.0	37.1	27.3	22.4	33.3	30.2
30.000	62.3	59.0	60.8	57.4	62.0	58.7	22.9	11.0	28.7	26.8	36.3	29.0
40.000	60.2	56.9	58.7	55.4	59.9	56.6	24.9	-3.2	43.4	38.8	35.8	29.1
50.000	57.5	54.4	56.0	52.8	57.2	54.0	31.6	26.7	43.1	38.3	35.8	29.7
60.000	54.0	51.1	52.3	49.4	53.6	50.6	22.3	12.1	35.0	30.2	32.4	26.7
70.000	48.5	46.0	46.2	43.9	47.8	45.3	32.3	27.9	23.4	11.0	23.2	21.1
80.000	33.8	34.6	23.4	29.4	30.3	32.2	28.0	13.4	30.6	24.6	28.0	19.8
90.000	43.2	37.8	43.8	38.6	44.0	38.9	28.2	26.3	19.9	0.5	28.9	25.2
100.000	49.9	45.7	49.6	45.4	50.2	46.0	31.6	24.4	31.6	24.4	27.8	19.9

Table 7.10. Effect of bundling on the EMI for a 362-kV transposed line using radiation method

Lateral distance, m	EMI level in dB 1 μV/m											
	Frequency = 1 MHz						Frequency = 100 MHz					
	Horizontal		Vertical		Triangular		Horizontal		Vertical		Triangular	
	N=1	N=2	N=1	N=2	N=1	N=2	N=1	N=2	N=1	N=2	N=1	N=2
0.000	66.1	62.6	64.0	60.4	65.8	62.2	43.7	38.2	39.6	35.1	41.8	35.7
1.875	66.0	62.6	64.0	60.4	65.7	62.2	34.8	32.2	37.8	33.6	41.6	36.7
3.750	66.0	62.5	63.9	60.3	65.7	62.1	42.7	36.8	-2.1	13.5	40.5	34.7
5.625	65.9	62.4	63.8	60.2	65.5	62.0	37.5	33.5	37.6	32.7	47.7	43.3
7.500	65.7	62.3	63.6	60.1	65.4	61.9	32.2	27.4	31.4	25.7	29.1	19.7
10.000	65.5	62.0	63.4	59.9	65.1	61.6	44.3	40.7	40.0	34.5	40.0	34.7
20.000	64.1	60.6	62.1	58.7	63.7	60.2	42.9	37.2	29.2	23.2	19.8	-4.7
30.000	62.2	58.9	60.5	57.0	61.9	58.5	30.1	26.2	11.7	16.1	37.4	31.3
40.000	60.1	56.8	58.4	55.0	59.8	56.5	32.3	27.5	42.2	37.0	36.9	31.1
50.000	57.5	54.3	55.7	52.5	57.1	53.9	31.3	27.3	43.0	38.1	37.3	32.3
60.000	53.9	51.0	51.9	48.9	53.5	50.4	31.1	25.7	36.9	32.2	34.5	30.0
70.000	48.4	45.9	45.8	43.4	47.6	45.1	31.5	27.5	30.3	25.7	20.8	18.7
80.000	33.7	34.5	18.9	27.5	29.6	31.6	32.9	27.8	31.3	27.1	31.4	26.3
90.000	43.1	37.7	44.0	38.9	44.0	39.0	22.5	19.9	27.1	20.7	28.4	24.7
100.000	49.8	45.6	49.6	45.3	50.2	46.0	33.5	28.9	33.9	29.4	30.9	25.7

Table 7.11. Quasi-static method vs. radiation method for a 362-kV untransposed horizontal line (N = 1)

Lateral distance, m	EMI level in dB above 1 μV/m													
	Quasi-Static Method							Radiation Method						
	Frequency, MHz							Frequency, MHz						
	0.5	1	5	10	50	100	500	0.5	1	5	10	50	100	500
0.000	74.1	70.2	59.4	54.2	40.9	34.5	19.6	65.9	66.2	54.9	60.0	27.5	42.6	33.5
1.875	74.0	70.1	59.8	54.1	40.8	34.5	19.5	65.9	66.1	54.6	59.9	40.0	35.8	39.4
3.750	73.7	69.8	59.0	53.8	40.6	34.2	19.2	65.9	66.1	53.8	59.8	49.1	43.1	28.6
5.625	73.3	69.4	58.6	53.4	40.2	33.8	18.8	65.8	66.0	52.2	59.6	51.2	34.5	39.2
7.500	72.7	68.8	58.0	52.8	39.6	33.2	18.2	65.7	65.8	49.6	59.2	41.7	37.0	31.4
10.000	71.6	67.7	56.9	51.8	38.5	32.2	17.2	65.5	65.6	42.4	58.3	41.1	43.6	23.9
20.000	65.5	61.6	50.9	45.7	32.5	26.1	11.1	64.5	64.1	55.6	36.1	50.5	43.0	21.4
30.000	59.7	55.8	45.0	39.8	26.6	20.2	5.2	63.5	62.3	58.4	50.8	44.0	22.9	32.0
40.000	55.0	51.1	40.3	35.2	21.9	15.6	0.6	62.5	60.2	51.8	44.1	44.3	24.9	29.0
50.000	51.3	47.4	36.6	31.4	18.2	11.9	-3.2	61.5	57.5	49.1	41.6	43.7	31.6	29.2
60.000	48.2	44.3	33.6	28.3	15.1	8.8	-6.3	60.5	54.0	55.4	46.9	38.3	22.3	29.9
70.000	45.6	41.7	30.9	25.7	12.5	6.1	-8.9	59.5	48.5	50.1	39.5	26.1	32.3	21.1
80.000	43.3	39.4	28.6	23.4	10.2	3.8	-11.2	58.3	33.8	46.4	40.3	39.1	28.0	11.0
90.000	41.2	37.3	26.5	21.4	8.1	1.8	-13.2	57.0	43.2	53.7	44.9	38.3	28.2	4.2
100.000	39.4	35.5	24.7	19.6	8.3	-0.0	-15.0	55.6	49.9	48.8	37.1	21.2	31.6	-3.5

Table 7.12. Quasi-static method vs. radiation method for a 362-kV untransposed vertical line (N = 1)

Lateral distance, m	EMI level in dB above 1 μV/m													
	Quasi-Static Method							Radiation Method						
	Frequency, MHz							Frequency, MHz						
	0.5	1	5	10	50	100	500	0.5	1	5	10	50	100	500
0.000	72.0	68.1	57.2	52.1	38.8	32.5	17.5	64.4	64.4	39.3	51.9	37.1	39.8	26.1
1.875	71.9	67.9	57.1	51.9	38.6	32.3	17.4	64.4	64.3	40.4	51.9	34.1	38.4	26.5
3.750	71.5	67.6	56.7	51.5	38.3	31.9	17.0	64.4	64.3	43.0	51.8	28.8	22.2	24.4
5.625	70.9	67.0	56.2	51.0	37.7	31.4	16.4	64.3	64.2	45.9	51.6	45.2	34.1	35.9
7.500	70.2	66.3	55.4	50.3	37.0	30.7	15.7	64.2	64.0	48.7	50.9	50.5	37.5	32.6
10.000	69.1	65.1	54.3	49.2	35.9	29.6	14.6	64.0	63.8	51.7	48.8	46.2	42.4	33.7
20.000	64.2	60.3	49.5	44.4	31.1	24.8	9.8	63.2	62.5	58.1	51.9	36.1	27.3	25.7
30.000	59.8	55.9	45.2	40.0	26.8	20.5	5.5	62.3	60.8	57.5	50.0	12.4	28.7	34.4
40.000	56.1	52.2	41.4	36.3	23.1	16.7	1.7	61.4	58.7	45.3	54.0	38.6	43.4	29.8
50.000	52.9	49.0	38.2	33.1	19.9	13.6	-1.4	60.5	56.0	53.1	20.5	36.9	43.1	23.4
60.000	50.1	46.2	35.5	30.3	17.1	10.8	-4.2	59.5	52.3	56.0	52.7	24.2	35.0	26.1
70.000	47.7	43.8	33.0	27.9	14.7	8.4	-6.6	58.4	46.2	47.8	50.7	31.2	23.4	23.4
80.000	45.5	41.6	30.9	25.8	12.6	6.2	-8.8	57.3	23.4	49.8	40.6	32.6	30.6	15.9
90.000	43.6	39.7	29.0	23.8	10.7	4.3	-10.7	56.0	43.8	54.5	52.0	20.5	19.9	31.1
100.000	41.8	37.9	27.2	22.1	8.9	2.6	-12.4	54.6	49.6	47.8	47.9	38.0	31.6	27.4

Table 7.13. Quasi-static method vs. radiation method for a 362-kV untransposed triangular line (N = 1)

Lateral distance, m	EMI level in dB above 1 μV/m													
	Quasi-Static Method							Radiation Method						
	Frequency, MHz							Frequency, MHz						
	0.5	1	5	10	50	100	500	0.5	1	5	10	50	100	500
0.000	74.1	70.1	59.3	54.1	41.0	34.8	19.8	65.8	65.9	51.5	59.0	50.4	42.8	34.0
1.875	74.0	70.0	59.2	54.0	40.9	34.7	19.7	65.7	65.9	51.1	59.0	47.6	42.2	32.7
3.750	73.6	69.7	58.8	53.7	40.6	34.3	19.4	65.7	65.8	49.7	59.0	31.3	41.1	25.3
5.625	73.1	69.1	58.3	53.1	40.0	33.8	18.8	65.6	65.7	46.9	59.0	37.3	47.0	37.7
7.500	72.3	68.4	57.5	52.3	39.3	33.0	18.0	65.5	65.5	41.1	58.7	27.0	35.7	24.8
10.000	71.0	67.1	56.3	51.1	38.0	31.8	16.8	65.3	65.3	35.6	57.8	36.7	38.4	37.9
20.000	65.1	61.1	50.3	45.2	32.1	25.9	10.9	64.4	63.8	57.6	44.3	50.0	33.3	33.4
30.000	59.8	55.9	45.1	39.9	26.9	20.6	5.6	63.4	62.0	59.0	54.2	47.6	36.3	28.9
40.000	55.5	51.6	40.8	35.7	22.6	16.4	1.4	62.4	59.9	50.8	51.9	47.4	35.8	15.3
50.000	52.0	48.1	37.3	32.2	19.1	12.9	-2.1	61.4	57.2	51.7	42.6	47.3	35.8	16.3
60.000	49.1	45.1	34.3	29.2	16.2	9.9	-5.1	60.4	53.6	56.5	52.6	44.2	32.4	31.0
70.000	46.5	42.6	31.8	26.6	13.6	7.4	-7.6	59.3	47.8	50.2	47.5	31.3	23.2	25.8
80.000	44.3	40.3	29.6	24.4	11.4	5.2	-9.9	58.2	30.3	48.7	44.4	37.9	28.0	18.7
90.000	42.3	38.4	27.6	22.4	9.4	3.2	-11.9	56.9	44.0	54.8	51.1	41.2	28.9	28.5
100.000	40.5	36.6	25.8	20.6	7.6	1.4	-13.7	55.5	50.2	49.2	44.8	35.9	27.8	24.2

Table 7.14. Quasi-static method vs. radiation method for a 362-kV transposed horizontal line (N = 1)

Lateral distance, m	EMI level in dB above 1 μV/m													
	Quasi-Static Method							Radiation Method						
	Frequency, MHz							Frequency, MHz						
	0.5	1	5	10	50	100	500	0.5	1	5	10	50	100	500
0.000	73.9	69.9	59.1	54.0	40.7	34.4	19.4	65.8	66.1	54.5	59.9	28.7	43.7	29.2
1.875	73.8	69.9	59.1	53.9	40.7	34.3	19.3	65.8	66.0	54.2	59.9	36.5	34.8	39.4
3.750	73.6	69.6	58.8	53.7	40.4	34.1	19.1	65.8	66.0	53.4	59.7	49.3	42.7	27.2
5.625	73.2	69.3	58.5	53.3	40.0	33.7	18.7	65.7	65.9	51.9	59.4	52.0	37.5	38.6
7.500	72.6	68.7	57.9	52.8	39.5	33.1	18.1	65.6	65.7	49.3	59.0	43.8	32.2	29.3
10.000	71.6	67.7	56.9	51.7	38.5	32.1	17.1	65.4	65.5	42.1	58.0	40.9	44.3	21.4
20.000	65.6	61.7	50.9	45.7	32.4	26.1	11.1	64.5	64.1	55.4	38.1	50.4	42.9	23.8
30.000	59.7	55.8	45.0	39.8	26.6	20.2	5.2	63.5	62.2	58.2	50.1	43.5	30.1	33.3
40.000	55.0	51.1	40.3	35.1	21.9	15.5	0.5	62.5	60.1	51.7	42.3	43.7	32.3	29.3
50.000	51.3	47.4	36.6	31.4	18.1	11.8	-3.2	61.5	57.5	48.8	41.7	43.3	31.3	28.9
60.000	48.2	44.3	33.5	28.3	15.0	8.7	-6.3	60.5	53.9	55.2	45.9	38.5	31.1	29.4
70.000	45.5	41.6	30.8	25.7	12.4	6.0	-9.0	59.4	48.4	50.0	37.3	19.8	31.5	13.1
80.000	43.2	39.3	28.5	23.4	10.1	3.8	-11.3	58.2	33.7	46.0	40.1	37.9	32.9	13.9
90.000	41.2	37.3	26.5	21.3	8.1	1.7	-13.3	57.0	43.1	53.4	43.8	38.0	22.5	17.2
100.000	39.4	35.5	24.7	19.5	6.2	-0.1	-15.1	55.5	49.8	48.7	34.7	25.3	33.5	19.5

Table 7.15. Quasi-static method vs. radiation method for a 362-kV transposed vertical line (N = 1)

Lateral distance, m	EMI level in dB above 1 μV/m													
	Quasi-Static Method							Radiation Method						
	Frequency, MHz							Frequency, MHz						
	0.5	1	5	10	50	100	500	0.5	1	5	10	50	100	500
0.000	71.4	67.5	56.7	51.6	38.3	32.0	17.0	64.1	64.0	44.1	49.1	34.0	39.6	15.1
1.875	71.3	67.4	56.6	51.4	38.2	31.8	16.8	64.1	64.0	44.7	49.1	30.6	37.8	31.3
3.750	71.0	67.0	56.3	51.1	37.8	31.5	16.5	64.1	63.9	46.2	49.0	29.5	-2.1	11.5
5.625	70.4	66.5	55.7	50.5	37.3	30.9	15.9	64.0	63.8	48.1	48.7	44.0	37.6	34.7
7.500	69.7	65.8	55.0	49.8	36.6	30.2	15.2	63.9	63.6	50.1	47.9	49.3	31.4	33.5
10.000	68.7	64.8	54.0	48.8	35.5	29.2	14.2	63.8	63.4	52.5	45.2	44.7	40.0	31.0
20.000	64.1	60.2	49.4	44.2	30.9	24.6	9.6	63.0	62.1	57.9	51.6	38.6	29.2	23.4
30.000	59.9	55.9	45.1	40.0	26.7	20.4	5.4	62.1	60.5	56.9	48.0	20.4	11.7	34.3
40.000	56.2	52.3	41.5	36.3	23.1	16.7	1.7	61.2	58.4	43.3	53.6	40.4	42.2	24.8
50.000	53.1	49.1	38.4	33.2	19.9	13.6	-1.4	60.3	55.7	53.2	32.4	39.6	43.0	23.7
60.000	50.3	46.4	35.6	30.5	17.2	10.9	-4.2	59.3	51.9	55.7	52.0	32.7	36.9	29.8
70.000	47.9	44.0	33.2	28.1	14.8	8.5	-6.6	58.2	45.8	47.0	50.6	21.0	30.3	22.7
80.000	45.8	41.9	31.1	25.9	12.7	6.3	-8.7	57.1	18.9	49.9	38.5	28.8	31.3	23.9
90.000	43.9	40.0	29.2	24.0	10.8	4.4	-10.6	55.8	44.0	54.3	51.6	17.3	27.1	28.6
100.000	42.2	38.2	27.4	22.3	9.0	2.7	-12.3	54.4	49.6	47.2	48.0	35.5	33.9	26.8

Table 7.16. Quasi-static method vs. radiation method for a 362-kV transposed triangular line (N = 1)

Lateral distance, m	EMI level in dB above 1 μV/m													
	Quasi-Static Method							Radiation Method						
	Frequency, MHz							Frequency, MHz						
	0.5	1	5	10	50	100	500	0.5	1	5	10	50	100	500
0.000	73.8	69.9	59.0	53.9	40.8	34.5	19.5	65.6	65.8	49.7	58.5	49.5	41.8	35.5
1.875	73.7	69.8	58.9	53.8	40.7	34.4	19.4	65.6	65.7	49.2	58.5	46.4	41.6	26.0
3.750	73.4	69.4	58.6	53.4	40.4	34.1	19.1	65.6	65.7	47.6	58.5	22.0	40.5	28.8
5.625	72.8	68.9	58.1	52.9	39.8	33.6	18.5	65.5	65.5	44.2	58.4	40.3	47.7	35.1
7.500	72.1	68.1	57.3	52.1	39.1	32.8	17.8	65.4	65.4	35.3	58.1	24.3	29.1	30.2
10.000	70.9	66.9	56.1	50.9	37.9	31.6	16.6	65.2	65.1	40.6	57.1	36.8	40.0	37.0
20.000	65.1	61.1	50.3	45.1	32.1	25.8	10.8	64.3	63.7	57.7	46.2	49.2	19.8	33.8
30.000	59.9	56.0	45.2	40.0	26.9	20.7	5.6	63.3	61.9	58.9	53.8	47.6	37.4	30.7
40.000	55.7	51.8	41.0	35.8	22.7	16.5	1.4	62.3	59.8	50.3	52.2	47.5	36.9	25.7
50.000	52.2	48.3	37.5	32.3	19.3	13.0	-2.0	61.4	57.1	51.9	41.3	47.5	37.3	4.8
60.000	49.3	45.4	34.5	29.4	16.3	10.0	-5.0	60.3	53.5	56.5	52.6	44.9	34.5	28.5
70.000	46.8	42.8	32.0	26.8	13.8	7.5	-7.5	59.3	47.6	49.9	48.0	34.6	20.8	26.0
80.000	44.5	40.6	29.8	24.6	11.6	5.3	-9.7	58.1	29.6	48.8	43.9	36.8	31.4	-12.6
90.000	42.6	38.6	27.8	22.6	9.6	3.3	-11.7	56.8	44.0	54.8	51.1	41.6	28.4	28.4
100.000	40.8	36.8	26.0	20.8	7.8	1.5	-13.5	55.4	50.2	49.1	45.2	38.0	30.9	25.9

Table 7.17. Quasi-static method vs. radiation method for a 362-kV untransposed horizontal line (N = 2)

Lateral distance, m	EMI level in dB above 1 μV/m													
	Quasi-Static Method							Radiation Method						
	Frequency, MHz							Frequency, MHz						
	0.5	1	5	10	50	100	500	0.5	1	5	10	50	100	500
0.000	70.6	66.8	56.0	50.7	36.5	30.0	15.2	62.4	62.7	53.2	55.8	35.6	36.4	30.3
1.875	70.5	66.7	56.0	50.6	36.4	29.9	15.1	62.4	62.7	53.0	55.8	39.0	34.0	34.7
3.750	70.3	66.4	55.7	50.3	36.1	29.7	14.8	62.3	62.6	52.3	55.8	44.7	37.1	26.3
5.625	69.8	66.0	55.3	49.9	35.7	29.2	14.3	62.2	62.5	51.1	55.7	46.4	26.6	34.5
7.500	69.2	65.3	54.7	49.3	35.1	28.6	13.7	62.1	62.4	49.1	55.4	37.6	34.2	27.1
10.000	68.1	64.3	53.6	48.3	34.0	27.6	12.6	61.9	62.1	44.3	54.8	37.3	39.6	22.0
20.000	62.0	58.1	47.5	42.2	27.9	21.5	6.5	61.0	60.7	51.2	37.2	45.1	37.1	9.0
20.000	56.1	52.3	41.6	36.3	22.1	15.6	0.7	60.0	59.0	55.1	47.5	38.2	11.0	26.6
40.000	51.5	47.7	37.0	31.7	17.4	11.0	-4.0	59.0	56.9	49.5	39.7	39.5	-3.2	23.2
50.000	47.8	43.9	33.3	27.9	13.7	7.2	-7.7	58.1	54.4	44.2	39.3	39.5	26.7	24.1
60.000	44.7	40.8	30.2	24.8	10.6	4.1	-10.8	57.1	51.1	52.0	43.6	34.6	12.1	25.9
70.000	42.0	38.2	27.5	22.2	7.9	1.5	-13.4	56.1	46.0	47.7	35.0	19.3	27.9	19.3
80.000	39.8	35.9	25.2	19.9	5.7	-0.8	-15.7	54.9	34.6	41.3	37.9	34.8	13.4	14.0
90.000	37.7	33.9	23.2	17.9	3.6	-2.8	-17.7	53.7	37.8	50.2	41.6	34.5	26.3	12.2
100.000	35.9	32.1	21.4	16.0	1.8	-4.6	-19.6	52.3	45.7	46.4	32.5	19.4	24.4	9.1

Table 7.18. Quasi-static method vs. radiation method for a 362-kV untransposed vertical line (N = 2)

Lateral distance, m	EMI level in dB above 1 μV/m													
	Quasi-Static Method							Radiation Method						
	Frequency, MHz							Frequency, MHz						
	0.5	1	5	10	50	100	500	0.5	1	5	10	50	100	500
0.000	68.4	64.6	53.8	48.5	34.3	27.9	13.1	60.8	60.9	17.9	48.9	34.3	34.9	24.8
1.875	68.3	64.4	53.7	48.3	34.2	27.8	13.0	60.8	60.8	24.3	48.9	31.9	34.1	14.9
3.750	67.9	64.0	53.3	48.0	33.8	27.4	12.6	60.7	60.8	32.4	48.9	17.7	25.0	21.7
5.625	67.3	63.5	52.7	47.4	33.2	26.8	12.0	60.7	60.7	38.2	48.8	40.2	24.0	32.6
7.500	66.6	62.7	52.0	46.7	32.5	26.1	11.3	60.6	60.5	42.4	48.3	46.3	34.5	27.2
10.000	65.5	61.6	50.9	45.6	31.4	25.0	10.2	60.4	60.3	46.6	46.6	43.5	38.2	29.8
20.000	60.6	56.8	46.1	40.8	26.6	20.2	5.3	59.6	59.0	54.4	47.7	34.4	22.4	23.6
30.000	56.2	52.4	41.7	36.4	22.2	15.8	0.9	58.7	57.4	54.5	48.0	10.0	26.8	30.0
40.000	52.4	48.6	38.0	32.7	18.5	12.1	-2.8	57.9	55.4	44.5	50.2	31.8	38.8	27.6
50.000	49.2	45.4	34.8	29.5	15.3	8.9	-6.0	56.9	52.8	48.7	30.9	29.5	38.3	15.9
60.000	46.4	42.6	32.0	26.7	12.5	6.1	-8.8	56.0	49.4	52.7	49.7	1.8	30.2	18.6
70.000	44.0	40.2	29.6	24.3	10.1	3.7	-11.2	54.9	43.9	46.0	46.1	28.7	11.0	17.2
80.000	41.8	38.0	27.4	22.1	8.0	1.5	-13.4	53.8	29.4	45.2	40.5	29.1	24.6	-14.7
90.000	39.9	36.1	25.5	20.2	6.0	-0.4	-15.3	52.6	38.6	51.1	48.7	16.0	0.5	27.4
100.000	38.2	34.3	23.8	18.5	4.3	-2.1	-17.0	51.2	45.4	45.6	42.9	34.3	24.4	22.5

Table 7.19. Quasi-static method vs. radiation method for a 362-kV untransposed triangular line (N = 2)

Lateral distance, m	EMI level in dB above 1 μV/m													
	Quasi-Static Method							Radiation Method						
	Frequency, MHz							Frequency, MHz						
	0.5	1	5	10	50	100	500	0.5	1	5	10	50	100	500
0.000	70.6	66.7	56.0	50.7	36.7	30.2	15.4	62.2	62.4	50.3	55.4	47.5	37.2	29.4
1.875	70.5	66.6	55.8	50.6	36.6	30.1	15.3	62.2	62.4	49.9	55.4	45.1	37.5	29.7
3.750	70.1	66.2	55.5	50.2	36.2	29.8	14.9	62.1	62.4	48.9	55.5	34.3	35.6	17.7
5.625	69.6	65.7	54.9	49.7	35.7	29.2	14.4	62.0	62.2	46.9	55.5	28.6	42.3	34.0
7.500	68.8	64.9	54.2	48.9	34.9	28.5	13.6	61.9	62.1	43.3	55.4	26.6	31.6	17.8
10.000	67.5	63.6	52.9	47.6	33.6	27.2	12.3	61.7	61.8	27.9	54.8	33.5	31.7	33.8
20.000	61.5	57.6	47.0	41.7	27.7	21.2	6.3	60.8	60.4	53.6	35.4	45.5	30.2	28.5
30.000	56.2	52.3	41.7	36.4	22.4	16.0	1.0	59.8	58.7	55.8	51.3	42.0	29.0	23.3
40.000	51.9	48.1	37.4	32.2	18.2	11.7	-3.2	58.9	56.6	48.7	47.5	42.1	29.1	1.5
50.000	48.4	44.5	33.9	28.7	14.7	8.2	-6.8	57.9	54.0	47.2	42.1	42.5	29.7	11.4
60.000	45.4	41.6	30.9	25.7	11.7	5.2	-9.7	56.9	50.6	53.1	49.3	39.9	26.7	27.6
70.000	42.9	39.0	28.4	23.1	9.2	2.7	-12.3	55.9	45.3	47.8	42.5	29.2	21.1	20.7
80.000	40.6	36.8	26.1	20.9	6.9	0.5	-14.5	54.8	32.2	43.9	42.8	32.0	19.8	17.1
90.000	38.6	34.8	24.2	18.9	4.9	-1.5	-16.5	53.5	38.9	51.4	47.6	36.3	25.2	23.7
100.000	36.9	33.0	22.4	17.1	3.1	-3.3	-18.3	52.1	46.0	46.8	39.3	31.5	19.9	18.2

Table 7.20. Quasi-static method vs. radiation method for a 362-kV transposed horizontal line (N = 2)

Lateral distance, m	EMI level in dB above 1 μV/m													
	Quasi-Static Method							Radiation Method						
	Frequency, MHz							Frequency, MHz						
	0.5	1	5	10	50	100	500	0.5	1	5	10	50	100	500
0.000	70.3	66.5	55.8	50.4	36.2	29.7	14.9	62.3	62.6	52.8	55.7	11.9	38.2	25.1
1.875	70.3	66.4	55.7	50.4	36.1	29.7	14.8	62.2	62.6	52.5	55.7	34.3	32.2	34.7
3.750	70.0	66.2	55.5	50.1	35.9	29.4	14.6	62.2	62.5	51.9	55.6	44.9	36.8	23.7
5.625	69.6	65.8	55.1	49.8	35.5	29.1	14.2	62.1	62.4	50.6	55.4	47.8	33.5	34.0
7.500	69.1	65.2	54.5	49.2	35.0	28.5	13.6	62.0	62.3	48.7	55.1	40.9	27.4	24.7
10.000	68.1	64.2	53.5	48.2	34.0	27.5	12.6	61.9	62.0	44.0	54.4	36.7	40.7	17.3
20.000	62.0	58.2	47.5	42.2	27.9	21.5	6.6	60.9	60.6	50.9	39.0	45.0	37.2	17.3
30.000	56.2	52.3	41.6	36.3	22.0	15.6	0.7	59.9	58.9	54.8	46.6	37.3	26.2	28.5
40.000	51.5	47.6	36.9	31.6	17.4	10.9	-4.0	59.0	56.8	49.3	36.7	38.4	27.5	24.1
50.000	47.7	43.9	33.2	27.9	13.6	7.2	-7.7	58.0	54.3	43.7	39.6	38.7	27.3	23.8
60.000	44.6	40.8	30.1	24.8	10.5	4.1	-10.8	57.0	51.0	51.8	42.2	34.9	25.7	24.9
70.000	42.0	38.1	27.4	22.1	7.9	1.4	-13.5	56.0	45.9	47.5	30.8	1.1	27.5	8.2
80.000	39.7	35.8	25.2	19.8	5.6	-0.9	-15.8	54.8	34.5	40.7	37.8	32.7	27.8	9.4
90.000	37.7	33.8	23.1	17.8	3.5	-2.9	-17.8	53.6	37.7	49.9	40.1	33.8	19.9	12.4
100.000	35.8	32.0	21.3	16.0	1.7	-4.7	-19.6	52.2	45.6	46.2	27.9	24.1	28.9	14.8

Table 7.21. Quasi-static method vs. radiation method for a 362-kV transposed vertical line (N = 2)

Lateral distance, m	EMI level in dB above 1 μV/m													
	Quasi-Static Method							Radiation Method						
	Frequency, MHz							Frequency, MHz						
	0.5	1	5	10	50	100	500	0.5	1	5	10	50	100	500
0.000	67.8	63.9	53.2	47.9	33.7	27.2	12.3	60.5	60.4	35.0	45.8	31.7	35.1	12.2
1.875	67.7	63.8	53.1	47.8	33.5	27.1	12.2	60.4	60.4	36.1	45.8	29.6	33.6	26.5
3.750	67.3	63.5	52.8	47.4	33.2	26.7	11.8	60.4	60.3	38.6	45.8	13.6	13.5	3.0
5.625	66.8	62.9	52.2	46.9	32.6	26.2	11.3	60.3	60.2	41.6	45.7	38.1	32.7	30.4
7.500	66.1	62.2	51.5	46.2	31.9	25.5	10.6	60.2	60.1	44.4	45.2	44.5	25.7	28.5
10.000	65.0	61.2	50.5	45.1	30.9	24.4	9.6	60.1	59.9	47.5	43.2	41.5	34.5	26.5
20.000	60.4	56.6	45.9	40.5	26.3	19.8	5.0	59.3	58.7	54.0	47.0	36.4	23.2	19.3
30.000	56.2	52.4	41.7	36.6	22.1	15.6	0.7	58.5	57.0	53.8	45.9	10.1	16.1	29.6
40.000	52.6	48.7	38.0	32.7	18.4	12.0	-2.9	57.6	55.0	42.7	49.6	35.9	37.0	20.7
50.000	49.4	45.6	34.9	29.5	15.3	8.8	-6.1	56.7	52.5	48.8	20.6	35.1	38.1	18.3
60.000	46.7	42.8	32.1	26.8	12.6	6.1	-8.8	55.7	48.9	52.3	48.9	28.9	32.2	25.3
70.000	44.3	40.4	29.7	24.4	10.2	3.7	-11.2	54.7	43.4	45.1	46.1	13.3	25.7	17.1
80.000	42.2	38.3	27.6	22.3	8.0	1.6	-13.3	53.6	27.5	45.3	38.8	24.7	27.1	19.1
90.000	40.2	36.4	25.7	20.4	6.1	-0.3	-15.2	52.4	38.9	50.8	48.1	0.1	20.7	24.1
100.000	38.5	34.7	24.0	18.6	4.4	-2.1	-17.0	51.0	45.3	45.0	43.0	30.3	29.4	21.7

Table 7.22. Quasi-static method vs. radiation method for a 362-kV transposed triangular line (N = 2)

Lateral distance, m	EMI level in dB above 1 μV/m													
	Quasi-Static Method							Radiation Method						
	Frequency, MHz							Frequency, MHz						
	0.5	1	5	10	50	100	500	0.5	1	5	10	50	100	500
0.000	70.2	66.3	55.6	50.4	36.3	29.9	15.0	62.0	62.2	48.7	54.7	46.3	35.7	31.1
1.875	70.1	66.2	55.5	50.3	36.2	29.8	14.9	62.0	62.2	48.3	54.7	43.7	36.7	20.9
3.750	69.8	65.9	55.2	49.9	35.9	29.5	14.5	61.9	62.1	47.1	54.8	29.5	34.7	23.7
5.625	69.2	65.4	54.7	49.4	35.4	28.9	14.0	61.9	62.0	44.7	54.8	34.6	43.3	30.3
7.500	68.5	64.6	53.9	48.7	34.6	28.2	13.3	61.8	61.9	40.1	54.6	22.2	19.7	26.1
10.000	67.3	63.4	52.7	47.4	33.4	26.9	12.0	61.6	61.6	21.9	53.9	33.6	34.7	32.7
20.000	61.5	57.6	46.9	41.7	27.6	21.2	6.2	60.7	60.2	53.7	39.0	44.2	-4.7	29.2
30.000	56.3	52.5	41.8	36.5	22.5	16.0	1.1	59.7	58.5	55.6	50.8	42.0	31.3	26.2
40.000	52.1	48.3	37.6	32.3	18.3	11.8	-3.1	58.8	56.5	48.2	47.8	42.1	31.1	21.8
50.000	48.7	44.8	34.1	28.8	14.8	8.3	-6.6	57.8	53.9	47.4	40.9	42.8	32.3	-10.8
60.000	45.7	41.9	31.2	25.9	11.8	5.4	-9.5	56.8	50.4	53.0	49.2	40.9	30.0	24.3
70.000	43.2	39.3	28.6	23.3	9.3	2.9	-12.1	55.8	45.1	47.5	43.1	32.7	18.7	20.8
80.000	41.0	37.1	26.4	21.1	7.1	0.6	-14.3	54.7	31.6	44.2	42.3	30.0	26.3	-14.9
90.000	39.0	35.1	24.4	19.1	5.1	-1.4	-16.3	53.4	39.0	51.3	47.7	36.9	24.7	23.8
100.000	37.2	33.3	22.6	17.4	3.3	-3.1	-18.1	52.0	46.0	46.6	40.0	34.4	25.7	21.0

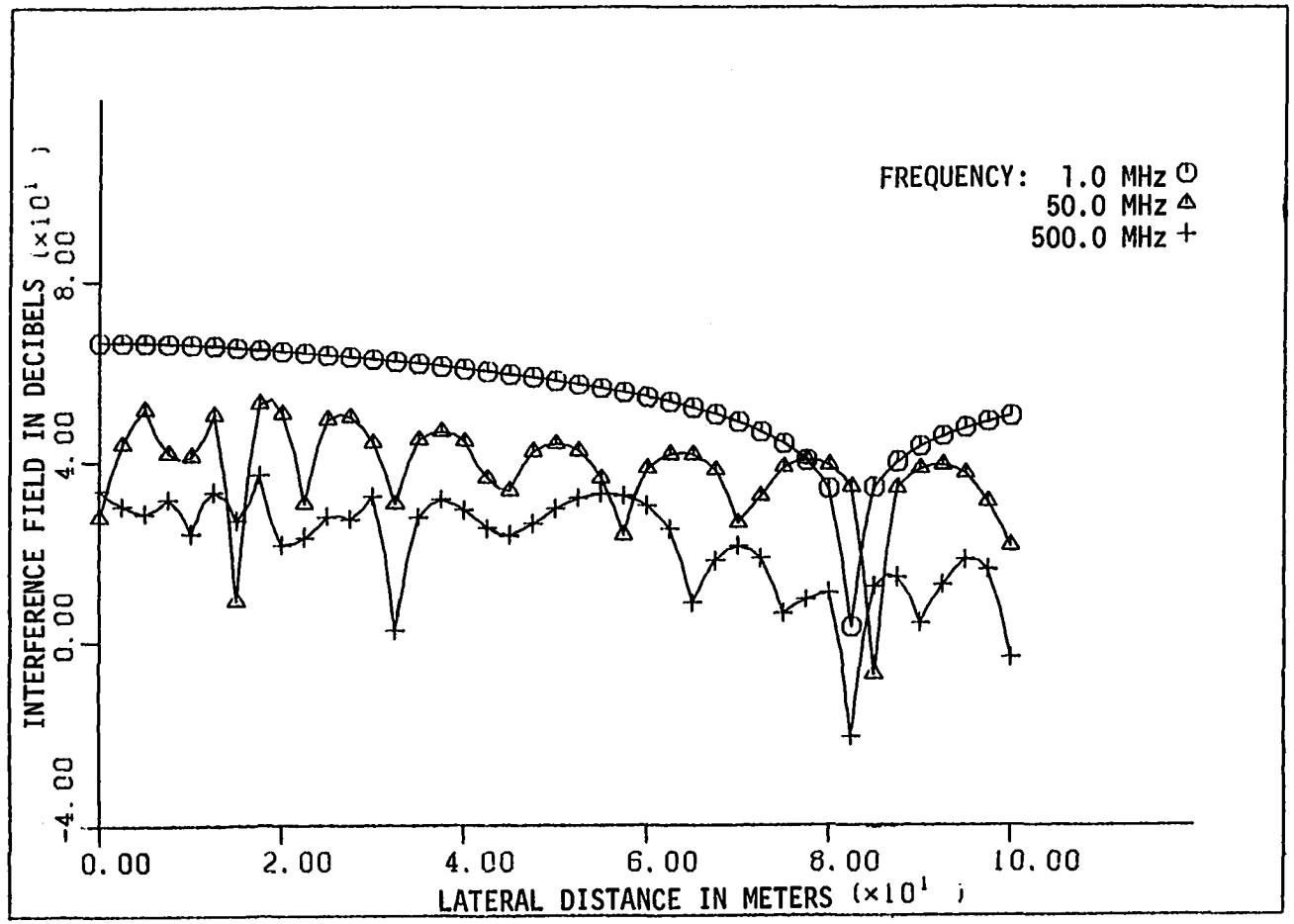

Fig. 7.20. Untransposed horizontal 362 kV line - single circuit using radiation method

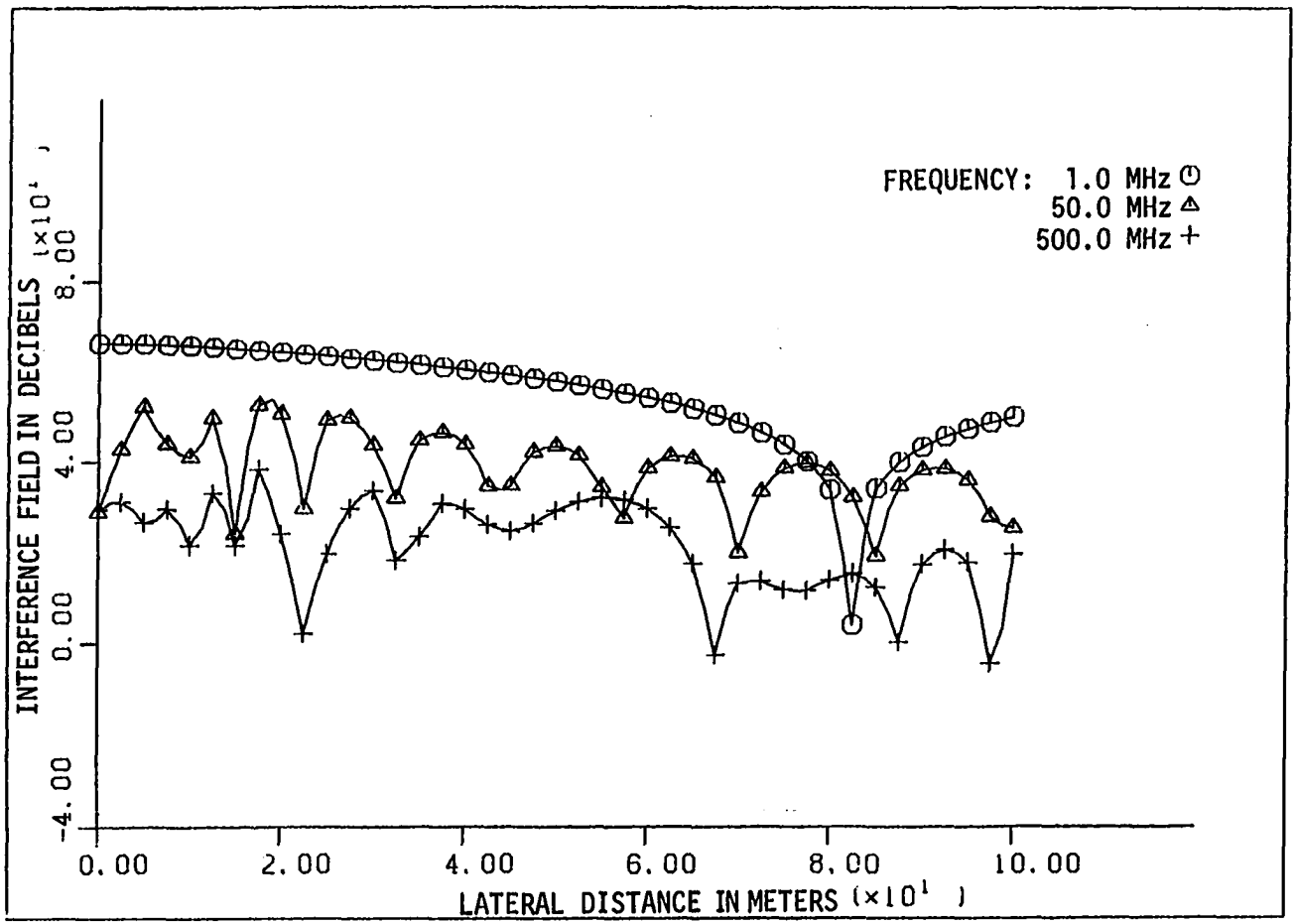

Fig. 7.20. Untransposed horizontal 362 kV line - single circuit using radiation method

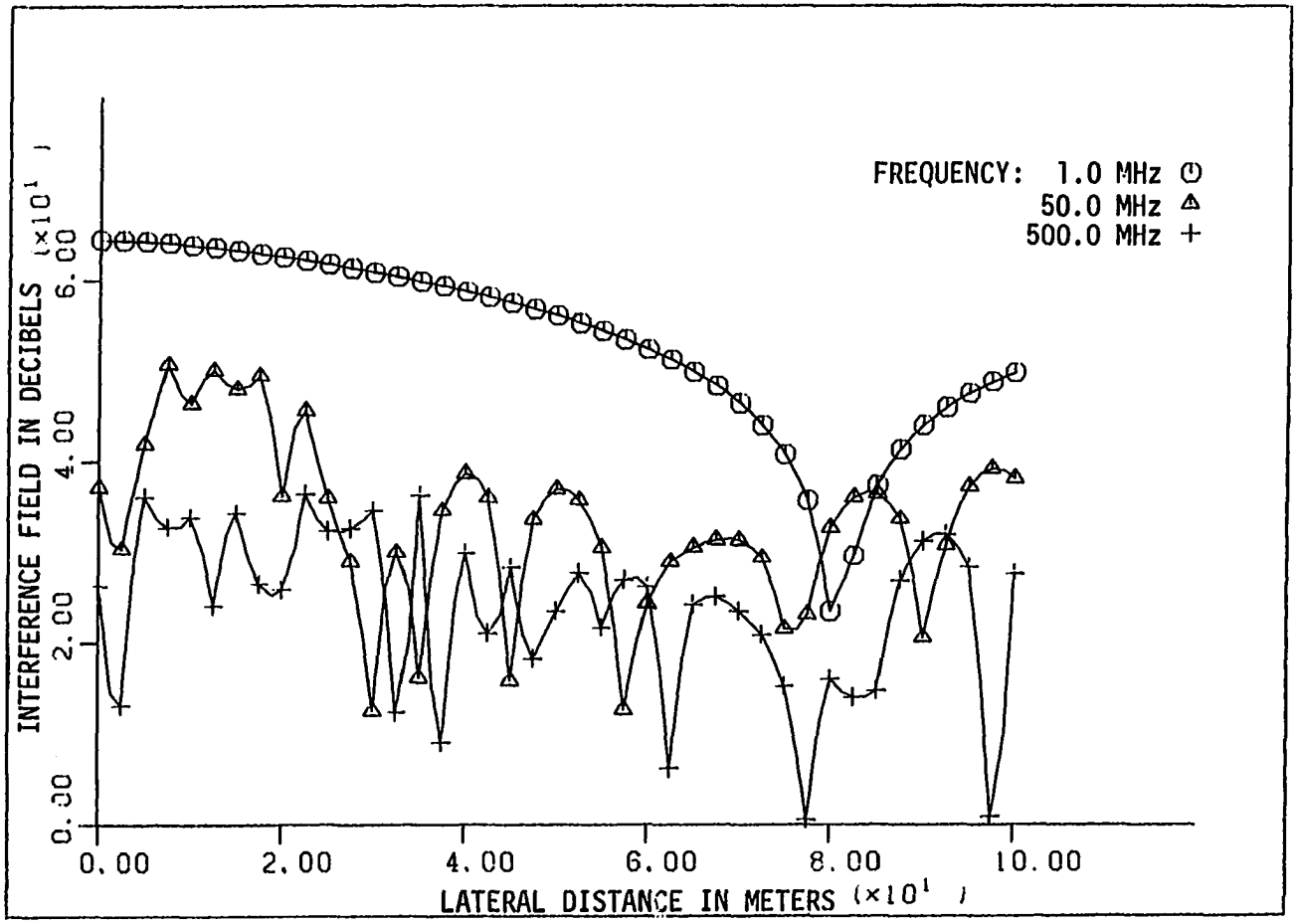

Fig. 7.22. Untransposed vertical 362 kV line - single circuit using radiation method

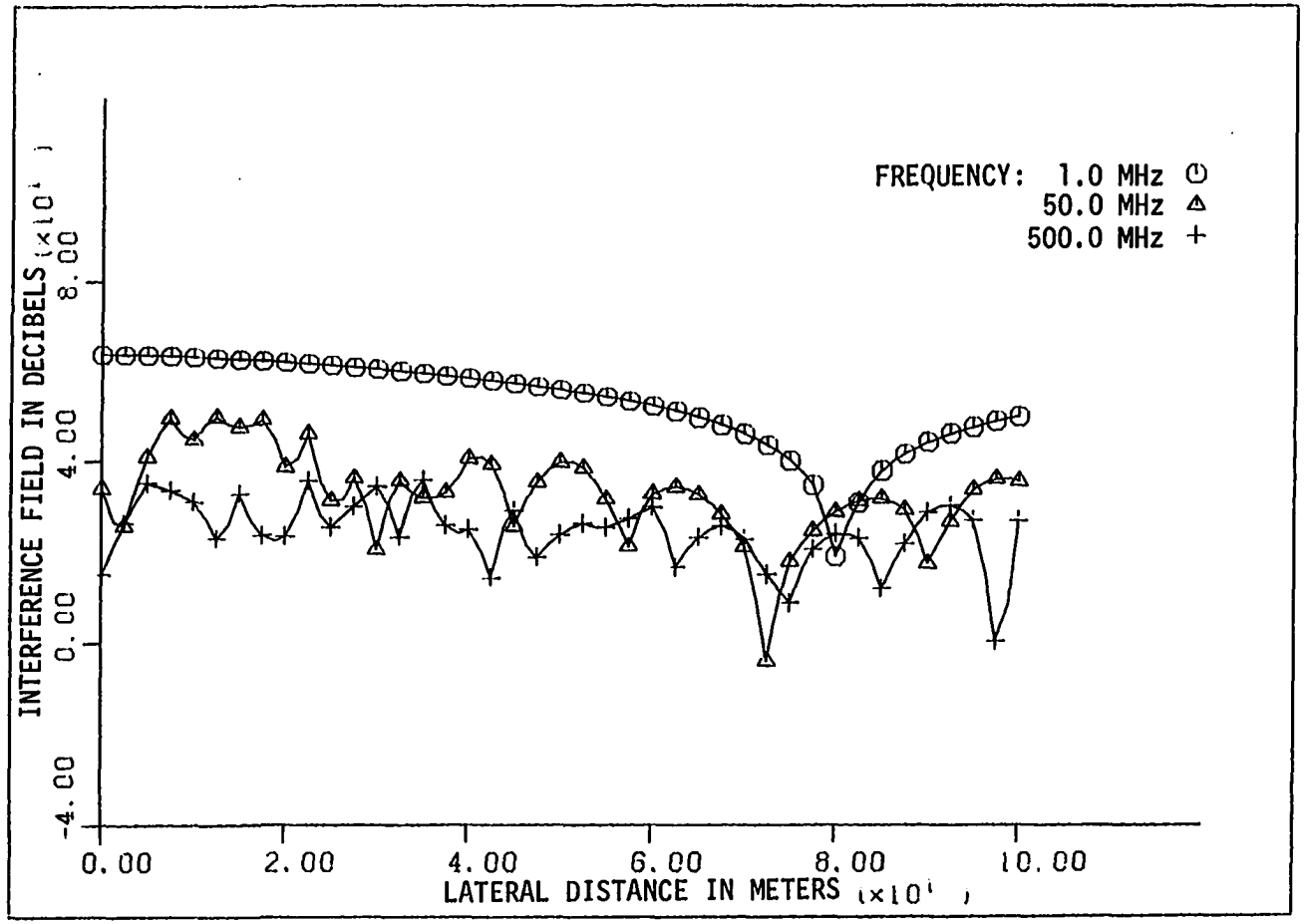

Fig. 7.23. Transposed vertical 362 kV line - single circuit using radiation method

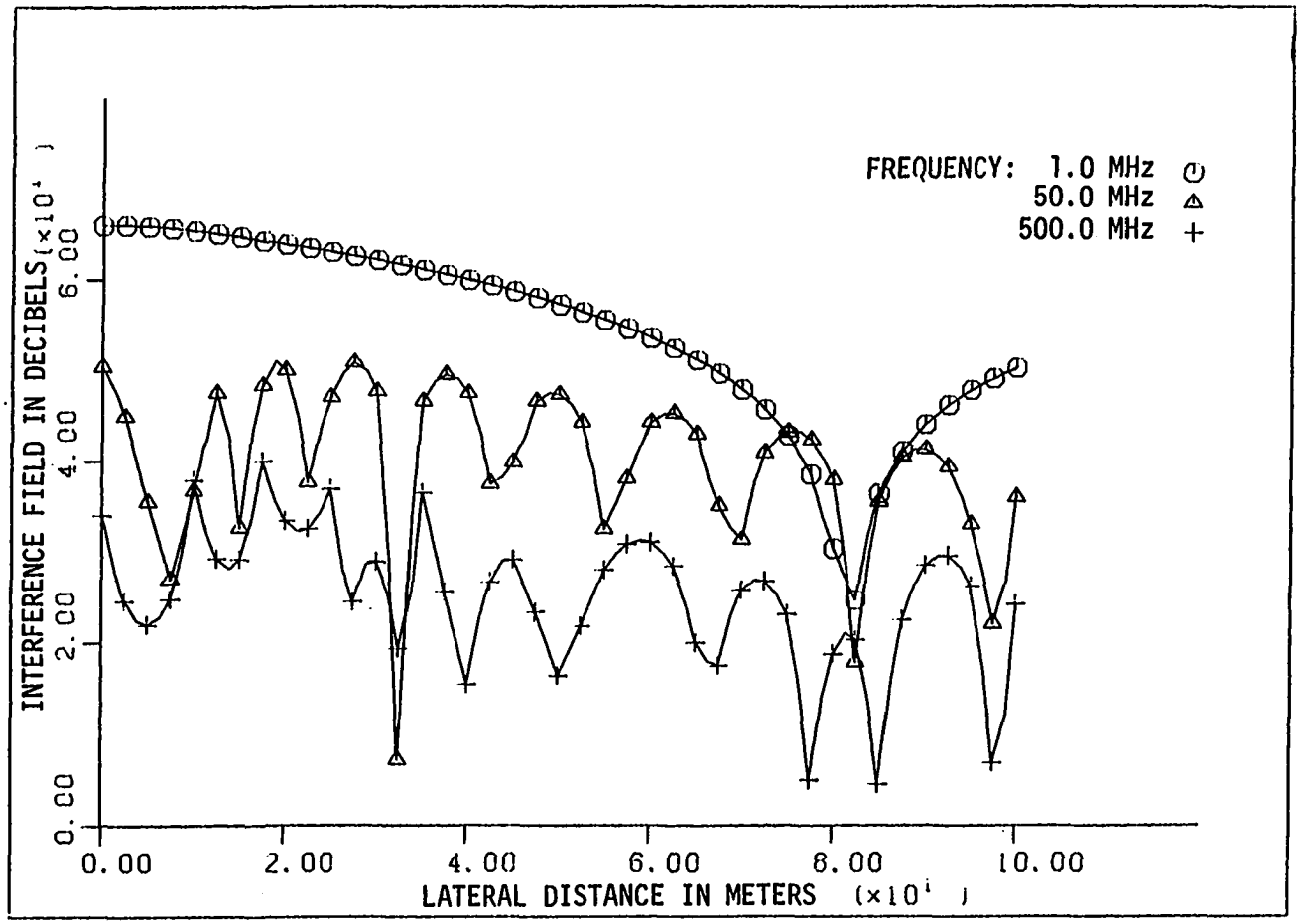

Fig. 7.24. Untransposed triangular 362 kV line - single circuit using radiation method

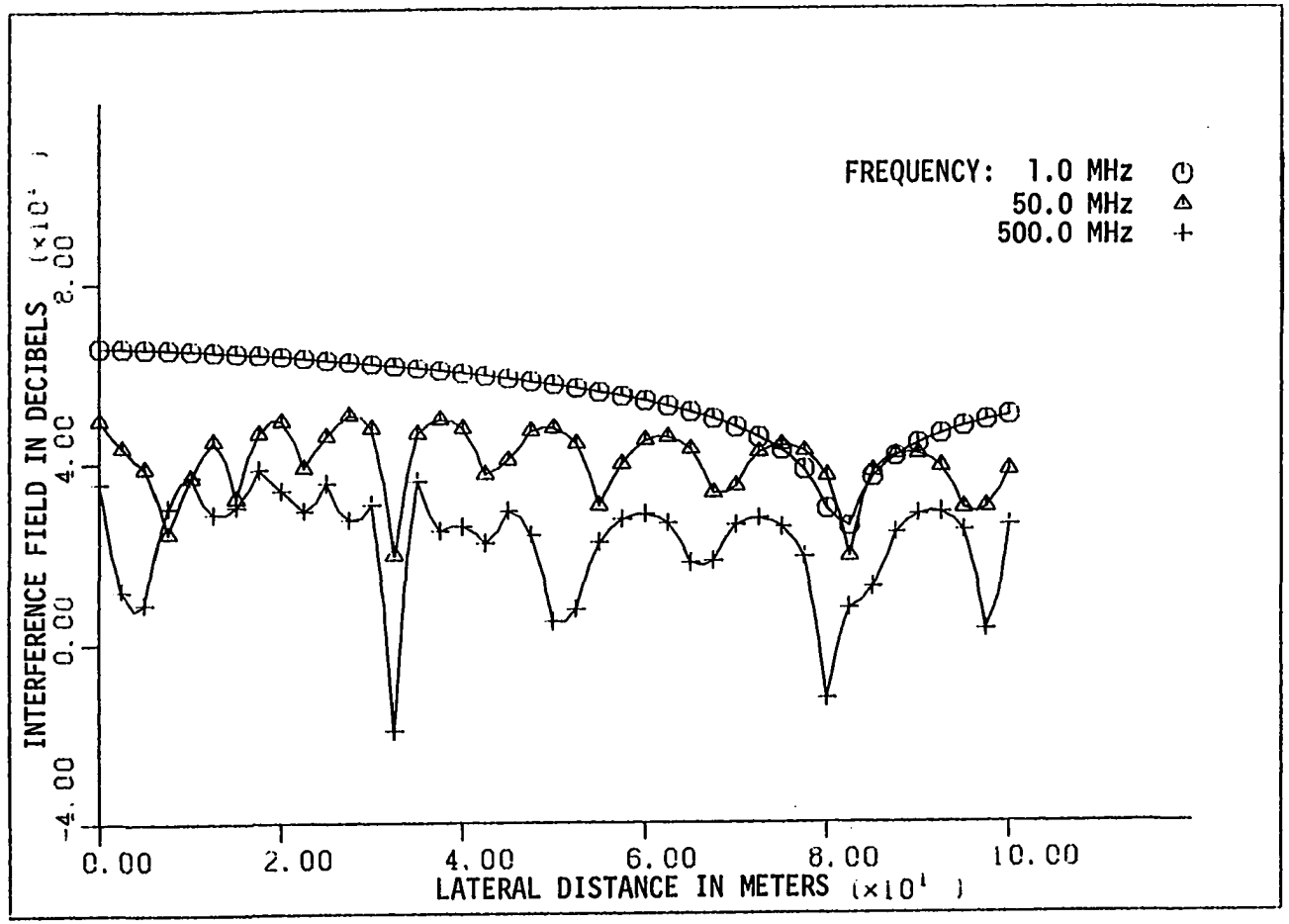

Fig. 7.25. Transposed triangular 362 kV line - single circuit using radiation method

The EMI is evaluated based on the availability of the HF corona currents or the HF corona voltages information. The classical procedure to calculate the EMI is based on the quasi-static method. In this research, the EMI was investigated by a newly developed method as well as by the use of the quasi-static method. The newly developed method has the advantage to extend and validate the study of the EMI spectrum to the FM radio and television range of frequencies.

The interference fields were computed for various transmission line configurations (Figs. 7.1-7.2) using the newly developed method and associated algorithm. The algorithm requires minimum input data such as the conductor radius, the coordinates of each conductor, the earth resistivity, the frequency and the voltage level.

Both methods prove that there is no advantage in using the transposed transmission lines as far as the improvement of the EMI level is concerned. Besides, geometrical configuration has almost no effect on the EMI. This result is valid for both methods.

At low frequencies and small distances, the EMI level computed by the quasi-static method was in all cases higher than the EMI level evaluated by the radiation method. However, at large distances and any frequency, the quasi-static method underestimated the EMI level compared to that evaluated by the radiation method. The method comparison is mainly displayed in Tables 7.11-7.16 for the one conductor per phase case and Tables 7.17-7.22 for the two subconductor per phase case.

The static EMI lateral profile and the radiated EMI lateral survey seem to follow the same pattern at low frequencies. However, at higher

frequencies, the radiated EMI level variations have some fluctuations and do not coincide with the static EMI profile. This is mainly due to the fact that the quasi-static method is no longer valid at frequencies beyond 5 MHz.

Few measurements of the EMI level have been done by the CIGRE working group 36.01 at television frequencies. These measurements, shown in Fig. 7.26, exhibit the same variations and fluctuations as the one resulting from the newly developed method. Therefore, besides the extension and validation of the study of EMI spectrum to FM radio and television frequency range, the newly developed method promises a good explanation for the few measurements undertaken by the CIGRE working group. Therefore, the newly developed method opens a new vision to the electromagnetic interference field study at high frequencies.

It is suggested to do experimental work at high frequencies for a better understanding and compare the results with the newly developed method, that is the radiation method.

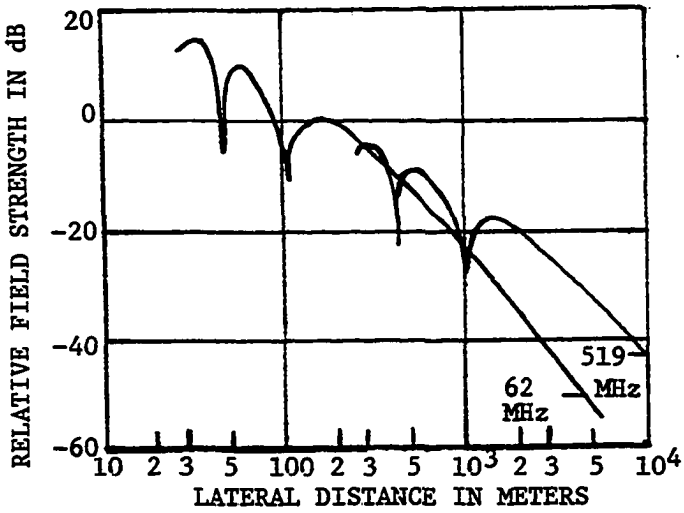

Fig. 7.26. Lateral profile of T.V.I. field [60]

VIII. LITERATURE CITED

1. Ryan, H. J. "The Conductivity of the Atmosphere at High Voltages." AIEE Transactions, Power Apparatus and Systems 23 (1940):101-34.

2. Ryan, H. J.; and Henline, H. H. "Hysteresis Character of Corona Formation." AIEE Transactions, Pt. III, Power Apparatus and Systems 43 (1924):1118-1124.

3. Pélissier, R.; and Renaudia, D. "Mechanism of the Corona Effec on AC Transmission Lines." Bulletin, Société Francais des Électriciens, Malakoff, France, 9 (1919):57-71.

4. Peek, F. W., Jr. "Law of Corona and the Dielectric Strength of Air." AIEE Transactions, Pt. III, Power Apparatus and Systems 30 (1911):1889-1965.

5. Peek, F. W., Jr. Dielectric Phenomena in High-Voltage Engineering. 3rd ed. New York: McGraw-Hill, 1929.

6. General Electric Company. Transmission Line Reference Book 345 kV and Above. Project UHV. Palo Alto, CA: Electric Power Research Institute, 1975.

7. Adams, G. E. "An Analysis of the Radio-Interference Characteristics of Bundled Conductors." AIEE Transactions, Pt. III, Power Apparatus and Systems 75 (February 1956):1569-1584.

8. Adams, G. E. "The Calculations of the Radio Interference Level of Transmission Lines Caused by Corona Discharges." AIEE Transactions, Pt. III, Power Apparatus and Systems 75 (June 1956):411-418.

9. Adams, G. E. "Radio Interference from High Voltage Transmission Lines as Influenced by the Line Design." IEEE Transactions, Power Apparatus and Systems 77 (April 1958):54.

10. Adams, G. E.; Liao, T. W.; Poland, M. G.; and Trebby, F. J. "Radio Noise Propagation and Attenuation on the Bonneville Power Administration McNary-Ross 345 kV Line." AIEE Transactions, Pt. III, Power Apparatus and Systems 78 (1959):380-388.

11. Adams, G. E.; and Barthold, L. O. "The Calculation of Attenuation Constants for Radio Noise Analysis of Overhead Lines." AIEE Transactions, Pt. III, Power Apparatus and Systems 79 (December 1960):975-981.

12. Bartenstein, R.; and Schafer, E. "Continuous Measurements of the High-Frequency Interference Levels of High Voltage Lines and Their Statistical Evaluation." CIGRE, 1954, report no. 409.

13. Boulet, L.; Cahill, L.; Jordan, J. B.; Slemon, G. R.; Janischewskyj, W.; Nigol, O.; Reichman, J.; Morris, R. M.; Khalifa, M.; and Morse, A. R. "Environmental Studies of Radio Interference from Conductor and Hardware." CIGRE, 1966, report no. 408.

14. Bernadelli, P. D.; Cortina, R.; and Sforzini, M. "Laboratory Investigation on the Radio Interference Performance of Insulators in Different Ambient Conditions." IEEE Transactions, PAS-92 (January-February 1973):14-24.

15. Cladé, J.; and Gary, C. "Les Perturbations Radioèlectriques Engendrées par les Lignes de Transport d'energie." RGE 75 (Mai 1966):5.

16. Cortina, R. et al. "Radio Interference Long-Term Recording on an Operating 420 kV Line." IEEE Transactions, PAS-89 (May/June 1970:881-892.

17. Chartier, V. L. "Interference Sources, Complaint Statistics and Limits." The Location, Correction and Prevention of RI and TVI Sources from Overhead Power Lines. IEEE Tutorial Course, IEEE Publication No. 76CH1163-5-PWR.

18. Davey, J.; Deloney, H. L.; and LaForest, J. J. "Effect of Station Radio Noise Sources on Transmission Line Noise Levels--Environmental Results." IEEE Transactions, PAS-86 (August 1967):1007-1011.

19. Clade, J. J.; and Gary, C. H. "Predetermination of Corona Losses Under Rain. Experimental Interpreting and Checking of a Method to Calculate Corona Losses." IEEE Transactions, PAS-89 (May/June 1970):853-859.

20. Clade, J. J.; Gary, G. H.; and Lefevre, C. A. "Calculation of Corona Losses Beyond the Critical Gradient in Alternating Voltage." IEEE Transactions, PAS-88 (1969):695-703.

21. Gary, C.; and Moreau, M. "Predetermination of the Radio-Interference Level of High Voltage Transmission Lines - Part 1. Predetermination of the Excitation Function." Paper 71 TP661-PWR (1971).

22. Gary, C.; and Moreau, M. "Predetermination of the Interference Level for High Voltage Transmission Lines - Part II. Field Calculating Method." Paper 71 TP662-PWR (1971).

23. Clade, J. J.; Gary, C. H.; and Moreau, M. R. "Usage and Checking of the Theoretical Relations Between Fields, Currents, and Excitation Functions in Radio Frequencies in the Case of Short Test Lines." IEEE Transactions 69 TP64-PWR, Winter Power Meeting, January, 1969.

24. Hedman, D. E. "Propagation on Overhead Transmission Lines." IEEE Transactions, PAS-84 (March 1965):205-211.

25. Wedepohl, M. "Application of Matrix Methods to the Solution of Traveling-Wave Phenomena in Polyphase Systems." IEE 110, No. 12 (December 1963):1200-1212.

26. Howatson, A. M. An Introduction to Gas Discharges. 2nd ed. Oxford: Pergamon Press, 1976.

27. Hermstein, W. "The Streamer Discharge and Its Transition into Glow." Archiv fur Elektrotechnik 45 (1960):209-224.

28. Loeb, Leonard B. Electrical Coronas: Their Basic Physical Mechanisms. Berkeley: University of California Press, 1965.

29. Mahmoud, Aly A. "High Voltage Engineering." Unpublished classroom notes, Department of Electrical Engineering, Iowa State University, 1979.

30. Kuffel, E.; and Abdullah, M. High Voltage Engineering. Oxford: Pergamon Press, 1970.

31. Nasser, E. Fundamentals of Gaseous Ionization and Plasma Electronics. New York: John Wiley and Sons, 1971.

32. Raether, H. Electron Avalanches and Breakdown in Gases. London: Butterworths, 1964.

33. Meek, J. M.; and Craggs, J. D. Electrical Breakdown of Gases. Oxford: Clarendon Press, 1953.

34. Nasser, E. "Theoretical and Experimental Studies of the Electrical Breakdown of Gases." Final report submitted to the National Science Foundation, Engineering Research Institute, Iowa State University, Ames, August 1968.

35. Trichel, G. W. "The Mechanism of the Negative Point to Plane Corona Near Onset." Physical Review 51 (1938):1078-84.

36. Giao, T. N.; and Jordan, J. B. "Modes of Corona Discharges in Air." IEEE Winter Power Meeting Papers, Technical Session on Radio Noise, Jan.-Feb., 1967, paper no. 31c 44-a.

37. Denholm, A. S. "The Pulses and Radio Interference Voltage of Power Frequency Corona." AIEE Transactions, Pt. III, Power Apparatus and Systems 79 (October 1960):698.

38. Rakoshodas, B. "Pulses and Radio-Interference Voltage of Direct Voltage Corona." IEEE Transactions, Power Apparatus and Systems 83 (May 1964):483.

39. El-Debeiky, Soliman Mohamed. "Calculating the Corona Characteristics as Influenced by Atmospheric Humidity." Ph.D. dissertation, Cairo University, Cairo, U.A.R., 1970.

40. Ryzhik, Graolshteyn. Table of Integrals, Series, and Products. New York: Academic Press, 1980.

41. Guile, A. E.; and Paterson, W. Electrical Power Systems. Vol. 1. 2nd ed. Oxford: Pergamon Press, 1977.

42. Weeks, Walter L. Transmission and Distribution of Electrical Energy. New York: Harper and Row, Publishers, 1981.

43. Ramo, Simon; Whinnery, John R.; and Van Duzer, Theodore. Fields and Waves in Communications Electronics. New York: John Wiley and Sons, 1965.

44. Wagner, C. F.; and Evans, R. D. Symmetrical Components. New York: McGraw-Hill Book Co., 1933.

45. Clarke, Edith. Circuit Analysis of A-C Power Systems. Vol. 1. General Electric Series, March 1961.

46. Anderson, P. M. Analysis of Faulted Power Systems. Ames, Iowa: Iowa State University Press, 1976.

47. IEEE Committee Report. "CIGRE/IEEE Survey on Extra High Voltage Transmission Line Noise." IEEE Transactions, PAS-92 (May/June 1973):1019-1028.

48. IEEE Committee Report. "Comparison of Radio Noise Prediction Methods with CIGRE/IEEE Survey Results." IEEE Transactions, PAS-92 (May/June 1973):1029-1042.

49. Juette, G. W.; and Zaffanella, L. E. "Radio Noise Audible Noise and Corona Loss of EHV and UHV Transmission Lines Under Rain: Predetermination Based on Cage Tests." IEEE Transactions, PAS-89 (July/August 1970):1168-1178.

50. Gary, C. H. "The Theory of the Excitation Function: A Demonstration of its Physical Meaning." IEEE Transactions, PAS-91 (1972): 305-310.

51. Stevenson, William D., Jr. Elements of Power System Analysis. New York: McGraw-Hill, Inc., 1975.

52. Nelson, J. K. "Propagation of Traveling Waves on Transmission Lines - Frequency Dependent Parameters." IEEE Transactions, PAS-91 (Jan./Feb. 1972):85.

53. Dommel, H. W. "Digital Computer Solution of Electromagnetic Transients in Single and Multiphase Networks." IEEE Transactions, PAS-88 (1969):388.

54. Fadeev, D. K.; and Fadeeva, V. N. Computational Methods for Linear Algebra. San Francisco: W. H. Freeman, 1963.

55. Pakala, W. E.; and Chartier, V. L. "Radio Noise Measurements on Overhead Power Lines from 2.4 to 800 kV." IEEE Transactions, PAS-90 (May/June 1971):1155-1165.

56. Harrington, Roger F. Time Harmonic Electromagnetic Fields. New York: McGraw-Hill, 1961.

57. Stinson, Donald C. Intermediate Mathematics of Electromagnetics. Englewood Cliffs, N.J.: Prentice-Hall, 1976.

58. Stratton, Julius A. Electromagnetic Theory. New York: McGraw-Hill, 1941.

59. Jones, D. S. Methods in Electromagnetic Wave Propagation. Oxford: Clarendon Press, 1979.

60. "Interferences produced by corona effect of electric systems: Description of phenomena, practical guide for calculation." CIGRE, Int. Conf. Large High Voltage Electric Systems, Paris, 1974.

61. Glorious Qur'an. Translation and Commentary, A. Yusuf Ali. 2nd ed. Indianapolis, IN: American Trust Publication, 1977.

IX. ACKNOWLEDGMENTS

God enjoined man to think and have an insight in the infinite natural phenomena at his disposal: "O my Lord! Advance me in knowledge" [61].

It is through God's grace and blessings that the present attempt, to think of and calculate one of the complex natural phenomena facing high voltage transmission line engineers, was accomplished.

> God will raise up, to suitable ranks and degrees, those of you who believe and who have been granted knowledge [61].

This research was carried out by the author with the special encouragement and guidance of Professors Aly A. Mahmoud and Robert E. Post. Once again, the author is grateful to his co-major professors, Dr. A. A. Mahmoud and Dr. R. E. Post, for providing the opportunity for this study, for their continuous advice and supervision throughout the author's stay in Ames.

My thanks are also extended to Dr. R. J. Lambert for his valuable discussions and encouragement in many mathematical problems.

The author also wishes to thank Drs. K. C. Kruempel, A. L. Day and J. D. Musil, who provided helpful comments and useful advice during his graduate work.

Special thanks go to J. Hoekstra (Application Systems Consultant, ISU Computation Center) for his assistance in programming and to Mrs. Carolyn Taylor for typing the manuscript.

Acknowledgment must be made to the Iowa Test and Evaluation Facility and the Power Affilitate Research Program for their financial support

which helped the author to carry out this research.

The author offers his heartfelt gratitude to his wife for her understanding, patience and unfailing encouragement. Further thanks go to my son Abdouallah whose special love and care, whenever the author goes home, have sustained the author through many dark days and nights; to my daughter Soumya, for her smile; and to my newborn daughter As-sma for being so quiet during the nights.

X. APPENDIX: EMI FORTRAN PROGRAM

```
C THE FOLLOWING 15 CARDS ARE JOB CONTROL CARDS TO CONVERT
C AND TRANSLATE A WATFIV COMPILER INTO FORTRANH COMPILER.
C A LOAD MODULE IS CREATED AND STORED INTO LOADMD1(SAL1) FILE.
C
C
C
//B211 JOB
/*JOBPARM  LINES=15
//S1    EXEC  WATFIV,REGION=192K
//GO.FT11F001    DD  DSN=S.I4349.EMI1,DISP=SHR,DCB=BUFNO=1
//GO.FT12F001    DD  DSN=&TEMP,DISP=(NEW,PASS),
//    UNIT=SCRTCH,SPACE=(TRK,(20,20)),
//    DCB=(RECFM=FB,LRECL=80,BLKSIZE=6160,BUFNO=1)
//GO.SYSIN  DD  *
$JOB       CONVERT
       CALL TRANSL(11,12) ; STOP ; END
$ENTRY
//S2   EXEC   FORTHCL,D=DOUBLE
//FORT.SYSIN   DD  DSN=&TEMP,DISP=(OLD,DELETE)
//LKED.SYSLMOD   DD  DSN=S.I4349.LOADMD1(SAL1),DISP=(NEW,CATLG),
//   SPACE=(TRK,(10,5,1),RLSE),UNIT=DISK
C
C END OF THE JCL CARDS.
C
C
C
C THE FOLLOWING CARDS INCLUDE THE MAIN PROGRAM AND THE NECESSARY
C SUBROUTINES.
C
C
C
C MAIN PROGRAM
C TRANSFORMATION METHOD TO COMPUTE CORONA CURRENTS & VOLTAGES.
C QUASI STATIC METHOD OR RADIATION METHOD TO COMPUTE EMI & HMI PROFILE.
C FTEPRI: RED BOOK EXAMPLE USING EQUIVALENT MODEL FOR TRANSPOSITION.
C
      REAL*8 NBC
      REAL*8 F1,F2,F3
      REAL*8 WA(18)
      REAL*8 DIST(6),YH,H(6),RBC,DAA,DIA,COR,GRR,F
      REAL*8 VOLT
      REAL*8 DIMAG,DREAL,DSQRT,DLOG,DLOG10
C
      REAL*8 SDX(22),SEMI(22),SHMI(22),E1(15,7,2),E2(15,14)
C
      COMPLEX*16 TRIV(3),TRIC(3)
      COMPLEX*16 ZABC(3,3),YABC(3,3)
      COMPLEX*16 INNER,U1(3,3)
      COMPLEX*16 VECTOR(3,3),VECTO2(3,3),CVET(3,3),TVEC(3,3)
      COMPLEX*16 GAM(3),TGAM(3)
```

```
      COMPLEX*16 C(3,3),E1XF(3,3)
      COMPLEX*16 CDSQRT
C
      COMMON /A1/ F1,F2,F3
      COMMON /C1/ VECTOR,TVEC,CVET,C,GAM
      COMMON /C3/ DIST,H,DIA,COR,GRR,DAA,RBC,NBC
C
C
C
C
C READ DATA
      READ(5,1) NBC,VOLT,RBC,DIA
  1   FORMAT(4X,4F10.5)
      WRITE(6,2)
  2   FORMAT(4X,15HINPUT DATA ARE:)
      WRITE(6,3) NBC
  3   FORMAT(4X,31HNUMBER OF SUBCONDUCTOR/PHASE = ,F10.5)
      WRITE(6,4) VOLT
  4   FORMAT(4X,21HLINE VOLTAGE IN KV = ,F10.4)
      WRITE(6,5) RBC
  5   FORMAT(4X,21HRADIUS OF A BUNDLE = ,F10.4)
      WRITE(6,6) DIA
  6   FORMAT(4X,24HSUBCONDUCTOR DIAMETER = ,F10.4)
C
C WE ARE USING 3 CONFIGURATIONS (HORIZONTAL,VERTICAL,TRIANGULAR).
C
      DO 7000 ICONFI=1,3
C
      DO 8 J=1,6
  8    READ(5,7) DIST(J),H(J)
C (DIST(J),H(J)) ARE THE CORDINATES OF THE JTH CONDUCTOR.
  7    FORMAT(4X,2F10.5)
C
C ITRANS DESIGNATES UNTRANSPOSED OR TRANSPOSED LINE.
      DO 9000 ITRANS=1,2
        IF(ITRANS.EQ.1) THEN
              F1=1.D0
              F2=0.D0
              F3=0.D0
         ELSE
              F1=.3333333D0
              F2=F1
              F3=F1
         ENDIF
C
C
       IF(ITRANS.EQ.1) THEN
      WRITE(6,400)
 400  FORMAT(1H, 17HUNTRANSPOSED CASE)
       ELSE
```

```
       WRITE(6,401)
 401     FORMAT(1H,15HTRANSPOSED CASE)
       ENDIF
C
C
      IF(ICONFI.EQ.1) THEN
      WRITE(6,403)
 403    FORMAT(4X,24HHORIZONTAL CONFIGURATION)
      ELSE IF(ICONFI.EQ.2) THEN
      WRITE(6,404)
 404     FORMAT(4X,22HVERTICAL CONFIGURATION)
      ELSE IF(ICONFI.EQ.3) THEN
      WRITE(6,405)
 405     FORMAT(4X,24HTRIANGULAR CONFIGURATION)
      ELSE IF(ICONFI.EQ.4) THEN
      WRITE(6,406)
406       FORMAT(4X,25HRECTANGULAR CONFIGURATION)
      ENDIF
C
       WRITE(6,9)
  9    FORMAT(4X,13H   NUMBER    ,15H   X-CORDINATES,15H   Y-CORDINATES)
       DO 11 K=1,6
 11    WRITE(6,10) K,DIST(K),H(K)
 10    FORMAT(I10,6X,F10.4,3X,F10.4)
C
C
C VARIATION OF FREQUENCY FROM 0.5 MHZ TO 1000 MHZ.
C
       DO 7001 IFREQ=1,7
C
       IF(IFREQ.EQ.1 ) THEN
        F=500000.D0
       ELSE IF(IFREQ.EQ.2 ) THEN
        F=1000000.D0
       ELSE IF(IFREQ.EQ.3 ) THEN
        F=5000000.D0
       ELSE IF(IFREQ.EQ.4 ) THEN
       F=10000000.D0
       ELSE IF(IFREQ.EQ.5 ) THEN
       F=50000000.D0
       ELSE IF(IFREQ.EQ.6 ) THEN
       F=100000000.D0
       ELSE IF(IFREQ.EQ.7 ) THEN
       F= 500000000.D0
       ENDIF
C
C
      CALL PARM(F,ZABC,YABC)
       CALL EXFUN(F,C,VOLT,E1XF)
        CALL CORONA(E1XF,TRIC,TRIV)
```

```
C
C
C
C CALL SUBROUTINE RADIATION OR QUASI TO COMPUTE EMI & HMI PROFILE.
C IMETH MEANS EITHER QUASI STATIC OR RADIATION METHOD.
C
       DO 7002 IMETH=1,2
C
      IF(IMETH.EQ.1) THEN
      WRITE(6,780)
 780  FORMAT(1H1,47HEMI & HMI PROFILE USING THE QUASI STATIC METHOD)
C
          CALL QUASI(H,DIST,TRIV,SDX,SEMI,SHMI)
      ELSE
      WRITE(6,781)
 781  FORMAT(1H1,2X,44HEMI & HMI PROFILE USING THE RADIATION METHOD)
C
          CALL RADIA(F,H,DIST,TRIC,SDX,SEMI,SHMI)
      ENDIF
C
C
          WRITE(6,32)
 32     FORMAT(17X,16HLATERAL DISTANCE,9X,6HEFIELD,11X,6HHFIELD)
          DO 33 IY=1,15
          WRITE(6,34) SDX(IY),SEMI(IY),SHMI(IY)
          WRITE(15,35) SDX(IY),SEMI(IY),SHMI(IY)
 33     CONTINUE
 34     FORMAT(15X,F16.6,5X,2F16.6)
  35       FORMAT(3F16.8)
C
C
C
          DO 7003 IL=1,15
               E1(IL,IFREQ,IMETH)=SEMI(IL)
 7003      CONTINUE
C
 7002  CONTINUE
       DO 7004 IL=1,15
            E2(IL,IFREQ)=E1(IL,IFREQ,1)
            E2(IL,IFREQ+7)=E1(IL,IFREQ,2)
 7004   CONTINUE
 7001  CONTINUE
              WRITE(6,7006)
 7006         FORMAT(4X, 'QUASI VS. RADIA')
         WRITE(6,7005) ((E2(I,J),J=1,14),I=1,15)
 7005     FORMAT(2X,14F8.1)
 9000 CONTINUE
 7000  CONTINUE
      STOP
      END
```

```
C
C
C
C SUBROUTINE 'PARM' TO CALCULATE THE ELECTRICAL PARAMETER OF THE LINE
C
C
      SUBROUTINE PARM(F,ZABC,YABC)
C
       REAL*8 NBC
C
      REAL*8 F1,F2,F3
      REAL*8 DIST(6),H(6),DLTA(6,6),RBC,DAA,DIA,COR,GRR,F,WO
      REAL*8 DIMAG,DREAL,DSQRT,DLOG,DLOG10
      REAL*8 P(3,3)
      REAL*8 WK(30)
      REAL*8 RBSYM(18),RVEC(18),RTBSYM(18),RTVEC(18),WA(18)
      REAL*8 RGAM(6),RTGAM(6)
      REAL*8 GR,CGR,XAA,XAB,XAC,XBC,CA
C
      COMPLEX*16 ZINT
      COMPLEX*16 ZPA(3,3),CPA(3,3),ZABC(3,3),YABC(3,3)
      COMPLEX*16  BSYM(3,3),VECTOR(3,3),GAM(3)
      COMPLEX*16 TBSYM(3,3),TVEC(3,3),TGAM(3)
      COMPLEX*16 INNER,U1(3,3)
      COMPLEX*16 CDSQRT,CVET(3,3),C(3,3)
C
      EQUIVALENCE (BSYM(1,1),RBSYM(1)),(VECTOR(1,1),RVEC(1))
      EQUIVALENCE (GAM(1),RGAM(1))
      EQUIVALENCE (TBSYM(1,1),RTBSYM(1)),(TVEC(1,1),RTVEC(1))
      EQUIVALENCE (TGAM(1),RTGAM(1))
C
      COMMON /A1/ F1,F2,F3
      COMMON /C1/ VECTOR,TVEC,CVET,C,GAM
      COMMON /C3/ DIST,H,DIA,COR,GRR,DAA,RBC,NBC
C
C
C
            WRITE(6,13) F
 13         FORMAT('1', 2X, 11HFREQUENCY: ,F16.2)
C
        WO=2*3.1415927D0*F
C
C COMPUTE DLTA(I,J): DISTANCE FROM CONDUCTOR I TO CONDUCTOR J.
C
      DO 800 I=1,6
      DO 800 J=1,6
         DLTA(I,J)=DSQRT((DIST(J)-DIST(I))**2+(H(J)-H(I))**2)
 800  CONTINUE
C
C
```

```
C
      WRITE(6,999)
 999  FORMAT('-', 6H DATA:)
      WRITE(6,998) F1,F2,F3
 998  FORMAT(2X, 4HF1= ,F10.7,5X, 4HF2= ,F10.7,5X, 4HF3= ,F10.7)
      WRITE(6,992)
 992  FORMAT('   DELTA(I,J): ' )
      WRITE(6,997) ((DLTA(I,J),J=1,6),I=1,6)
 997  FORMAT(2X, 6F12.7)
      WRITE(6,995) (H(I),I=1,6)
 995  FORMAT(2X, 9HHEIGHTS= ,6F10.4)
C
C COR=CONDUCTOR RESISTANCE (OHM/METER).
C GRR=GOUND RETURN RESISTANCE (OHM/METER).
C WO IS IN RADIAN PER SECONDS (RAD/SEC)
C
C COMPUTE THE IMPEDANCE AND THE ADMITTANCE MATRICES OF THE LINE
C
       CALL SKIN(F,ZINT)
C
      DE=2160.D0*DSQRT(100.D0/F)*.3048D0
C
C DAA: EQUIVALENT DIAMETER OF THE BUNDLE CONDUCTOR IN METER.
C RBC: RADIUS OF BUNDLE IN METER.
C NBC: NUMBER OF CONDUCTOR /BUNDLE.
C DIA:DIAMETER OF A CONDUCTOR IN A BUNDLE IN METER.
      DAA=2.D0*RBC*(NBC*0.779D0*DIA/(2.D0*RBC))**(1.D0/NBC)
      WRITE(6,7) DAA
  7   FORMAT(4X,22HEQUIVALENT DIAMETER = ,F10.4)
C
      COR=DREAL(ZINT)
      GRR=9.869D-07*F
      WRITE(6,996) COR,GRR,WO
 996  FORMAT(2X, 5HCOR= ,F12.5,5X, 5HGRR= ,F12.5,5X, 4HWO= ,F16.5 )
C
C CALCULATON OF THE INDUCTANCES
      XAA=DIMAG(ZINT)+(25.132741D-7/2.D0)*F*DLOG(DE*2.D0/DAA)
      XAB=25.132741D-7*F*DLOG(DE/DLTA(1,2))/2.D0
      XAC=25.132741D-7*F*DLOG(DE/DLTA(1,3))/2.D0
      XBC=25.132741D-7*F*DLOG(DE/DLTA(2,3))/2.D0
C
      CGR=COR+GRR
      GR=GRR
C
C DETERMINATION OF THE IMPEDANCES
      ZPA(1,1)=DCMPLX(CGR,XAA)
      ZPA(1,2)=DCMPLX(GR,XAB)
      ZPA(1,3)=DCMPLX(GR,XAC)
C
      ZPA(2,1)=ZPA(1,2)
```

```
      ZPA(2,2)=ZPA(1,1)
      ZPA(2,3)=DCMPLX(GR,XBC)
C
      ZPA(3,1)=ZPA(1,3)
      ZPA(3,2)=ZPA(2,3)
      ZPA(3,3)=ZPA(1,1)
C
       ZABC(1,2)=F1*ZPA(1,2)+F2*ZPA(2,3)+F3*ZPA(3,1)
       ZABC(1,3)=F1*ZPA(1,3)+F2*ZPA(1,2)+F3*ZPA(2,3)
        ZABC(2,3)=F1*ZPA(2,3)+F2*ZPA(1,3)+F3*ZPA(1,2)
      ZABC(2,1)=ZABC(1,2)
      ZABC(3,1)=ZABC(1,3)
      ZABC(3,2)=ZABC(2,3)
        ZABC(1,1)=ZPA(1,1)
         ZABC(3,3)=ZPA(3,3)
         ZABC(2,2)=ZPA(2,2)
C
C
C
      WRITE(6,4)
  4   FORMAT(4X,22HPHASE IMPEDANCE MATRIX)
      WRITE(6,2002) ((ZABC(I,J),J=1,3),I=1,3)
C
C CALCULATION OF THE POTENTIAL COEFFICIENTS
      P(1,1)=18.D09*DLOG(4.D0*H(1)*(0.779D0**(1.D0/NBC))/DAA)
      P(1,2)=18.D09*DLOG(DLTA(1,5)/DLTA(1,2))
      P(1,3)=18.D09*DLOG(DLTA(1,6)/DLTA(1,3))
C
      P(2,1)=P(1,2)
      P(2,2)=18.D09*DLOG(4.D0*H(2)*(0.779D0**(1.D0/NBC))/DAA)
      P(2,3)=18.D09*DLOG(DLTA(2,6)/DLTA(2,3))
C
      P(3,1)=P(1,3)
      P(3,2)=P(2,3)
      P(3,3)=18.D09*DLOG(4.D0*H(3)*(0.779D0**(1.D0/NBC))/DAA)
C
C FIND THE INVERSE OF THE POTENTIAL COEFFICIENTS MATRIX.CALL IT CPA
      DO 21 I=1,3
      DO 22 J=1,3
      U1(I,J)=DCMPLX(P(I,J) , 0.D0)
C C IS THE CAPACITANCE MATRIX
  22  CPA(I,J)=(0.D0 , 0.D0)
  21  CPA(I,I)=(1.D0,0.D0)
C CALL SUBROUTINE LEQT1C TO INVERT A COMPLEX MATRIX.
      CALL LEQT1C(U1,3,3,CPA,3,3,0,WA,IER)
      IF(IER.NE.0) GOTO 100
  100 WRITE(6,200) IER
  200 FORMAT('0',I10)
C
      C(1,1)=F1*CPA(1,1)+F2*CPA(2,2)+F3*CPA(3,3)
```

```
      C(1,2)=F1*CPA(1,2)+F2*CPA(2,3)+F3*CPA(3,1)
      C(1,3)=F1*CPA(1,3)+F2*CPA(1,2)+F3*CPA(2,3)
C
      C(2,1)=C(1,2)
      C(2,2)=F1*CPA(2,2)+F2*CPA(3,3)+F3*CPA(1,1)
      C(2,3)=F1*CPA(2,3)+F2*CPA(1,3)+F3*CPA(1,2)
C
      C(3,1)=C(1,3)
      C(3,2)=C(2,3)
      C(3,3)=F1*CPA(3,3)+F2*CPA(1,1)+F3*CPA(2,2)
C
      WRITE(6,5)
    5 FORMAT(4X,18HCAPACITANCE MATRIX)
      WRITE(6,2002) ((C(I,J),J=1,3),I=1,3)
C
C
C
C CALCULATION OF THE ADMITTANCE MATRIX YABC
C
      DO 30 I=1,3
      CA=CDABS(C(I,I))
      YABC(I,I)=DCMPLX(0.D0,CA*WO)
      DO 23 J=1,3
      IF(I.EQ.J) GO TO 23
      CA=-CDABS(C(I,J))
      YABC(I,J)=DCMPLX(0.0D0,CA*WO)
   23 CONTINUE
   30 CONTINUE
C
C
      WRITE(6,6)
    6 FORMAT(4X,23HPHASE ADMITTANCE MATRIX)
      WRITE (6,2002) ((YABC(I,J),J=1,3),I=1,3)
C
      CALL MULTI(ZABC,YABC,BSYM)
      WRITE(6,8)
    8 FORMAT(4X,17HBSYM IS ZABC*YABC)
      WRITE(6,2002) ((BSYM(I,J),J=1,3),I=1,3)
C
      DO 50 I=1,3
      DO 50 J=1,3
      TBSYM(I,J)=BSYM(J,I)
   50 CONTINUE
 2002 FORMAT(6G15.6)
C
C CALL EIGENVALUES AND EIGENVECTORS SUBROUTINE.
      CALL EIGCC(RBSYM,3,3,1,RGAM,RVEC,3,WK,IER)
      CALL EIGCC(RTBSYM,3,3,1,RTGAM,RTVEC,3,WK,IER)
C
      DO 2 IT=1,3
```

```
          GAM(IT)=CDSQRT(GAM(IT))
          TGAM(IT)=CDSQRT(TGAM(IT))
 2     CONTINUE
C
      WRITE(6,1753)
 1753 FORMAT('-', 5H GAM:)
      WRITE(6,2000) (GAM(I),I=1,3)
      WRITE(6,1754)
 1754 FORMAT('-', 6H TGAM:)
      WRITE(6,2000) (TGAM(I),I=1,3)
      WRITE(6,1900)
 1900 FORMAT('-', 5H VEC:)
      WRITE(6,2001) ((VECTOR(I,J),J=1,3),I=1,3)
      WRITE (6,1925)
 1925 FORMAT('-', 6H TVEC:)
      WRITE(6,2001) ((TVEC(I,J),J=1,3),I=1,3)
 2000 FORMAT(12G15.6)
 2001 FORMAT(6G15.6)
C
C
C FIND THE INVERSE OF THE EIGENVECTOR MATRIX.CALL IT CVET
      DO 220 I=1,3
      DO 222 J=1,3
      U1(I,J)=DCMPLX(DREAL(TVEC(I,J)),DIMAG(TVEC(I,J)))
C C VECTOR IS THEINVERSE TRANSFORMATION MATRIX
  222 CVET(I,J)=(0.0 , 0.0)
  220 CVET(I,I)=(1.0,0.0)
C CALL SUBROUTINE LEQT1C TO INVERT A COMPLEX MATRIX.
      CALL LEQT1C(U1,3,3,CVET,3,3,0,WA,IER)
      IF(IER.NE.0) GOTO 101
  101 WRITE(6,205) IER
  205 FORMAT('0',I10)
C
      RETURN
      END
C
C
C SUBROUTINE 'MULTI' TO MULTIPLY TWO SQUARE MATRICES.
C
      SUBROUTINE MULTI(A,B,C)
      COMPLEX*16 A(3,3),B(3,3),C(3,3)
      DO 10 I=1,3
      DO 10 J =1,3
      C(I,J)=(0.0,0.0)
      DO 10 K=1,3
   10 C(I,J)=C(I,J)+A(I,K)*B(K,J)
      RETURN
      END
C
C
```

```
C SUBROUTINE 'MULTI1' TO MULTIPLY A SQUARE MATRIX BY A VECTOR.
C
      SUBROUTINE MULTI1(A,B,C)
      COMPLEX*16 A(3,3),B(3,1),C(3,1)
      DO 10 I=1,3
      J=1
      C(I,J)=(0.0,0.0)
      DO 10 K=1,3
  10  C(I,J)=C(I,J)+A(I,K)*B(K,J)
      RETURN
      END
C
C
C FUNCTION 'INNER' TO DETERMINE THE INNER PRODUCT OF TWO VECTORS.
C
      FUNCTION INNER(A,B)
      COMPLEX*16 A(3,1),B(3,1),INNER,AT(1,3)
      INNER=(0.0,0.0)
      DO 10 I=1,3
      AT(1,I)=A(I,1)
  10  INNER=INNER+DCONJG(AT(1,I))*B(I,1)
      RETURN
      END
C
C SUBROUTINE 'TRANSP' TO TRANSPOSE A MATRIX.
C
C SUBROUTINE TO DETERMINE THE TRANSPOSED MATRIX.
      SUBROUTINE TRANSP(A,AT)
       COMPLEX*16 A(3,3),AT(3,3)
        DO 1 I=1,3
        DO 1 J=1,3
        AT(I,J)=A(J,I)
 1      CONTINUE
        RETURN
        END
C
C
C SUBROUTINE 'SKIN' TO CALCULATE THE INTERNAL IMPEDANCE AS A FUNCTION
C OF FREQUENCY.
C
      SUBROUTINE SKIN(F,ZINT)
C
      INTEGER IER,NBSL
      REAL*8 DIMAG,DREAL,DSQRT,DLOG,DLOG10
      REAL*8 F,RDC,BSLR(2),BSLI(2),RZINT,XR,XI,XRXI
      COMPLEX*16 ZINT
C
C F=FREQUENCY IN HZ
C RDC=DC RESISTANCE OF EACH CONDUCTOR IN OHM/METER
      RDC=0.0426D0/1609.D0
```

```
C USE BESSEL FUNCTIONS TO DETERMINE THE INTERNAL IMPEDANCE.
        NBSL=2
        XR=-DSQRT(12.56637D-7*F/RDC)/2.D0
        XI=-XR
C
       XRXI=DSQRT(XR*XR+XI*XI)
       IF((XRXI.GT.1D4).OR.(XI.GT.110))      GO TO  15
       CALL MMBZJN(XR,XI,NBSL,BSLR,BSLI,IER)
      WRITE(6,1) IER
  1   FORMAT(4X,21HERROR FROM MMBZJN IS:,I4)
      WRITE(6,32) (BSLR(I),I=1,2)
  32  FORMAT(4X,15HREAL BSL ARE = ,F16.8)
      WRITE(6,3) (BSLI(I),I=1,2)
  3   FORMAT(4X,20HIMAGINARY BSL ARE = ,F16.8)
C
C ZINT=INTERNAL IMPEDANCE OF EACH CONDUCTOR IN OHM/METER.
       ZINT=RDC*DCMPLX(BSLR(1),BSLI(1))/DCMPLX(BSLR(2),BSLI(2))
       ZINT=ZINT*DCMPLX(XR,XI)/2.D0
       GO TO 16
 15   RZINT=DSQRT(RDC*12.56637D-7*F)/2.D0
      ZINT=DCMPLX(RZINT,RZINT)
C
 16   WRITE(6,12) ZINT
 12   FORMAT(2X, 6HZINT= ,2F16.5)
C
      RETURN
      END
C
C
C
C
C SUBROUTINE 'EXFUN' TO EVALUATE THE EXCITATION FUNCTION.
C
        SUBROUTINE EXFUN(F,C,VOLT,E1XF)
C
       REAL*8 NBC
      REAL*8 DIMAG,DREAL,DSQRT,DLOG,DLOG10
      REAL*8 VOLT,GRD(3),GRDMX(3),CHARGM(3),EXF(3)
      REAL*8 DIST(6),H(6),RBC,DAA,DIA,DX(3),COR,GRR,F
      COMPLEX*16 KVOLT(3),CHARG(3)
      COMPLEX*16 CDSQRT,E1XF(3,3),C(3,3)
C
      COMMON /C3/ DIST,H,DIA,COR,GRR,DAA,RBC,NBC
      KVOLT(1)=DCMPLX(VOLT/1.732D0,0.D0)
      KVOLT(2)=DCMPLX(-VOLT/3.464D0,-VOLT/2.D0)
      KVOLT(3)=DCMPLX(-VOLT/3.464D0,VOLT/2.D0)
C
      WRITE(6,1) (KVOLT(K), K=1,3)
   1  FORMAT(4X,27HPHASE VOLTAGES IN KV ARE = ,F10.4)
      CALL MULTI1(C,KVOLT,CHARG)
```

```
      DO 8000 I=1,3
          CHARGM(I)=CDABS(CHARG(I))
          GRD(I)=18.D09*CHARGM(I)/((1.D2*DIA/2.D0)*NBC)
          GRDMX(I)=GRD(I)*(1+((NBC-1.D0)*DIA/(2.D0*RBC)))
      EXF(I)=78.D0-(580.D0/GRDMX(I))+38.D0*DLOG10(1.D2*DIA/3.8D0)
 8000 CONTINUE
C
C THE BASE FREQUENCY,F0, IN THE RED BOOK MEASUREMENT IS:
      F0=1000000.D0
          EXF(1)=(10**(EXF(1)/20.D0))*DSQRT((2.D0*F0)/(F0+F))
          EXF(2)=(10**(EXF(2)/20.D0))*DSQRT((2.D0*F0)/(F0+F))
          EXF(3)=(10**(EXF(3)/20.D0))*DSQRT((2.D0*F0)/(F0+F))
C
      DO 45 I=1,3
      DO 45 J=1,3
      E1XF(I,J)=DCMPLX(0.D0,0.D0)
      IF(I.NE.J)  GO TO 45
      E1XF(I,J)=DCMPLX(EXF(I),0.D0)
 45   CONTINUE
C
       WRITE(6,3) (CHARGM(I),I=1,3)
  3    FORMAT(4X,19HLINE CHARGES ARE = ,F16.8)
       WRITE(6,4) (GRDMX(I),I=1,3)
  4    FORMAT(4X,32HMAXIMUM VOLTAGE GRADIENTS ARE = ,F10.4)
      WRITE(6,2) (EXF(K),K=1,3)
  2   FORMAT(4X,32HEXCITATION FUNCTION IN DB ARE = ,F10.4)
C
         RETURN
         END
C
C
C
C
C SUBPROGRAM TO CALCULATE CORONA CURRENTS & CORONA VOLTAGES.
C
      SUBROUTINE CORONA(E1XF,TRIC,TRIV)
       REAL*8 F1,F2,F3
      REAL*8 DIMAG,DREAL,DSQRT,DLOG,DLOG10
      REAL*8 TRIVM(3),TRI(3)
C
      COMPLEX*16 TRIV(3),TRIC(3)
      COMPLEX*16 Q(3),W(3,3),WN(3,3),RI(3,3),RIC(3)
      COMPLEX*16 CDSQRT,ACO(3,3)
      COMPLEX*16 VECTOR(3,3),VECTO2(3,3),CVET(3,3),TVEC(3,3)
      COMPLEX*16 GAM(3),TGAM(3)
      COMPLEX*16 C(3,3),E1XF(3,3)
C
      COMMON /A1/ F1,F2,F3
      COMMON /C1/ VECTOR,TVEC,CVET,C,GAM
C
```

```
C
      DO 91 I=1,3
      DO 91 J=1,3
      ACO(I,J)=18.D09*C(I,J)
 91   CONTINUE
      CALL MULTI(ACO,E1XF,RI)
      DO 201 I=1,3
      RIC(I)=RI(I,1)+RI(I,2)+RI(I,3)
 201  CONTINUE
      WRITE(6,12) (RIC(I),I=1,3)
 12   FORMAT(4X,20HTOTAL RI CURRENTS = ,F10.4)
C
        CALL MULTI(CVET,RI,W)
        DO 200 I=1,3
           Q(I)=W(I,1)+W(I,2)+W(I,3)
        DO 200 J=1,3
           WN(J,I)=Q(I)*TVEC(J,I)
 200    CONTINUE
C
      IF(F1.EQ.F2) GO TO 811
C
C COMPUTE TRI FOR UNIFORMELY DISTRIBUTED CORONA OVER THE ENTIRE LENGTH
C
C COMPUTE TRI (UNTRANSPOSED CASE) USING W(I,J).
C
      DO 94 K11=1,3
      TRIC(K11)=(0.D0,0.D0)
      DO 95 IK=1,3
      DO 95 J=1,3
 95   TRIC(K11)=TRIC(K11)+(WN(K11,IK)*WN(K11,J))/(GAM(IK)+GAM(J))
      TRIC(K11)=CDSQRT(2.D0*TRIC(K11))
 94     TRI(K11)=CDABS(TRIC(K11))
C
      WRITE(6,13) (TRI(I),I=1,3)
 13   FORMAT(4X,34HTRI CURRENTS (UNTRANSPOSED) ARE = ,F10.4)
      GO TO 820
C
 811  CONTINUE
C
C COMPUTE TRI (TRANSPOSED CASE) USING W(I,J).
      DO 812 I=1,3
      TRIC(I)=(WN(I,1)**2)/(4.D0*GAM(1)**3)+WN(I,2)**2/(2.D0*GAM(2))
      TRIC(I)=TRIC(I)+WN(I,3)**2/(2.D0*GAM(3))
      TRIC(I)=TRIC(I)+2.D0*(WN(I,3)*WN(I,1))/((GAM(3)+GAM(1))**2)
      TRIC(I)=TRIC(I)+2.D0*(WN(I,2)*WN(I,1))/((GAM(1)+GAM(2))**2)
      TRIC(I)=TRIC(I)+2.D0*(WN(I,2)*WN(I,3))/(GAM(2)+GAM(3))
C
      TRIC(I)=CDSQRT(2.D0*TRIC(I))
      TRI(I)=CDABS(TRIC(I))
C
```

```
 812  CONTINUE
      WRITE(6,14) (TRI(I),I=1,3)
 14   FORMAT(4X,32HTRI CURRENTS (TRANSPOSED) ARE = ,F10.4)
  820  CONTINUE
       DO 92 I=1,3
       TRIV(I)=60.D0*TRIC(I)
       TRIVM(I)=CDABS(TRIV(I))
 92    CONTINUE
      WRITE(6,15) (TRIVM(I),I=1,3)
 15   FORMAT(4X,32HTOTAL RI VOLTAGES (TRIVM) ARE = ,F10.4)
C
C
       RETURN
       END
C
C
C
C THIS SUBPROGRAM COMPUTES THE EMI & HMI PROFILE BY RADIATION METHOD.
C
       SUBROUTINE RADIA(F,H,DIST,TRIC,SDX,SEMI,SHMI)
C
C
      INTEGER NB,NORDER,IER
      REAL*8 DIMAG,DREAL,DSQRT,DLOG,DLOG10
      REAL*8 DIST(6),YH,H(6),RBC,DAA,DIA,DX(3),F
      REAL*8 VOLT,EXF(3),LAMBDA,EPSIF,CMUF,RK,EFM(6),HFM(6),HTOTM,ETOTM
C
      REAL*8 SDX(22),SEMI(22),SHMI(22)
      REAL*8 TRI(3),TRIVM(3),CONST
      REAL*8 BSL1(3),BSL2(3),ARG,ORDER
C
      COMPLEX*16 HANKL2,DHANKL,TRIC(3),TRIV(3)
      COMPLEX*16 RIC(3),HFIELD(6),EFIELD(6)
      COMPLEX*16 EPSI,CMU,RKJ,ACO(3,3)
      COMPLEX*16 HTOTAL,ETOTAL
      COMPLEX*16 C(3,3)
      COMPLEX*16 CDSQRT
C
      RK=2.094395D-8*F
      RKJ=-DCMPLX(0.D0,RK)
      ETHA=377.D0
      LAMBDA=6.2831853D0/RK
      SPEED=3.D8
      EPSIF=0.055555556D-9*F
      CMUF=-78.956835D-7*F
      EPSI=DCMPLX(0.D0,EPSIF)
      CMU=DCMPLX(0.D0,CMUF)
C
       NB=3
       NORDER=3
```

```
       ORDER=0.D0
C
        YH=0.D0
      DX(2)=-1.875D0
C
C LATERAL SURVEY AT DIFFERENT FREQUENCIES.
C
       DO 31 IR=1,15
       IF(IR.LE.5) THEN
        DX(2)=DX(2)+1.875D0
       ELSE IF(IR.EQ.6) THEN
        DX(2)=10.D0
       ELSE
       DX(2)=DX(2)+10.D0
       ENDIF
C
      DX(1)=DX(2)+(DIST(2)-DIST(1))
      DX(3)=DX(2)-(DIST(3)-DIST(2))
C
      DO 90 I=1,6
      IF(I.GT.3) GO TO 780
      DENO=DSQRT((H(I)-YH)**2+DX(I)**2)
      ARG=RK*DENO
      CALL MMBSJN(ARG,NORDER,BSL1,IER)
       WRITE(6,1001) IER
 1001  FORMAT(4X,18HIER FROM BSL1 IS : ,I5)
C       WRITE(6,1002)
C1002   FORMAT(4X,32HFIRST KIND BESSEL FUNCTIONS ARE:)
C       WRITE(6,1003) (BSL1(IU),IU=1,3)
C 1003  FORMAT(4X,3F16.8)
       CALL MMBSYN(ARG,ORDER,NB,BSL2,IER)
       WRITE(6,1005) IER
 1005  FORMAT(4X,18HIER FROM BSL2 IS : ,I5)
C      WRITE(6,1004)
C 1004 FORMAT(4X,33HSECOND KIND BESSEL FUNCTIONS ARE:)
C      WRITE(6,1003) (BSL2(IY),IY=1,3)
        HANKL2=DCMPLX(BSL1(1),-BSL2(1))
C       WRITE(6,1006) HANKL2
C 1006  FORMAT(4X,44HSECOND KIND (ZERO ORDER) HANKEL FUNCTION IS:,F16.8)
        DHANKL=DCMPLX(BSL1(2),-BSL2(2))
C       WRITE(6,781)  DHANKL
C 781  FORMAT(4X,45HSECOND KIND (FIRST ORDER) HANKEL FUNCTION IS:,F16.8)
      PATF=TRIC(I)*HANKL2
      DPATF=TRIC(I)*DHANKL
      GO TO 782
  780   DENO=DSQRT((-H(I)+YH)**2+DX(I-3)**2)
      ARG=RK*DENO
      CALL MMBSJN(ARG,NORDER,BSL1,IER)
       WRITE(6,1001) IER
C       WRITE(6,1002)
```

```
C       WRITE(6,1003) (BSL1(IU),IU=1,3)
        CALL MMBSYN(ARG,ORDER,NB,BSL2,IER)
        WRITE(6,1005) IER
C       WRITE(6,1004)
C       WRITE(6,1003) (BSL2(IY),IY=1,3)
         HANKL2=DCMPLX(BSL1(1),-BSL2(1))
C        WRITE(6,1006) HANKL2
         DHANKL=DCMPLX(BSL1(2),-BSL2(2))
C        WRITE(6,781)  DHANKL
       PATF=TRIC(I-3)*HANKL2
       DPATF=TRIC(I-3)*DHANKL
  782   HFIELD(I)=DPATF*DCMPLX(0.D0,-1.D0)/4.D0
       HFM(I)=CDABS(HFIELD(I))
       HFM(I)=20.D0*DLOG10(HFM(I))
       EFIELD(I)=PATF*CMU*DCMPLX(0.D0,-1.D0)/4.D0
       EFM(I)=CDABS(EFIELD(I))
       EFM(I)=20.D0*DLOG10(EFM(I))
 90    CONTINUE
C
C DETERMINATION OF THE TOTAL H & E FIELD.
       HTOTAL=HFIELD(1)+HFIELD(2)+HFIELD(3)+HFIELD(4)+HFIELD(5)+HFIELD(6)
       ETOTAL=EFIELD(1)+EFIELD(2)+EFIELD(3)+EFIELD(4)+EFIELD(5)+EFIELD(6)
       HTOTM=CDABS(HTOTAL)
       ETOTM=CDABS(ETOTAL)
       HTOTM=20.D0*DLOG10(HTOTM)
       ETOTM=20.D0*DLOG10(ETOTM)
C
C STORE LATERAL DISTANCE,EFIELD,HFIELD FOR PLOT.
C
         SDX(IR)=DX(2)
         SEMI(IR)=ETOTM
         SHMI(IR)=HTOTM
  31    CONTINUE
C
       RETURN
       END
C
C
C THIS SUBPROGRAM COMPUTES EMI & HMI PROFILE BY THE QUASI STATIC METHOD.
C
        SUBROUTINE QUASI(H,DIST,TRIV,SDX,SEMI,SHMI)
       REAL*8 DIMAG,DREAL,DSQRT,DLOG,DLOG10
C
C
       REAL*8 FDL(3),DIST(6),YH,H(6),RBC,DAA,DIA,DX(3),F
       REAL*8 EFM(6),HFM(6),HTOTM,ETOTM
       REAL*8 DIMAG,DREAL,DSQRT,DLOG,DLOG10
       REAL*8 SDX(22),SEMI(22),SHMI(22)
C
       COMPLEX*16 CDSQRT,C(3,3),TRIV(3)
```

```
      COMPLEX*16 HFIELD(6),EFIELD(6),HTOTAL,ETOTAL
C
      YH=0.D0
      DX(2)=-1.875D0
C
C LATERAL SURVEY AT DIFFERENT FREQUENCIES.
C
       DO 31 IR=1,15
       IF(IR.LE.5) THEN
        DX(2)=DX(2)+1.875D0
       ELSE IF(IR.EQ.6) THEN
        DX(2)=10.D0
       ELSE
       DX(2)=DX(2)+10.D0
       ENDIF
C
      DX(1)=DX(2)+(DIST(2)-DIST(1))
      DX(3)=DX(2)-(DIST(3)-DIST(2))
       DO 90 I=1,3
       FDL(I)=((H(I)-YH)/((H(I)-YH)**2+DX(I)**2))
       FDL(I)=FDL(I)+((H(I)+YH)/((H(I)+YH)**2+DX(I)**2))
 90    CONTINUE
      DO 910 I=1,3
      EFIELD(I)=TRIV(I)*FDL(I)
      EFM(I)=CDABS(EFIELD(I))
      EFM(I)=20.D0*DLOG10(EFM(I))
      HFIELD(I)=EFIELD(I)/377.D0
      HFM(I)=CDABS(HFIELD(I))
      HFM(I)=20.D0*DLOG10(HFM(I))
 910   CONTINUE
C
C DETERMINATION OF THE TOTAL H & E FIELD.
      HTOTAL=HFIELD(1)+HFIELD(2)+HFIELD(3)
      ETOTAL=EFIELD(1)+EFIELD(2)+EFIELD(3)
      HTOTM=CDABS(HTOTAL)
      ETOTM=CDABS(ETOTAL)
      HTOTM=20.D0*DLOG10(HTOTM)
      ETOTM=20.D0*DLOG10(ETOTM)
C
C STORE LATERAL DISTANCE,EFIELD,HFIELD FOR PLOT.
                SDX(IR)=DX(2)
                SEMI(IR)=ETOTM
                SHMI(IR)=HTOTM
 31     CONTINUE
C
       RETURN
       END
C
C
END OF THE MAIN PROGRAM AND ITS RELEVANT SUBROUTINES.
```

```
C
C
C
THE FOLLOWING CARDS CORESPOND TO THE JCL CARDS FOR THE DATA.
THE OUPUT IS STORED INTO A FILE CALLED OUTPUT.
C
C
//B211 JOB
/*JOBPARM  LINES=15
//S1    EXEC  WATFIV,REGION=192K
//GO.FT12F001    DD  DSN=&TEMP,DISP=(NEW,PASS),
//    UNIT=SCRTCH,SPACE=(TRK,(20,20)),
//    DCB=(RECFM=FB,LRECL=80,BLKSIZE=6160,BUFNO=1)
//GO.SYSIN  DD  *
$JOB           DATACONVERT
      REAL*8 D(12)
      READ, NBC,VOLT,RBC,DIA
      WRITE(12,1) NBC,VOLT,RBC,DIA
  1   FORMAT(4X,4F10.5)
      DO 2 I=1,3
C     READ IN PAIRS OF DIST(J),H(J),J=1,6
      READ, D
      WRITE(12,4) D
  2   CONTINUE
  4   FORMAT(4X,2F10.5)
      STOP
      END
$ENTRY
2.D0,362.D0,0.2285D0,0.0281D0
-7.5D0,12.5D0,0.D0,12.5D0,7.5D0,12.5D0
-7.5D0,-12.5D0,0.D0,-12.5D0,7.5D0,-12.5D0
0.D0,12.5D0,0.D0,20.D0,0.D0,27.5D0
0.D0,-12.5D0,0.D0,-20.D0,0.D0,-27.5D0
-3.75D0,12.5D0,0.D0,20.D0,3.75D0,12.5D0
-3.75D0,-12.5D0,0.D0,-20.D0,3.75D0,-12.5D0
//S2   EXEC   PGM=SAL1,REGION=128K,TIME=(,30)
//STEPLIB   DD  DSN=S.I4349.LOADMD1,DISP=SHR
//FT06F001  DD  SYSOUT=A,DCB=(RECFM=FBA,LRECL=133,BLKSIZE=133)
//FT05F001  DD  DSN=&TEMP,DISP=(OLD,DELETE),DCB=BUFNO=1
//FT15F001  DD  DSN=S.I4349.OUTPUT,DISP=(NEW,CATLG),
//    SPACE=(TRK,(1,1)),UNIT=DISK,
//    DCB=(RECFM=FB,LRECL=48,BLKSIZE=6192,BUFNO=1)
```